Life Cycle Assessment of Greenhouse Gas Emissions and Non-CO_2 Combustion Effects from Alternative Jet Fuels

by

Russell William Stratton

B.Sc. Engineering Physics, 2008
Queen's University

Submitted to the Department of Aeronautics and Astronautics in Partial Fulfillment of the Requirements for the Degree of

Master of Science in Aeronautics and Astronautics

at the

MASSACHUSETTS INSTITUTE OF TECHNOLOGY

May 2010
[June 2010]

Signature of Author.....
Department of Aeronautics and Astronautics
May 21, 2010

Certified by.....
James I. Hileman
Principal Research Engineer, Department of Aeronautics and Astronautics
Thesis Supervisor

Accepted by.....
Eytan H. Modiano
Associate Professor of Aeronautics and Astronautics
Chair, Committee on Graduate Students

[Page Intentionally Left Blank]

Life Cycle Assessment of Greenhouse Gas Emissions and Non-CO_2 Combustion Effects from Alternative Jet Fuels

by

Russell William Stratton

Submitted to the Department of Aeronautics and Astronautics on
May 21, 2010 in Partial Fulfillment of the Requirements for the Degree of
Master of Science in Aeronautics and Astronautics

Abstract

The long-term viability and success of a transportation fuel depends on both economic and environmental sustainability. This thesis focuses specifically on assessing the life cycle greenhouse gas (GHG) emissions and non-CO_2 combustion effects from conventional jet fuel and synthetic paraffinic kerosene (SPK). The research expands upon the work of Wong (2008) by examining Fischer-Tropsch jet fuel from coal and biomass, and hydroprocessed renewable jet (HRJ) fuel from rapeseed, jatropha, algae and salicornia. Each fuel option is a "drop-in" alternative in that they are compatible with existing aviation infrastructure. Using a modified version of the APMT climate impacts module, the additional climate forcing from non-CO_2 combustion effects is combined with the fuel life cycle GHG inventories.

Life cycle GHG emissions are only one of many aspects that must be considered when evaluating the feasibility and sustainability of an alternative fuel option. While cost and fresh water availability are important constraints, fuel yield and land requirements for select biomass-based fuel pathways are quantified. This is most important for feedstocks requiring cropland for cultivation. For example, current global production of soy, palm and rapeseed oil translate to only 34%, 43% and 18% of US jet fuel demand, respectively; hence, even small fractions of the petroleum industry translate to massive production scales in absolute terms. By comparison, HRJ from algal oil can yield more than an order of magnitude higher fuel production per hectare of land.

Few biofuels were identified with zero life cycle GHG emissions. This contradicts previous studies and likely results from avoiding the displacement method to allocate emissions. Considerable inter and intra fuel option variability was found in life cycle GHG emissions; land use change contributed much to the variability of many pathways. The range in life cycle GHG emissions of all fuel options examined ranged from 0 to 9.1 times those of conventional jet fuel.

The uncertainty in treating non-CO_2 combustion effects was found to have a larger influence on the life cycle emissions of each fuel option than the variability of the life cycle GHG inventories; however, including non-CO_2 combustion effects reduced the overall range in emissions of all fuel options considered to only 0 to 4.7 times those of conventional jet fuel. Hence, the inclusion of non-CO_2 effects in the fuel life cycle increases the absolute uncertainty of each fuel option but reduces the overall variability in the life cycle emissions of alternative fuels relative to conventional jet fuel.

Thesis Supervisor: Dr. James I. Hileman
Title: Principal Research Engineer, Department of Aeronautics and Astronautics

[Page Intentionally Left Blank]

Acknowledgements

I would first like to thank my advisor, Dr. Jim Hileman, for sharing his knowledge and experience with me over the course of this research. I sincerely appreciate the guidance he has offered, both academic and non-academic. The quality and breadth of the research was also greatly improved through the help of Hsin Min Wong, Dr. Malcolm Weiss, Mr. Matthew Pearlson, Dr. Kristen Lewis and Prof. Ian Waitz, (all from MIT).

I would like to thank the following individuals for their detailed reviews of all or parts of the material in this thesis: Michael Griffin (Carnegie Mellon University), Ray Dums (Chevron), David Shonnard (Michigan Technological University), Dennis Bushnell (NASA), Bob Dillmore, Tim Skone (both from National Energy Technology Laboratory), Wagner Daraia Rocha, Joanna Bauldreay, Trevor Stephenson, and Paul Bogers (all from Shell Global Solutions), Carl Hodges (The Seawater Foundation), Tom Kalnes (UOP LLC), and Kristin Lewis (Volpe National Transportation Systems Center). Their efforts contributed to a much-improved finished product.

My experience at MIT has been greatly improved through my interactions with Warren Gillette and Lourdes Maurice, of FAA, Bill Harrison of AFRL and all the other individuals who are part of the Aviation Fuels Life Cycle Analysis Working Group. Each of these people treated me with the respect of a colleague in our interactions and I am genuinely grateful for the opportunity to work with each of them.

Finally, I must thank my family for their love and support throughout my time at MIT. They were there to listen and help even when faced with their own challenges. Included in the family category is Georgia Smith who has been my rock, even when an ocean away. She has stood by me unconditionally over the past 2 years and helped me get the most business and fun out of living in Boston.

[Page Intentionally Left Blank]

Table of Contents

[Page Intentionally Left Blank]

List of Figures

List of Tables

Units, Notation, Abbreviations and Acronyms

Units

Bpd	Barrels per day	LHV	Lower Heating Value
Btu	British Thermal Unit	Mg	Megagram (metric tonne)
Bu	Bushel	MJ	Megajoule
Ha	Hectare (10000 m^2)	mmBtu	Million British Thermal Units
HHV	Higher Heating Value	Ton	Imperial Ton (2000 pounds)
kWh	Kilowatt-hour	Tonne	Metric Ton (megagram)

Chemical Species Notation

C_n	Hydrocarbon chain of length 'n'	K_2O	Potassium Oxide
CH_4	Methane	N_2O	Nitrous Oxide
CO	Carbon Monoxide	NH_3	Ammonia
CO_2	Carbon Dioxide	NO_x	Nitrogen Oxide
CO_2e	Carbon Dioxide equivalent	P_2O_5	Phosphorous Pentoxide
H_2	Hydrogen Gas	SO_x	Sulfur Oxides

Acronyms and Abbreviations

AFLCAWG	Air Force Life Cycle Analysis Working Group	HRJ	Hydroprocessed Renewable Jet
API	American Petroleum Institute	IGCC	Integrated Gasification Combined Cycle
ASP	Aquatic Species Program	IPCC	Intergovernmental Panel on Climate Change
BTL	Biomass to Liquids (via F-T)	ISO	International Organization for Standardization
CBTL	Coal and Biomass to Liquids (via F-T)	LCA	Life Cycle Analysis
CCS	Carbon Capture and Sequestration	LPG	Liquefied Petroleum Gas
CRP	Conservation Reserve Program	LUC	Land Use Change
CTL	Coal to Liquids (via F-T)	MEA	Monoethanolamine
DME	Dimethyl Ether	NETL	National Energy Technology Laboratory
DOE	Department of Energy (US)	NREL	National Renewable Energy Laboratory
EIA	Energy Information Agency	PARTNER	Partnership for Air Transportation Noise and Emissions Reduction
EISA	Energy Independence and Security Act	SOC	Soil Organic Carbon
FAPRI	Food and Agricultural Policy Research Institute	SPK	Synthetic Paraffinic Kerosene
F-T	Fischer Tropsch	TSS	Total Suspended Solids (mass percent)
GHG	Greenhouse Gas	TTW	Tank to Wake
GREET	Greenhouse Gases, Regulated Emissions, and Energy Use in Transportation	ULS	Ultra Low Sulfur
GTL	Gas to Liquids (via F-T)	USDA	United States Department of Agriculture
GWP	Global Warming Potential (IPCC)	WTT	Well to Tank
HRD	Hydroprocessed Renewable Diesel	WTW	Well to Wake

[Page Intentionally Left Blank]

Chapter 1: Introduction

Both economic and environmental sustainability are required for any transportation fuel to be viable in the long term. An expansion of our energy portfolio to include alternative fuels would also result in the desirable consequence of energy diversity. This thesis presents results from ongoing research within the Partnership for AiR Transportation Noise and Emissions Reduction at MIT on alternative fuels. As shown by the diagram of Figure 1, the PARTNER alternative fuels research portfolio is considering many aspects of alternative fuel sustainability. This thesis focuses on aspects of environmental sustainability, with an emphasis on life cycle greenhouse gas emissions and fuel combustion effects in the upper atmosphere as they relate to impacts on global climate.

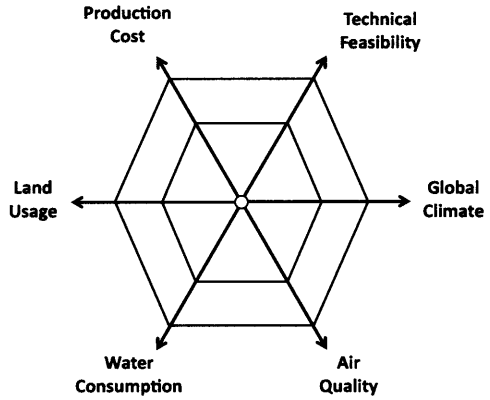

Figure 1: Aspects of alternative fuels that are being considered for alternative fuel feasibility and sustainability. This report has an emphasis on life cycle greenhouse gas emissions

Alternative jet fuels created from renewable resources offer the potential to reduce the greenhouse gas (GHG) emissions from aviation. This is due to a change in the GHG emissions that result from the extraction, production and combustion of the alternative fuel relative to conventional jet fuel, not because of a change in fuel composition change in engine efficiency. A life cycle accounting of the GHG emissions that starts with the well, mine, or field where the fuel feedstock is extracted, and extending to the wake behind the aircraft, can be developed to quantify the change in GHG emissions that result from the use of an alternative fuel. To emphasize the importance of life cycle analysis for an accurate comparison of GHG emissions, consider that the combustion of synthetic fuels, which are covered extensively in this work, results in approximately 4% less CO_2 emissions (per unit mass of fuel) as compared to conventional jet fuel. However, as will be shown in this report, the life cycle GHG emissions from various alternative fuels can vary by two orders of magnitude depending on the feedstock and the details of production.

There are many other issues that need to be considered when evaluating the potential of a specific alternative fuel. These include, but are not limited to, the efficient usage of water and land resources, the environmental impacts on air quality, and the economic cost of fuel production. This work touches on water and land usage, but not air quality or economic costs. Hileman et al. (2009) provide an extended discussion of these and other aspects of alternative jet fuel feasibility that is complementary to the work presented herein. This thesis does not consider whether our

limited biomass resources would provide greater societal benefit if they were used elsewhere, for example to create fuels for ground transportation or to generate heat and/or electricity. A recent analysis by Hedegaard et al. (2008) indicates that scarce biomass resources could be used more effectively, from perspectives of energy efficiency and CO_2 mitigation, for heat and electricity rather than ethanol for transportation. These topics are being considered as part of ongoing research.

The focus of this thesis is a comparison of the well-to-wake, life cycle GHG emissions from select feedstock-to-jet fuel pathways for the United States; only a partial list of potential alternative jet fuel options are assessed and should not be considered exhaustive. In some cases, details for a given fuel production pathway are expected to differ for other countries. The underlying data for each analysis have come from the literature, but each fuel pathways has been considered using a consistent methodology. The life cycle GHG inventories developed in this thesis improves and expands upon the work started by Wong (2008). The analysis framework and methodological assumption used by Wong (2008) are consistent with those adopted herein; hence, all results are complementary and are treated as a single data set.

This work is the first of its kind in that that a broad range of alternative fuels are analyzed for aviation using consistent methodologies that facilitate equitable comparisons. Each pathway is presented such that transparency of assumptions is maximized and the reader is able to identify the pivotal factors defining fuel production for each feedstock. This is one of the primary goals in communicating the results. As there is considerable variability in the life cycle GHG emissions from existing fuel production, and many of the fuel pathways considered in this report have not been commercialized, a range of life cycle GHG emissions has been provided for each feedstock-to-fuel pathway. In addition to the examination of life cycle GHG emissions, the manuscript provides a first order examination of the land and water usage that could accompany the development of a biofuel industry for aviation.

A complete well-to-wake analysis of emissions must also consider the climate impacts of non-CO_2 products of combustion, namely, soot and sulfate aerosols, water vapor, greenhouse gas precursors (NO_x), contrails and contrail cirrus.[1] Such products have both atmospheric warming and cooling effects but are typically ignored because the climate impacts of biofuels are primarily considered from the perspective of greenhouse gas (GHG) emissions (EISA, 2007; EPA, 2010). Recent research has emphasized that selecting environmental policies that balance society's economic and environmental needs requires that policymakers assess the full impact of candidate policies. Non-CO_2 combustion effects are particularly important for aircraft where near-term impacts are dominated by the non-CO_2 effects while long-term impacts are driven by only CO_2 and other long lived greenhouse gases (Marais et al., 2008). This thesis extends the life cycle GHG inventories of alternative fuels to consider the climate impacts of non-CO_2 combustion products and effects.

The contents of the report are structured as follows. Chapter 2 provides context for discussing fuel in the aviation industry while Chapter 3 presents the fuel pathways considered in this thesis. Chapter 4 outlines background information on creating a life cycle GHG emissions inventory and outlines a framework for considering non-CO_2 effects from fuel combustion in aircraft. Chapters 5 through 7 present life cycle GHG inventories for conventional jet fuel and various other alternative jet fuel pathways. Chapter 5 expands upon the work of Wong (2008) in considering

[1] Contrails are artificial clouds that are the visible trails of condensed water vapor made by the exhaust of aircraft engines. Contrail cirrus refers to atmospheric clouds that are characterized by thin, wisplike strands. The contrails left by aircraft can induce the formation of cirrus clouds in regions that are supersaturated with respect to ice.

conventional jet fuel petroleum. Chapter 6 examines Fischer-Tropsch synthesis as a means to create synthetic paraffinic kerosene (SPK) fuel by combining coal and biomass. Chapter 7 presents the analysis of hydroprocessed renewable jet fuels (HRJ) from rapeseed, jatropha, algae, and salicornia. Chapter 8 offers an analysis of fuel yields of the feedstocks considered both by Wong (2008) and in this thesis followed by a discussion of water consumption in fuel production and potential damages caused by the introduction of invasive species. Chapter 9 quantitatively evaluates the climate forcing of non-CO_2 combustion effects of both conventional jet fuel and SPK fuel. Chapter 10 presents a broad comparison of the life cycle GHG inventories from Wong (2008) and Chapters 5 through 7 of this thesis. The impact of including non-CO_2 combustion effects in the fuel life cycle is subsequently evaluated for each fuel pathway. A discussion synthesizing the findings of all previously chapters is given. Conclusions from this research with recommendations for future work are presented in Chapter 11

[Page Intentionally Left Blank]

Chapter 2: Background on Fuels and Aviation

2.1 Current State of the Jet Fuel Industry

The world demand for oil in 2008 was 85.6 million barrels per day. The United States accounted for 19.5 million barrels per day. In the US, 46% of oil goes to gasoline production, 27% goes to diesel and only 9% goes to jet fuel (EIA, 2010a). Although a producer can alter their distribution of products to some extent to meet market demands, the product slate is fundamentally driven by the oil composition. Given in Figure 2 is the average product slate of US refineries in 2009.

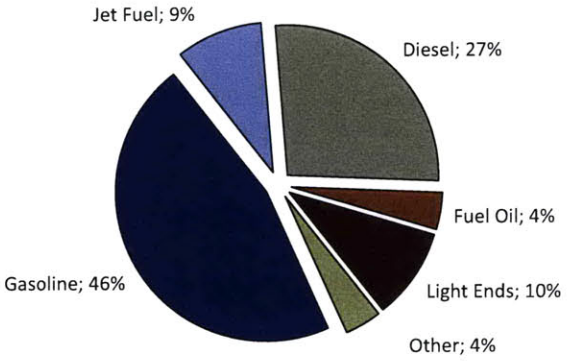

Figure 2: United States average distribution of petroleum products from a barrel of crude oil in 2009 (EIA, 2010a)

Despite jet fuel representing a relatively small fraction of the total, consider that a fully loaded Boeing 747-400 consumes approximately 1200 barrels of jet fuel to fly from Boston to Dubai. For comparison, a moderate sized airport, such as Boston Logan International, uses roughly 25,000 barrels per day and US aviation consumes 1.5 million barrels of jet fuel per day (Hileman, 2010). Hence, even small fractions of the petroleum industry translate to massive production scales in absolute terms.

Furthermore, a 2005 analysis of crude oil imports found that only 30% of all jet fuel produced in the US is made from domestic crude oil resources. The rest was imported from countries around the world, the largest supplier of which was Canada at 10.2% of the total (Skone and Gerdes, 2008). Although domestic resources could easily meet the demands of the Department of Defense (EIA, 2010b; Edwards, 2009), the commercial sector and overall economy are dependent on foreign sources.

Fuel use by airlines is related to the demand for aviation productivity and the fuel cost. Shown in Figure 3 are historical fuel cost, aviation productivity (defined here as the total system revenue ton miles) and fuel consumption from 1996 through 2009. The right-hand plot shows that total productivity has been steadily increasing while jet fuel consumption has remained relatively constant.[2] Therefore, the overall efficiency of aircraft operations has been steadily increasing. The

[2] The financial crisis in 2008 has caused both these trends to change but this is ignored for this simple introductory discussion

data in the left-hand plot show that the changes in fuel cost have been more significant than changes in either productivity or fuel consumption. The fact that fuel costs were increasing more rapidly than the improvements in operational efficiency led to fuel overtaking labor as the dominant contributor to aviation operating costs for the first time in 2006 (Hileman et al., 2009).

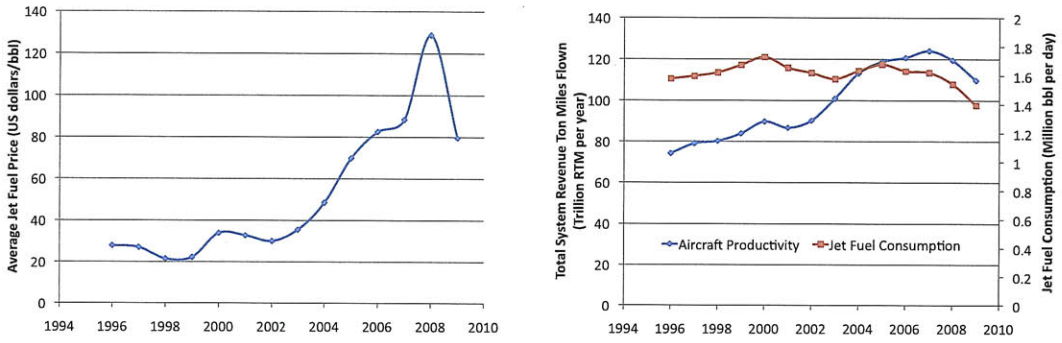

Figure 3: Annual US jet fuel cost, jet fuel consumption and aviation productivity from 1996 through 2009 (ATA, 2010a; ATA, 2010b; EIA, 2010c)

The volatility of the price of petroleum has caused an inconsistent interest in alternatives to conventional petroleum. Interest is provoked by a spike in the price of petroleum but quickly forgotten when oil prices and business return to normal. With environmental concerns likely providing a continuing reason for interest in alternative fuels, the shear magnitude and inertia of the petroleum industry must be kept in mind when discussing the potential influence of alternative fuels.

2.2 Potential for Alternative Fuels within the Aviation Industry

The motivations for exploring alternative fuels for aviation are rooted in environmental sustainability, concerns about high and volatile petroleum prices and energy security issues (Wong, 2008). Price and energy security issues were briefly outlined in the previous section. Environmental sustainability from a regulatory standpoint is focused on climate change, with a focus on GHG emissions (EPA, 2010; EISA, 2007). Although aviation contributes only 2% of global CO_2 emissions, there is considerable pressure on aviation to take actions to reduce its carbon footprint (Penner et al., 1999). Other factors affecting environmental sustainability for alternative fuels were outlined in the introduction.

Alternative fuels are considered within a larger effort for aviation to reduce its GHG emissions. Other parts of this effort are flight efficiency improvements that reduce fuel burn, operational improvements such as minimized route detours and more efficient ground based operations, and demand control through price signals. A future projection of GHG emissions from aviation under a scenario of moderate technological improvement is compared to a business as usual projection in Figure 4. Both projections are from the fourth meeting of the Group on International Aviation and Climate Change (ICAO, 2009).[3] Also shown is a notional goal for GHG emissions reductions from aviation framed loosely in the near-term on the goals put forth for the United States at the Copenhagen conference on climate change and outlined in the American Clean Energy and Security Act (AECS) (Broder, 2009; OpenCongress, 2009); specifically, the notional goal in

[3] Aircraft specific fuel burn was assumed to decrease 1.5% per annum. Operational improvements were assumed to reduce flight distances by 3% at 2015 and 10% at 2025 in the US. Flight distances for the rest of the world were assumed to decrease by 3% at 2020 and 10% at 2030.

Figure 4 is a 17% emissions reduction below 2005 levels by 2020 with subsequent carbon neutral growth to 2050.[4] The additional reductions required beyond those achieved through projected technological improvements is labeled the alternative fuels wedge. Under this particular scenario, the GHG emissions of the jet fuel mix consumed in the US would have to be 40% less than it is today to meet the emissions target in 2025. While this simple approach does not capture the potential for aviation to purchase emissions credits as outlined in the AECS (OpenCongress, 2009) it is sufficient to show a discontinuity between the public perception and the reality of using alternative fuels as a climate change mitigation technology.

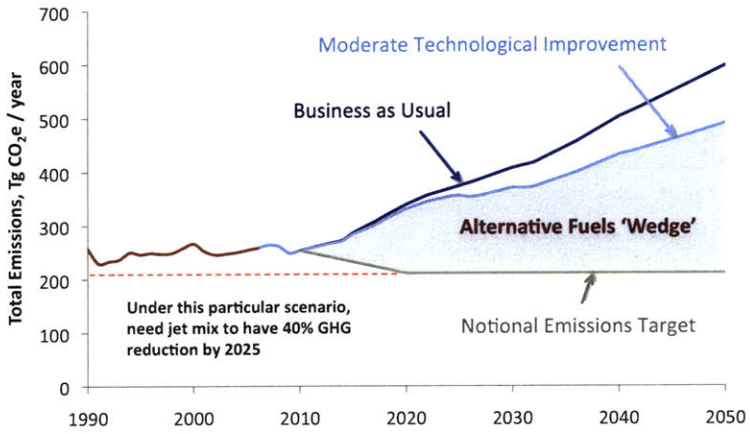

Figure 4: Historical and projected total GHG emissions from aviation under a business as usual scenario, a moderate technological improvement scenario and a notional emissions target

The reduction in GHG intensity of the US jet fuel mix can be met with either a strong proliferation of a fuel with moderate GHG reduction potential or moderate proliferation of a fuel with major GHG reduction potential. The trade between these factors is shown in Figure 5 for a 40% reduction and 10% reduction. In all cases, the upper left corner is the utopia point for this system. Also shown are two notional examples of how fuel options can be represented in this space. The focus of this thesis is quantifying the position of fuel options on the horizontal axis. Fuel options are positioned on the vertical axis based on the scale of total jet fuel production, fuel yield (per unit of land) and resource constraints such as land availability, freshwater consumption and economic cost. As emphasized in Section 2.1, the scale of jet fuel production is the biggest limitation facing any alternative fuel intended to meet a percentage emissions reduction. In the case of a 40% reduction, even a zero carbon fuel would have to grow from existing production levels, which are suitable for testing purposes, to commercialized production of 600,000 barrels per day in a span of 15 years.

These simple arguments demonstrate the need for realism in setting expectations for alternative fuels to reduce GHG emissions from aviation. All the above arguments can also be applied at a large scale to the transportation sector as a whole.

[4] The official US goal is 17% below 2005 emissions levels by 2020 and 83% by 2050. The notional goal used here is less stringent in the year 2030 through 2050.

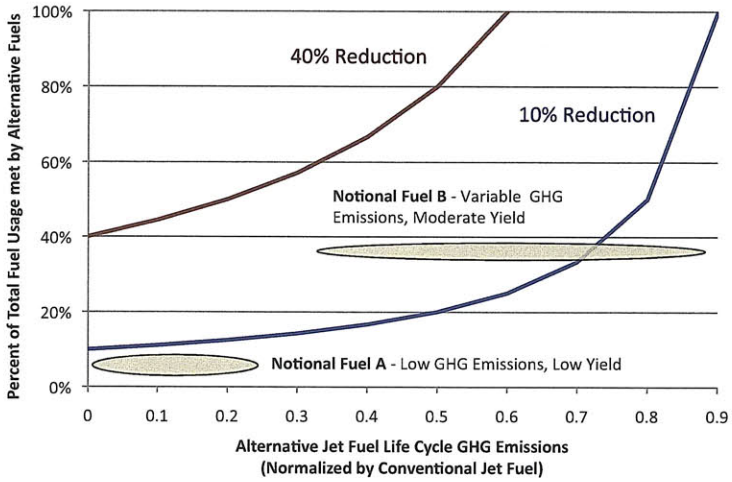

Figure 5: Trade space between alternative fuel proliferation and life cycle GHG emissions for meeting percentage reductions in total emissions from aviation

2.3 Fuel Viability for Aviation

The fuel options considered herein are limited to "drop-in" alternatives in that they have the potential to serve as a direct replacement for conventional jet fuel, requiring little or no modification to existing infrastructure or aircraft. With 20,000 commercial aircraft in service worldwide, each with a useful lifetime of several decades and representing an investment of tens to hundreds of millions of dollars, there is substantial incentive to use fuels that are compatible with existing infrastructure.

Furthermore, jet fuel is a valuable hydrocarbon fuel that is subject to stringent standards on composition and properties; the most notable of which necessitate a minimum specific energy, acceptable density range, maximum volatility, maximum flash point as well as adequate thermal stability (ASTM D1655-09, 2009). Any alternative fuel for aviation must meet the operational demands of the industry before it is considered in any further detail. Alcohols and biodiesel (fatty acid methyl esters) are not considered due to both the safety issues and the decrease in fuel efficiency that would accompany their use in aircraft operations (Hileman et al., 2009). The fuel compositions analyzed in this thesis are as follows:

- Conventional jet fuel (e.g., Jet A) from conventional petroleum (crude oil)
- Synthetic Paraffinic Kerosene (SPK) fuels created via Fischer-Tropsch (F-T) synthesis or hydroprocessing of renewable oils.

This should not be viewed an all-encompassing list of potential fuel compositions that could be used as a replacement or a blend stock in aviation gas turbine engines. Wong (2008) considered jet fuel from unconventional petroleum as well as Ultra Low Sulfur (ULS) jet fuel from conventional petroleum. Future fuel sources for aviation could also come via advanced fermentation or pyrolysis to create a jet fuel blendstock.[5]

[5] Note that pyrolysis is being examined to create synthetic aromatics that could be blended with SPK fuels to create a fully synthetic jet fuel while advanced fermentation is being examined to create a paraffinic fuel for aviation gas turbines.

SPK fuels have similar molecular composition to conventional jet fuel with the primary difference being a lack of aromatic compounds; conventional jet fuel typically contains 20% aromatic compounds. Because certain types of gas turbine seals require aromatic compounds for proper swelling, the certification of SPK fuels has thus far been limited to blends of up to 50% with conventional jet fuel to maintain a minimum aromatic content. As of September 2009, a 50% blend of SPK fuel derived via Fischer-Tropsch synthesis with conventional jet fuel was certified for use in commercial aviation under ASTM spec D7566-09 (ASTM D7566-09, 2009). The fuel specification and certification division of the Commercial Aviation Alternative Fuels Initiative (CAAFI) played a key role in the process of establishing D7566 and has outlined plans for a expanding the specification to include a 50% HRJ blend with conventional jet by 2010, 100% F-T derived SPK by 2011 and 100% HRJ by 2013 (Rumizen, 2010).

[Page Intentionally Left Blank]

Chapter 3: Alternative Fuel Pathways

Due to the closely related nature of the work of Wong (2008) and this thesis, this chapter is designed to outline all fuel pathways considered as part of the larger research effort and then clearly identify the contributions of this thesis to the assessment of alternative jet fuel pathways.

The current list of fuel production pathways that have been analyzed within the larger research effort are jet fuel from conventional crude oil, jet fuel from Canadian oil sands, jet fuel from oil shale, Fischer-Tropsch jet fuel from natural gas, coal and biomass, and jet fuel created by hydroprocessing soy oil, palm oil, rapeseed oil, algal oil, jatropha oil and salicornia oil. The fuel pathways are summarized in Table 1.

The specific contributions of this thesis to the overall research are outlined below:

- *Addition of country specific crude oil extraction profiles to the conventional jet fuel and ultra low sulfur jet fuel pathways from Wong (2008) (Chapter 5)*
- *Development of switchgrass cultivation and harvesting profile for use in Fischer Tropsch jet fuel pathways (Chapter 6)*
- *Development of a coal and biomass to Fischer-Tropsch jet pathway (Chapter 6)*
- *Development of mass and energy flow estimates of hydroprocessing renewable oils to HRJ (Chapter 7)*
- *Development of rapeseed to HRJ pathway (Chapter 7)*
- *Development of algae to HRJ pathway (Chapter 7)*
- *Development of jatropha to HRJ pathway (Chapter 7)*
- *Development of salicornia to HRJ and Fischer-Tropsch Jet pathway (Chapter 7)*
- *Fuel yield assessment of all pathways (Chapter 8)*
- *Development of a framework for assessing the climate impacts of non-CO_2 emissions from fuel combustion (Chapter 9)*

Table 1: Fuel pathways investigated

Source	Feedstock	Recovery	Processing	Final product
Petroleum	Conventional crude	Crude extraction	Crude refining	Jet Fuel
	Conventional crude	Crude extraction	Crude refining	Ultra low Sulfur Jet Fuel
	Canadian oil sands	Bitumen mining/ extraction and upgrading	Syncrude refining	Jet Fuel
	Oil shale	In-situ conversion	Shale oil refining	Jet Fuel
Natural gas	Natural gas	Natural gas extraction and processing	Gasification, F-T reaction and upgrading	F-T Jet Fuel (GTL)
Coal	Coal	Coal mining	Gasification, F-T reaction and upgrading (with and without carbon capture)	F-T Jet Fuel (CTL)
Coal and Biomass	Coal and switchgrass, corn stover and forest residues	Coal mining and biomass cultivation	Gasification, F-T reaction and upgrading (with carbon capture)	F-T Jet Fuel (CBTL)
Biomass	Switchgrass, corn stover and forest residues	Biomass cultivation	Gasification, F-T reaction and upgrading	F-T Jet Fuel (BTL)
	Soy oil	Cultivation and extraction of soy oils	Hydroprocessing	HRJ Fuel (Hydroprocessed Renewable Jet)
	Palm oil from Southeast Asia	Cultivation and extraction of palm oils	Hydroprocessing	HRJ Fuel
	Rapeseed Oil	Cultivation and extraction of soy oils	Hydroprocessing	HRJ Fuel
	Algae oil	Cultivation and extraction of algae oils	Hydroprocessing	HRJ Fuel
	Jatropha oil	Cultivation and extraction of jatropha oils	Hydroprocessing	HRJ Fuel
	Salicornia oil and solid biomass	Cultivation of salicornia and extraction of salicornia oils	Gasification, F-T reaction and upgrading (with carbon capture); Hydroprocessing	F-T Jet Fuel and HRJ Fuel

Chapter 4: Procedural Overview of Well-to-Wake Analyses

The life cycle analysis of alternative jet fuels encompasses emissions from the complete fuel cycle. This includes recovery and transportation of the feedstock from the well, field, or mine to the production facility, processing of these materials into fuels, transportation and distribution of the fuel to the aircraft tank, and finally, the combustion of the fuel in the aircraft. These "well-to-wake" (WtW) steps can be broadly grouped into fuel production and distribution, "well-to-tank" (WtT), and fuel combustion, "tank-to-wake" (TtW). This chapter first discusses the GHG emissions from well-to-tank steps and then separately considers the relevant climate impacts from the tank-to-wake combustion products of aircraft.

4.1 Functional Unit

Well-to-tank GHG emissions are presented using a metric that captures the mass of GHG per unit of energy (lower heating value) consumed by the aircraft. This is consistent with the framework developed by the US Air Force (AFLCAWG, 2009) and is given in units of grams of carbon dioxide equivalent per megajoule (g CO_2e/MJ), where

$$\left(CO_2e\right)_{\text{well-to-tank}} = \left(CO_2 + CH_4 \cdot GWP_{CH_4} + N_2O \cdot GWP_{N_2O}\right)_{\text{well-to-tank}} \qquad \text{Equation 1}$$

The tank-to-wake emissions from aircraft with known climate impacts are CO_2, soot and sulfate aerosols, water vapor, and greenhouse gas precursors (NO_x). Additionally, as the hot exhaust gases cool in the surrounding air they could precipitate a cloud of microscopic water droplets called contrails. The contrails left by aircraft can subsequently induce the formation of cirrus clouds, called contrail cirrus. Both contrails and contrail cirrus have been shown to have important climate impacts.

The CO_2 and non-CO_2 emissions from fuel combustion are presented per megajoule (LHV) of fuel consumed by the aircraft in the same manner as GHG emissions from well-to-tank steps. In some cases, only CO_2 emissions from combustion may be relevant to the analysis; the scope of other analyses may necessitate accounting for the climate impacts of all combustion products and effects. The CO_2 from fuel combustion is a well-known quantity for a specified fuel composition and is always given in conjunction with the GHG emissions from well-to-tank life cycle steps. Because of the limited time and geographical scales of their impact, there are no established global warming potentials to quantify the climate impacts of non-CO_2 and CO_2 effects using a single metric; therefore, a non-CO_2 ratio was derived to scale the CO_2 from combustion to account for the climate forcing from non-CO_2 combustion emissions. This approach draws from the process and results developed by Dorbian (Dorbian, 2010).

Consistent with established practices, 'tank-to-wake' is used to describe only the CO_2 emissions from combustion (Stratton et al., 2010; Hileman et al., 2009; AFLCAWG, 2009). This thesis introduces the new terminology of 'tank-to-wake (+)' to identify the combination of CO_2 and non-CO_2 effects from fuel combustion in aircraft.[6] This framework is shown explicitly in Equation 2. Further discussion of this approach is given in Section 4.3 and Chapter 9.

$$\left(CO_2e\right)_{\text{tank-to-wake}} = \left(CO_2\right)_{\text{combustion}} \cdot \left(\text{non-}CO_2\text{ ratio}\right) \qquad \text{Equation 2}$$

[6] Verbally pronounced as 'tank-to-wake plus'

4.2 Well-to-Tank Greenhouse Gas Emissions

The steps of a complete well-to-wake life cycle analysis are shown schematically in Figure 6. This section deals explicitly with the assessment of GHG emissions from the first four life cycle steps. The GHG covered in this analysis are carbon dioxide, methane and nitrous oxide using their 100-year global warming potentials (Solomon et al., 2007). Sensitivity studies are use in Section 10.3 to assess how the use of different time windows can affect the results developed herein. This analysis did not consider energy or GHG emissions associated with the initial creation of infrastructure such as extraction equipment, transportation vehicles, farming machinery, processing facilities, etc. This is consistent with Wong (2008), where the impact of such emissions on the total life cycle GHG emissions of the pathway was deemed within the uncertainty range of the analysis.

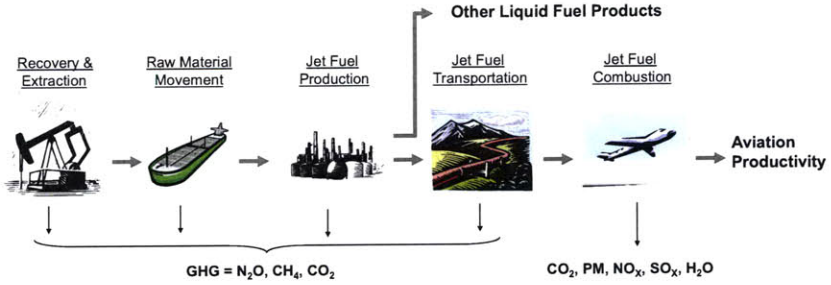

Figure 6: Steps considered, in the well-to-wake, life cycle GHG inventory of conventional jet fuel

Fossil feedstocks such as crude oil, coal or natural gas are created from geologically sequestered carbon sources, and the carbon is released as CO_2 when the fuel products are burned. Such combustion CO_2 has to be taken into account in the life cycle analysis (see Figure 6). Biomass feedstocks absorb CO_2 from the atmosphere when they grow and the CO_2 emitted during fuel combustion is equal to that absorbed during biomass cultivation. Hence, many biofuels have a "biomass credit" that offsets the combustion CO_2 in the life cycle analysis (see Figure 7). *This biomass credit is the primary difference between biomass and fossil fuels in terms of their GHG emissions.* However, a biofuel does not necessarily have GHG emissions that are below a fossil fuel.

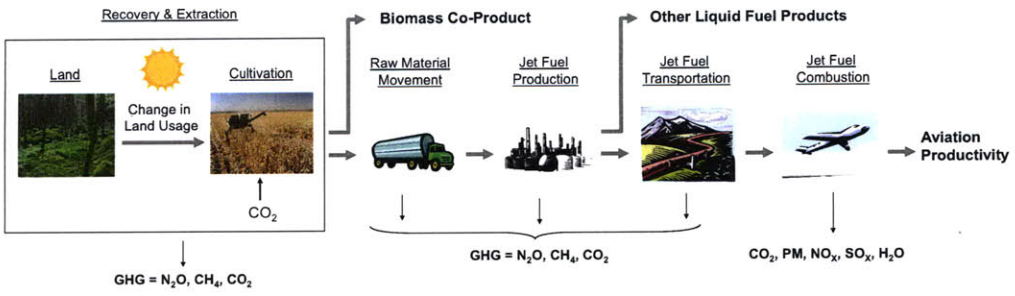

Figure 7: Steps considered in the well-to-wake, life cycle GHG inventory of bio-based alternative jet fuels

Biomass feedstocks also have the potential for CO_2 emissions or CO_2 sequestration from changes in land use (see first step of Figure 7). The CO_2 emissions or sequestration are due to changes in

the biomass, soil and organic waste contained on and within the land. In some instances, these emissions can dominate the life cycle GHG emissions of the biofuel pathway. The land use change can be a direct land conversion, (e.g., tropical rainforest being cleared for cropland to grow feedstocks), or it can be an indirect conversion resulting from land being converted elsewhere in the world due to economic signals induced by increased demand for agricultural products. In either case, it is assumed that a fixed quantity of biomass (e.g., vegetable oil) needs to be supplied to global food markets and that additional production (for biofuel creation) is met by land that has been converted from some previous use. The magnitude of land use change emissions depends primarily on the type of land being converted to cropland and the type of crops being grown. For fossil feedstocks, where conversion of land (e.g. forest land, grass land) for extraction of fossil resources (e.g. extraction of bitumen) or placement of fuel processing facilities (e.g. oil refineries) takes place, land use change emissions are negligible compared to other components of the fuel pathway. This is because a large throughput of fuel volume or mass (as well as energy) is created per unit area of converted land.

Only emissions from direct land use changes, where land is converted to facilitate biofuel production, were considered in this thesis. No attempt was made to quantify the magnitude of indirect land use change emissions resulting from fluctuations in supply and demand of other crops because of increased biofuel production. In order to properly capture these effects, a detailed economic model is required which falls beyond the capabilities of the modeling framework used for this analysis as well as the project scope. Other academic and government groups have invested a significant amount of effort to quantify indirect land use change emissions and the reader is directed to their publications for estimates of these effects (EPA, 2010; Melillo et al., 2009).

For biofuels produced from algae, sufficient growth rates cannot be achieved without the direct feeding of CO_2 during growth. This is because the atmospheric concentration of CO_2 is too dilute to support an economically viable growth rate (Putt, 2007). The CO_2 used to feed the biomass must be abundant and come from a source external to the biofuel production system. In this study, fossil energy resource-based electricity generation was chosen to meet these needs. One can imagine a coupled system in which the CO_2 source and algae facility are linked to one another, where a fossil fuel is the primary input and both electricity and algal biofuel are primary outputs. This concept is shown schematically in Figure 8 with the system boundary for a conventional biofuel pathway expanded to include an outside source of CO_2. In addition, direct land use changes should be small as compared to crop-based biofuels and indirect land use changes should be minimal because the necessary infrastructure can be created in wasteland and desert areas. Algae also have the capability to grow in saline water, meaning that fresh water is not a pre-requisite.

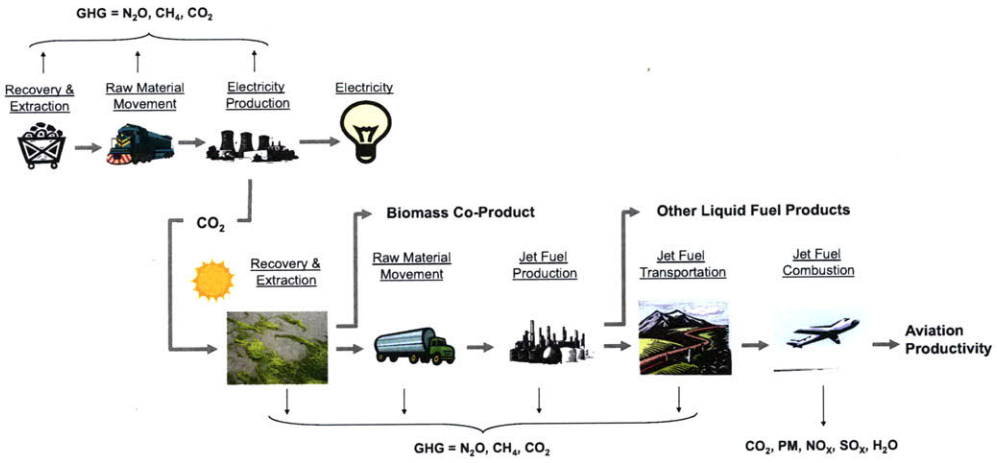

Figure 8: Steps considered in the well-to-wake, life cycle GHG inventory of bio-based fuels from algae

4.2.1 Co-Product Allocation Methodologies

Fuel production generally results in the creation of co-products in addition to the primary fuel product. For example, the systems shown in Figure 6, Figure 7 and Figure 8 generate biomass and liquid fuel co-products. These co-products have embodied value that can be quantified based on physical metrics, or their ability to displace some other product elsewhere in the greater marketplace. Four methods can be used to assign life cycle GHG emissions between the primary fuel product and any co-products that are created:

- Mass allocation
- Energy allocation
- Market-value allocation
- Displacement (or substitution, or system expansion)

The international organization for standardization (ISO) states in ISO 14044:2006(E) that processes shared with other product systems shall be identified and dealt with by preferentially using process disaggregation, system expansion, allocation by an underlying physical relationship and economic value, in this order. Inventories are based on material balances between input and output; therefore, allocation procedures should attempt to approximate such fundamental input/output relationships and characteristics (ISO, 2006).

The mass and energy allocation approaches distribute the life cycle GHG emissions based on either the mass or energy content, respectively, of the co-products and the fuel. In this work, the energy allocation method was used to allocate energy and emissions between co-products of the Fischer-Tropsch process as well as those in the hydroprocessing of renewable oils to make Hydroprocessed Renewable Jet (HRJ); this is because these co-products have utility as energy resources.

The market allocation approach apportions emissions based on the market prices of the co-products and primary fuel product. Unlike the mass or energy allocation approaches, the market value allocation can change with time. The sensitivity to market forces could be particularly useful when co-products are generated in quantities that stand to flood existing markets and drive the co-product price to zero. For example, if a fuel has a co-product that displaces some existing

product, then the market value method will capture the diminished utility of creating additional co-product by allocating more of the emissions to the fuel being produced. This is because increasing alternative fuel production will not change the price of the alternative fuel as this is set by the price of conventional fuel net subsidies and taxes. Co-product creation does, however, have the potential to alter the price of similar commodities. In this work, market valuation was used to allocate emissions between co-products leaving the system after oil extraction within the HRJ pathways.

The displacement method assumes that the production of the incidental co-product displaces the production of a substitute product. As a result, an emissions credit from the displaced product that is no longer produced is applied to the primary product. Although this methodology is desirable because it is time-invariant and it could in theory be applied to any co-product, it is hard to implement. This is because of difficulties in identifying a suitable product to be displaced, calculating the life cycle GHG emissions of that displaced product and determining the displacement ratio (Huo et al., 2008). In the case of biofuels, the issue of how to appropriately allocate land use change emissions further complicates the application of the displacement method. The life cycle analysis of algae in this work applied the displacement method to the fossil based electricity used as a CO_2 source.

The use of different allocation methodologies can lead to substantially different results, particularly in regards to biofuel pathways where significant quantities of co-products are being produced. The appropriate method may depend to a large extent on the question that the life cycle analyst attempting to answer. Regardless of which method is applied, it is important that those conducting life cycle analyses clearly state the allocation approach adopted.

4.2.2 Analysis Procedure

Analyses of well-to-tank GHG emissions for several jet fuel production pathways were carried out based on available information in the scholarly and technical literature. The Greenhouse Gases, Regulated Emissions, and Energy Use in Transportation (GREET) framework (version 1.8b) and its supporting data, both developed and maintained by Argonne National Laboratory, was the primary tool used for the analyses.[7] A simulation year of 2015 was used and default GREET assumptions were used in the analysis of the pathways, except where more recent data were obtained. For example, the average efficiencies of coal-fired power plants (utility boiler) and coal integrated gasification combined cycle (IGCC) plants were modified to be 36 percent and 41.5 percent, respectively, on a lower heating value basis[8] (Deutch and Moniz, 2007).

A key limitation of the GREET framework is that it is designed for ground transportation fuels and vehicle systems and does not include jet fuel production pathways. Also, most of the feedstocks analyzed in this thesis are not available in GREET (e.g. rapeseed, algae, etc.). Hence, this work utilized data from the literature on jet fuel and jet fuel alternatives where available (e.g. fuel properties, refining efficiency) and incorporated them into the GREET framework to derive life cycle GHG emissions. Where supporting data are presented in this report, mixed units are used for consistency with GREET version 1.8b.

---

[7] All fuel pathways analyzed in this thesis used GREET version 1.8b; however, the results from Wong (2008) used a combination of versions 1.8b and 1.8a. The impact on the results of using GREET version 1.8a or 1.8b is negligible compared to the inherent uncertainties of life cycle analysis.

[8] From Deutch and Moniz, 2007, the US coal fleet average generating efficiency is about 33% (HHV) and the generating efficiency for coal IGCC plants is 38.4% (HHV). Since the difference between HHV and LHV range from 2 to 4%, a 3% difference is assumed in this report. Hence, the efficiency of an average coal-fired power plant is assumed to be (33+3) 36% and the efficiency of a coal IGCC plants is assumed to be (38.4+3) 41.5%.

The GREET framework was primarily used as a database and calculation platform, where the quality of results depends on the quality of input assumptions such as energy efficiencies, fuel properties and emission allocation method for co-products. Wong (2008) developed a new approach by identifying and reviewing key inputs and assumptions for each pathway. Specifically, default GREET input assumptions were examined for the fuel pathways available in GREET. Key parameters with a significant impact on the life cycle GHG emissions of the pathway were identified. Default GREET values for these key parameters were updated wherever necessary using reviews of recent information available in the literature. Where a specific pathway was not available in GREET, the pathway was built within the GREET framework with all relevant input parameters gathered from the open literature.

The analysis methodology used in this work differs from that adopted by the US Environmental Protection Agency (EPA) in their Renewable Fuel Standard (RFS2) recently released in February 2010. Specifically, life cycle assessments can be categorized as either attributional or consequential. As defined by the EPA:

"An attributional approach to GHG emissions accounting provides information about the GHG emitted directly by a product and its life cycle. The product system includes processes that are directly linked to the product by material, energy flows or services through the supply-chain. A consequential approach to GHG emissions accounting in products provides information about the GHG emitted, directly or indirectly, as a consequence of changes in demand for the product. This approach typically describes changes in GHG emissions levels from affected processes, which are identified by linking causes with effects." (EPA, 2010)

Attributional and consequential life cycle analyses will tend to yield different results for an identical product; hence, comparing results from the two methodologies is inappropriate. This work implements an attributional methodology while the EPA has used a consequential analysis to more broadly consider the impact of future policy scenarios.

4.2.3 Goals and Practices

A life cycle analysis should be consistent with the goals of the study. As discussed in the "Framework and Guidance for Estimating Greenhouse Gas Footprints of Aviation Fuels", different levels of analysis fidelity originate primarily from robustness of assumptions, data quality and level of model completeness (AFLCAWG, 2009). These differences are summarized in Figure 9. As indicated, this work focuses on conducting high quality screening-level analyses using assumptions that attempt to capture industry averages.

Although a screening level analysis approach was chosen, uncertainty ranges were established using optimistic, nominal and pessimistic scenarios such that the result is presented as a range instead of a single point. In most cases, the GHG emissions inventories established for each pathway are not representative of an existing production configuration. As such, site-specific examinations of individual fuel pathways are still essential to quantifying specific GHG footprints such as would be required to meet Section 526 of EISA 2007. The results of this work do not replace such an analysis.

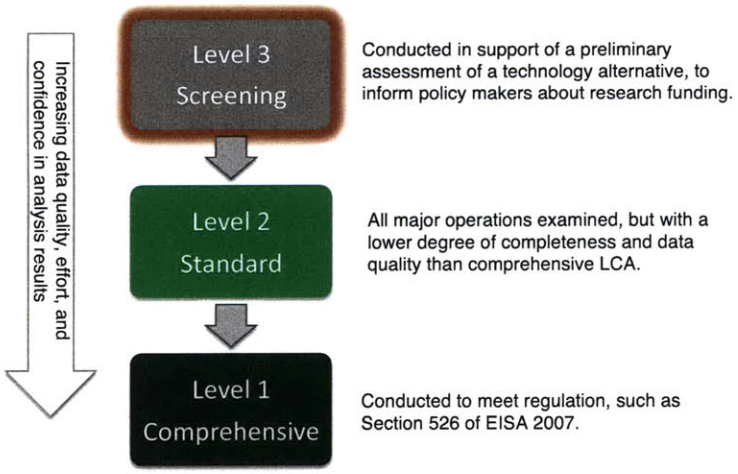

Figure 9: Levels of life cycle GHG studies used to ensure that the adopted practices are consistent with the goal of the work

4.2.4 Evaluation of Variability

To explore the impact of variability in key parameters values, three different scenarios – low GHG emissions, baseline or nominal GHG emissions, and high GHG emissions – were envisaged for each pathway. Key parameters were identified through examination of the GHG emissions that resulted from each individual life cycle step (see Figure 6 through Figure 8) and optimistic, nominal and pessimistic assumptions were developed for each. The engineering judgment of the author was used to identify parameters that had both variability as well as a considerable influence on the life cycle GHG emissions. Input parameters such as process efficiency and biomass feedstock yield have both of these qualities in that they exert considerable influence on the life cycle GHG emissions of the fuel pathway and their value a decade into the future could have considerable variability; hence, these parameters were varied as part of the three scenarios. Parameters with large variability but only a small impact on the life cycle emissions (such as the distance the feedstock needs to travel from the source to the refinery) were generally not examined.

By using key parameters to define the low, baseline, and high emissions scenarios, a range of GHG emissions, rather than a single value, was derived for each fuel pathway. Appropriate values for the key parameters were determined through literature review and consultation with relevant experts. In general, industry average values, rather than marginal values, were sought. If a marginal value for a key parameter was found that fell outside of typical values and if the marginal value indicates a potential industry trend, then the value was examined as a separate case study. Variation of the key parameter values across the three scenarios could arise from differences in time frame (e.g. historical data versus future projections), different feedstocks (e.g. bituminous coal versus sub-bituminous coal), different technologies or changes in process designs. While the upper and lower bounds of values found in the literature were generally used in the low and high emissions cases, baseline values were usually those which were deemed most likely, most frequently occurring, or were the average or mid-point of the range of values reported in the literature.

Some of the pathways under consideration result in nitrous oxide emissions that represent more than 50% of the total life cycle GHG emissions. This work applied IPCC Tier 1 methodology to

calculate N_2O emissions from each fuel pathway and is therefore subject to the full range of uncertainty associated with IPCC correlations. In many cases, the emission factors developed by the IPCC have uncertainty ranges in excess of 100% (De Klein et al., 2006). The large global warming potential of nitrous oxide (298 using a 100-year time window) further amplifies these uncertainties. While the focus of this work was not to assess the uncertainties within the IPCC methodology, the reader should be aware of their existence and that their impact is of larger consequence for pathways where N_2O is a significant contributor to the total life cycle GHG emissions.

4.3 Tank-to-Wake Combustion Emissions

The combustion of hydrocarbon fuels results in the release of CO_2 and water. The CO_2 from combustion can be quantified with minimal uncertainty (Hileman et al., 2010) and is added to the GHG inventories from well-to-tank life cycle steps. The combustion of jet fuel in aircraft also causes the formation of non-CO_2 products, namely, soot and sulfate aerosols, water vapor, greenhouse gas precursors (NO_x), contrails and contrail cirrus. A complete well-to-wake analysis of emissions must consider the climate impacts of non-CO_2 products of combustion in addition to those of CO_2.

The procedure used for this analysis was to first establish a basis for 'equivalence' between emissions of different species, such that the climate impacts of non-CO_2 combustion effects can be related to those of CO_2. Secondly, the climate impacts module of the Aviation Portfolio Management Tool (APMT) was modified to reflect the different combustion characteristics of SPK fuel (APMT, 2010). Finally, the climate impacts module was used to model the temporal evolution of all forcing agents resulting from SPK fuel and conventional jet fuel burned in the upper atmosphere.

4.3.1 Climate Metrics

Global warming potentials are commonly used to express the relative impact of long-lived gases such as methane, nitrous oxides and CFC's in terms of carbon dioxide[9] (Solomon et al., 2007; Wuebbles et al., 2008; Shine et al., 2005). The time window over which the radiative forcing is integrated is a value judgment rather than a matter of science, although 100 years is most commonly chosen. Clearly stating the chosen time window is essential in all situations. The IPCC provides global warming potentials for time windows of 20 years, 100 years and 500 years. Short time windows emphasize the climate forcing of short-lived effects while long time windows emphasize long-lived climate effects. Consistent time window choices is essential when assessing the climate impacts of non-CO_2 combustion effects, which have atmospheric lifetimes from hours to days, in conjunction with a greenhouse gas inventory that includes methane and nitrous oxide, which sustain in the atmospheric for decades or longer.

Other metrics can be used to relate the climate forcing of one substance to another. Shine et al. (2005) provide a detailed analysis of the Global Temperature Potential (GTP)[10] while Wuebbles et al. (2008) compare the benefits and drawbacks of both physical and economic metrics. Similar to the choice of time window, the consistency of metrics is essential when making comparisons. For example, the use of 100-year global warming potentials to express the methane and nitrous oxide in terms of CO_2 equivalent requires 100-year integrated radiative forcing to be used to assess the non-CO_2 effects.

The assessment of non-CO_2 effects in this thesis is limited to integrated-radiative forcing over 20

[9] The formal definition of GWP for a particular greenhouse gas is the ratio of the time-integrated radiative forcing (RF) from the instantaneous release of 1 kg of that gas relative to that of 1 kg of CO_2.

[10] GTP is the global temperature change as a function of time rather than integrated over a certain time window.

year, 100 year and 500 year time windows. The non-CO_2 ratio from Equation 2 is defined by Equation 3 for a given time window, Δt. The APMT climate impacts module is also capable of using other metrics (Dorbian, 2010) but only integrated radiative forcing was considered in this thesis to maintain consistency with the global warming potentials implemented in assessing life cycle methane and nitrous oxide emissions (Solomon et al., 2007).

$$\text{non-}CO_2 \text{ ratio} = \frac{\int_{t_0}^{t_0+\Delta t} \left[RF_{CO_2}(t) + RF_{NO_x}(t) + RF_{soot}(t) + RF_{sulfates}(t) + RF_{contrails}(t) + RF_{cirrus}(t) + RF_{H_2O}(t)\right] dt}{\int_{t_0}^{t_0+\Delta t} \left[RF_{CO_2}(t)\right] dt} \quad \text{Equation 3}$$

4.3.2 Overview of the APMT Climate Impacts Module

The APMT climate module has been extensively documented and tested in the literature (Marais et al., 2008; Mahashabde, 2009, Dorbian, 2010; APMT, 2010). The model is based on the Bern carbon-cycle impulse response function with a simplified analytical temperature change model to estimate climate impacts for aviation CO_2 and non-CO_2 effects. The modeling approach builds on work by Hasselmann et al. (1997), Sausen et al. (2000), Fuglestvedt et al. (2003) and Shine et al. (2005). The temporal resolution is limited to one year while the spatial resolution is an aggregated global mean level.

Inputs to APMT Climate are a demand scenario for aviation fuel burn and corresponding emissions inventories for CO_2 and NO_x. Radiative forcing estimates for NO_x are obtained by linearly scaling RF estimates from the literature based on NO_x emissions because the short lived nature of the species inhibits a well defined gas-cycle like the carbon cycle (Stevenson et al., 2004; Wild et al., 2001; Hoor et al., 2009). All short-lived effects are scaled linearly with fuel burn levels based on radiative forcing estimates from the literature (Sausen et al., 2005; Hansen et al., 2005; Solomon et al., 2007).

APMT uses Monte Carlo methods to propagate uncertainties in inputs and model parameters to outputs. This requires expressing inputs and parameters as random variables where possible. As described by Mahashabde (2009), in order to extract meaningful insights about the possible costs and benefits of a policy, it is helpful if the analysis options are synthesized into a set of pre-defined combinations of inputs and assumptions. These combinations of inputs and model parameters each describe a particular point of view or perspective on analysis. Each of these combinations is designated as a *lens* as it symbolizes a particular viewpoint through which one can assess environmental and economic impacts. There are currently three lenses implemented in the APMT climate module; namely, low impacts, mid-range impacts and high impacts. Each lens corresponds to the use of different values or distributions for the most influential parameters in the climate module. A description of each lens is provided in the APMT climate module supporting documentation (Mahashabde, 2009; APMT, 2010). The low lens, mid lens and high lens of APMT mirror the low emissions, baseline and high emissions scenarios described in Section 4.2 for assessing well-to-tank GHG emissions.

Parameters captured in the lenses are the projected growth of aviation, background emissions scenario, climate forcing of each non-CO_2 effect, climate sensitivity and a climate damage coefficient. Using only integrated radiative forcing to assess the impacts of non-CO_2 effects eliminates the use of the modules within APMT Climate which translate radiative forcing to changes in global mean temperature change and assign societal costs to these impacts. As such, no further details of these modules are given here.[11]

[11] Mahashabde (2009) and Marais et al. (2008) provide extensive documentation of the development of the APMT climate impact module.

As part of development, APMT Climate was validated against external sources for both long-lived species and NO_x related impacts. Mahashabde (2009) found the time evolution of long-lived species to agree well with those predicted by the IPCC MAGICC model and global warming potentials for NO_x-related impacts to be consistent with those from Stevenson et al. (2004) and Wild et al. (2001) after methodological differences are taken into consideration.

Chapter 5: Conventional Petroleum Baseline

Because this work focuses on fuels that could be used in gas turbine powered aircraft, the baseline for analysis is jet fuel from conventional petroleum. For the purposes of this thesis, jet fuel could represent JP-8, Jet A, or Jet A-1, which are the fuels in use by the U.S. Air Force, commercial aviation in the US, and commercial aviation in Europe as well as much of the rest of the world, respectively. The steps involved in the production of jet fuel from conventional petroleum sources include crude oil extraction, transportation of crude oil to U.S. refineries, refining of crude oil to jet fuel, and the transportation of jet fuel to the aircraft tank. Wong (2008) developed a life cycle GHG inventory for conventional jet fuel; however, those results have since been revised to reflect crude oil extraction, crude oil transportation and jet fuel transportation data from two recently published National Energy Technology Laboratory (NETL) studies on the life cycle GHG emissions of petroleum-based transportation fuels (Skone and Gerdes, 2008; Skone and Gerdes, 2009). Only the GHG inventory of crude oil processing to jet fuel has been retained from Wong (2008). Section 5.1 considers the extraction of conventional crude oil for jet fuel while Section 5.2 summarizes the work of Wong (2008) in refining petroleum to produce jet fuel. The crude oil extraction and transportation data presented in this chapter have also been applied to the ultra low sulfur jet fuel pathway from Wong (2008); updated results for this pathway are given in Chapter 10.

The emissions that result from crude oil refining were calculated by Wong (2008) using both a top-down and a bottoms-up perspective within GREET version 1.8a (GREET, 2007). This analysis of jet fuel from conventional petroleum differs from that of Skone and Gerdes (2008, 2009) in that the jet fuel pathway considers only jet fuel refined within the US and excludes jet fuel made from oil sands. Jet fuel from unconventional sources was treated explicitly in Wong (2008), with those results included in Chapter 10. Jet fuel refined within the US comprised 88.7% of all domestic jet fuel consumption in 2005 (Skone and Gerdes, 2008).

5.1 Crude Oil Recovery and Transportation

The source of crude oil is important in order to properly represent the range of GHG emissions associated with jet fuel production from petroleum. The GHG emissions from crude oil recovery and crude oil transportation are designated origin specific GHG emissions. The variation in these emissions by crude oil source is primarily due to specific hydrocarbon flaring and venting practices during extraction, the emissions resulting from local electricity production, equipment efficiency and the transportation distance of crude oil to a US port.

Imported crude oils are on average heavier (lower API gravity[12]) and contain higher levels of sulfur than domestic products (Skone and Gerdes, 2009). The changes in crude oil properties as well as processing technique drive a variation in processing emissions of converting crude oil into finished fuel products. Of the crude oil mix fed into US refineries in 2005, only 34% was domestically produced. The other 66% was imported from other counties located around the world. When including domestic production, over 90% of the crude oil mix came from only 11 countries (Skone and Gerdes, 2008). The remaining fraction of imported crude is designated 'other' and corresponds to the weighted average of all imported crude (excluding Canadian oil sands).

[12] API gravity is a measure of the density of a petroleum liquid relative to water. An API gravity greater than 10 indicates lighter than water while an API gravity less than 10 indicates heavier than water. *API gravity = 141.5/SG - 131.5, where SG = specific gravity*

In their 2008 life cycle GHG analysis of petroleum based fuels, Skone and Gerdes developed crude oil extraction profiles, including methane flaring and venting data, for each of these 11 countries. They also developed a transportation profile for each country by accounting for the transport of imported crude oil from its point of extraction to foreign ports, ocean tanker transport of waterborne imported crude oil to domestic ports and crude oil transport within the US. Domestic crude oil is only subject to transport within the US and 72% of Canadian crude imports are transported via pipeline and do not incur waterborne transport emissions; all other imports are subject to all three forms of transportation. The interested reader is directed to Skone and Gerdes (2008) for transportation distances and emissions factors for each leg of the transportation process.

Importing crude oil from Saudi Arabia and Kuwait results in substantially more GHG emissions from transportation than crude from other sources. The recovery and total transportation GHG emissions (by species) from 2005 are given for crude oil from each source in Figure 10. Beside the label for each source, the volumetric fraction of total crude fed into US refineries imported from that country is given in parentheses. The volumetric fractions do not add up to 100% because crude from Canadian oil sands are not listed.

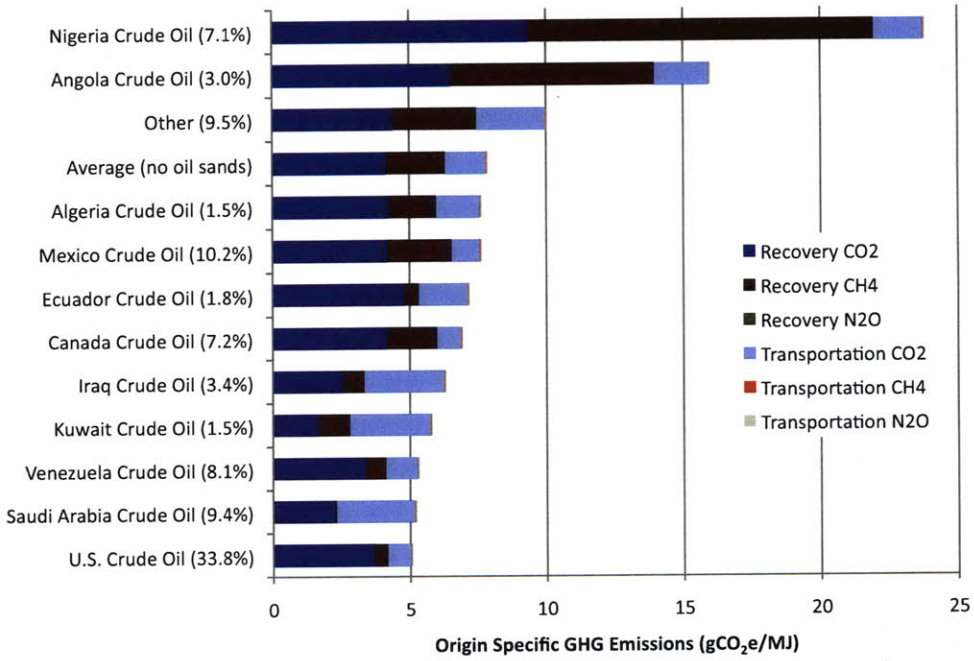

Figure 10: Origin specific GHG emissions by species of crude oil entering US refineries in 2005 (fraction of total imports in parentheses). Based on country profiles published in Skone and Gerdes (2008, 2009)

These data highlight that domestically produced crude oil results in lower GHG emissions than any other source because of reduced transportation emissions. Even though CO_2 emissions resulting from domestic oil extraction are higher than Iraq, Kuwait, Venezuela and Saudi Arabia, the combination of transportation emissions and methane venting causes these regions to have higher origin specific GHG emissions than the US. In the cases of Iraq, Kuwait and Saudi Arabia,

transportation emissions (primarily ocean transport emissions) represent 47%, 51% and 55% of the total origin specific GHG emissions.

The primary driver for countries with excessive origin-specific GHG emissions is methane venting. Methane emissions from Nigerian and Angolan crude extraction exceed all other origin specific GHG emissions. Mexican and Canadian crude also have non-negligible methane emissions from venting.

The variation in profiles shown in Figure 10 was used to establish the low emissions, baseline and high emissions scenarios for jet fuel and ULS jet fuel from conventional crude. The low emissions scenario was composed of purely domestic crude oil, the baseline scenario adopted the weighted average of all crude oil fed into US refineries, excluding Canadian oil sands, and the high emissions scenario used only Nigerian crude. The transportation of jet fuel from US refineries to the aircraft tank are independent of the source of crude oil; hence, a single result was used for all three emissions scenarios.

5.2 Processing of Crude Oil to Conventional Jet Fuel

The conventional jet fuel production pathway forms the baseline against which the life cycle GHG emissions of alternative jet fuels are compared. The GHG inventory of processing crude oil to conventional jet fuel was retained from Wong (2008). The properties of conventional crude oil were based on the projected average crude oil received by U.S. refineries in 2015, obtained using historical data provided by the EIA. There is a definite trend for crudes to become heavier and more sour (more sulfur) in the future; therefore, a business as usual scenario would likely see jet fuel production becoming more energy intensive as more hydroprocessing is required to maintain current product quality. This means that the energy intensity of refining may increase beyond the values used in this study. Some discussion of the impacts of crude oil quality on GHG emission from refining is given Section 5.3 (EIA, 2008a). [13]

The key parameter in analyzing the GHG emissions associated with the production of jet fuel from crude oil is fuel-refining efficiency. Two methods were employed in the derivation of jet fuel refining efficiency. The first method was a top-down approach, which derived the jet fuel refining energy efficiency from the overall U.S. refining energy efficiency. This formed the baseline case. The second method was a bottom-up approach, which estimated jet fuel-refining efficiency by summing the energy requirements for the individual refining processes. Specifically, two extreme cases were examined: straight-run fuel production and hydroprocessing of crude. The refining efficiencies obtained using the bottom-up approach were used for the low and high emissions cases, respectively, providing a bound on the range of possible values. Only the results of Wong's analysis are presented in this thesis. All additional details of the process assumptions and numerical inputs are left to Wong (2008) or Stratton et al. (2010).

5.3 Impact of Crude Oil Quality Compared to Processing Technique

The analysis of Wong (2008) was limited to establishing a range of processing emissions for conventional jet fuel while assuming US average crude oil properties. As shown by Skone and Gerdes (2009), imported crude oils are on average heavier and contain higher levels of sulfur than domestic products. Skone and Gerdes used the API gravity and sulfur content of crude oils fed into US refineries to establish origin-specific processing GHG emissions for diesel fuel in 2005. Based on these data, the origin-specific processing GHG emissions per barrel of crude oil were

[13] From data on sulfur content and API gravity of average crude oil input to U.S. refineries from 1995 to 2006 given by EIA (EIA, 2008a), it was estimated that there was approximately a 2% annual increase in sulfur content and 0.25% annual decrease in API gravity. From these trends, the average crude oil quality received by U.S. refineries in 2015 was estimated.

calculated and subsequently related to origin-specific processing GHG emissions for jet fuel.[14] The upper and lower bounds on the variation from crude oil quality correspond to Mexican crude (API gravity of 23.8 and sulfur content of 3.0%) and Algerian crude (API gravity of 44.8 and sulfur content of 0.1%), respectively (Skone and Gerdes, 2009).

The variation in processing GHG emissions introduced from crude oil quality and processing technique are shown graphically in Figure 11. The variation in processing emissions resulting from processing techniques is 70% larger than the variation from crude oil quality. This analysis emphasizes that there are two factors that impact the processing emissions of making jet fuel. Although they have been considered separately, the impacts of crude oil quality and processing technique on processing emissions are not necessarily independent. Namely, the impact of crude oil quality on straight run fuel production may not be the same as its impact on hydroprocessed jet fuel.

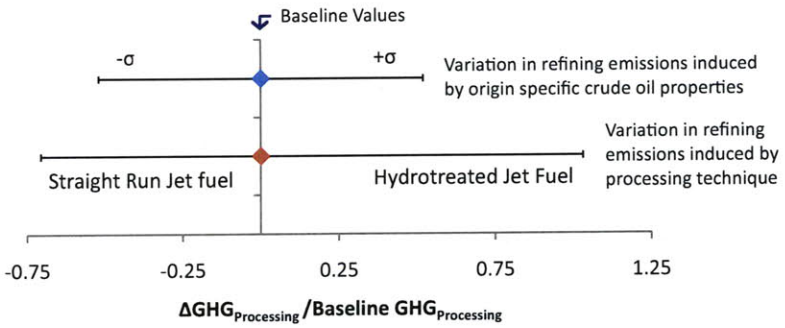

Figure 11: Variation in jet fuel processing emissions induced by origin specific crude oil properties and processing technique

5.4 Conventional Jet Fuel Results

The life cycle GHG emissions from the production of jet fuel from conventional crude are shown in Table 2. These results combine the recovery (crude extraction) and transportation results from Section 5.1 with the jet fuel processing emissions from Section 5.2 to form a complete life cycle GHG inventory. A comparison of the domestic results from this study with the average results presented by Skone and Gerdes (2008) is shown in the far right column of the table. Despite using a different approach to derive the GHG emissions in the processing of feedstock in the baseline case (top-down) from that used in the NETL study (bottom-up approach), similar results were obtained. These results assume average crude oil properties in all three scenarios; hence, they do not include any variation in processing emissions from crude oil quality.

In addition, the combustion CO_2 equivalent emissions used by Skone and Gerdes are slightly higher than those adopted here. This is due to their estimates of CH_4 and N_2O emissions from jet fuel combustion. These emissions were excluded in this thesis due to the high level of uncertainty associated with their estimation. Overall, the life cycle GHG emissions of jet fuel from conventional crude obtained by NETL (88.0 gCO_2e/MJ) are about 0.7% higher than the baseline results (87.5 gCO_2e/MJ) developed in this chapter.

[14] This calculation was based on the assumption that the difference in processing emissions per barrel of diesel between each source and the average is equal to the difference in processing emissions per barrel of jet between each source and the average. Average processing emissions for diesel are 9.0 gCO_2e/MJ while those for jet are 5.65 gCO_2e/MJ.

Table 2: Summary of results for jet fuel from conventional crude and a comparison of results to the NETL petroleum baseline study

	MIT Conventional Jet Fuel			NETL
	Low	**Baseline**	**High**	**Baseline**
Key Assumptions				
Crude oil origin	US	Average	Nigeria	n/a
Processing Technique	Straight Run	Average	Hydro-processed	n/a
Refining efficiency (LHV)	98.0%	93.5%	88.0%	n/a
Life Cycle CO_2 Emissions by Stage				
Recovery of feedstock (gCO_2/MJ)	3.7	4.2	9.4	4.3
Transportation of feedstock (gCO_2/MJ)	0.8	1.5	1.8	1.3
Processing of feedstock to fuel (gCO_2/MJ)	1.6	5.5	11.0	5.5
Transportation of jet fuel (gCO_2/MJ)	0.8	0.8	0.8	0.9
Combustion CO_2 (gCO_2/MJ)	73.2	73.2	73.2	73.7
WTT GHG Emissions by Species				
WTT CO_2 emissions (gCO_2/MJ)	7.0	11.9	22.9	12.0
WTT CH_4 emissions (gCO_2e/MJ)	0.5	2.3	13.0	2.3
WTT N_2O emissions (gCO_2e/MJ)	0.1	0.1	0.1	0.1
Total WTW GHG emissions (gCO_2e/MJ)	80.7	87.5	109.3	88.0
Life Cycle GHG Emissions Relative to Baseline Conventional Jet Fuel	**0.92**	**1.00**	**1.25**	1.01

[Page Intentionally Left Blank]

Chapter 6: Fischer Tropsch Fuel from Coal and Biomass

The Fischer Tropsch (F-T) process first involves the steam reforming or gasification of any carbon containing feedstock (e.g. natural gas, coal or biomass) to synthesis gas (syngas), which is a mixture of hydrogen and carbon monoxide. The syngas is subsequently converted to paraffinic hydrocarbons in the presence of an iron- or cobalt-based catalyst (Fischer-Tropsch synthesis). A third upgrading step cracks the longer hydrocarbon chains to maximize the production of synthetic paraffinic liquid fuels like diesel and jet fuel. Syngas must be cleaned before Fischer-Tropsch synthesis step to remove contaminants, particularly sulfur, to avoid poisoning the catalyst. Hence, the resultant Fischer-Tropsch liquid fuels are virtually free of contaminants and the jet fuel fraction of the product slate falls into the category of synthetic paraffinic fuels.

All jet fuels produced using F-T synthesis have similar characteristics, independent of feedstock type. Any small variations in fuel properties are primarily associated with the operating conditions (e.g., catalyst, temperature, and pressure) within the synthesis reactors and how the direct products of the synthesis are treated and processed. All jet fuels produced using the F-T process share common characteristics with regard to compatibility with existing infrastructure and aircraft, combustion emissions, and their relative merit for use in aviation. Feedstock choice, however, does have a strong influence on fuel production capacity, production cost, life cycle greenhouse gas emissions, and technology readiness (Hileman et al., 2009).

Fischer-Tropsch fuels created from natural gas, coal or biomass were analyzed in Wong (2008) while the combination of coal and biomass was analyzed in this thesis. Existing coal-to-liquids (CTL) capacity is limited to Sasol in South Africa where a production capacity of 160,000 bbl/day of oil equivalent has been consistently maintained. There is no commercial scale production of F-T fuels using biomass as the feedstock (BTL). This technology is still in the development phase; however, a German firm, CHOREN, began start-up operations of a 300 bbl/day facility in 2008 and Solena Group, with Rentech, announced plans for a 1,800 bbl/day BTL facility located in Gilroy, California. Experience with simultaneously gasifying a combination of coal and biomass in a single gasifier is presently limited to successful tests at an IGCC plant in the Netherlands (Hileman et al., 2009). The analysis of F-T jet fuel from the combination of coal and biomass was analyzed using GREET version 1.8b.

6.1 Analysis Overview

While both CTL and BTL hold promise as alternative jet fuels, they are each flawed. Even with 85% carbon capture, a CTL plant has life cycle GHG emissions over 110% of conventional jet fuel (i.e., the life cycle GHG emissions are 10% higher than conventional jet fuel); without carbon capture, CTL has 220% of the emissions of conventional jet fuel. If the goal is to reduce GHG emissions, then coal alone appears to be a poor choice. BTL plants without carbon capture have life cycle GHG emissions that are less than 20% of conventional jet fuel; however, considerable logistical challenges exist in obtaining sufficient biomass to operate at large scales because of the relatively low energy density of biomass (Stratton et al., 2010). Because current F-T plant designs are capital intensive, it is not economically feasible to build many small plants that are dispersed among the regions where biomass is being grown. Biomass must therefore be accumulated from considerable areas and transported to large central plants; hence, the infrastructure to move the biomass becomes a limiting factor. Emissions from the transportation of the biomass to the processing facility are included in the life cycle analysis, but represent a small fraction of the total emissions. In considering a coal and biomass to liquid (CBTL) plant,

the biomass offsets the high emissions from coal and coal offsets the low energy density and production limitations of biomass.

This analysis considered a stand-alone F-T liquid fuels plant designed to maximize liquid fuels production (e.g. through recycling of tail gas from F-T reactors). Sufficient electrical energy was produced to fuel all internal processes, with negligible excess electricity produced for export. The process included the upgrading (hydroprocessing) of long-chain liquids to a final product slate of diesel (C_9-C_{23}), jet fuel (C_8-C_{16}) and naphtha (C_4-C_6). The energy allocation method was adopted for assigning energy and emissions to various liquid products. Default GREET assumptions were adopted regarding the transportation profiles of F-T fuels.

The F-T process efficiency is a key parameter affecting the life cycle GHG emissions of the production of F-T jet fuel from natural gas. Equation 4 defines process efficiency for a general F-T facility.

$$\text{Process Efficiency} = \frac{1\ \text{MJ}_{\text{fuel}}}{1\ \text{MJ}_{\text{feedstock}} + \text{Process Energy}} \qquad \text{Equation 4}$$

Most studies in the literature focus on F-T reactor designs and conditions that produce diesel and naphtha. To produce jet fuel instead of diesel, additional hydrocracking and greater syngas recycle are needed, resulting in a small increase in hydrogen and power requirements for the plant. Furthermore, a moderate decrease in the CO_2 associated to jet fuel compared to diesel would ensue due to changes in the allocation fractions. As these additional energy requirements do not lead to substantial increases in CO_2 emissions from the facility (Gray et al., 2007), they were ignored in this analysis, (i.e. the production of F-T jet fuel is assumed to have the same emissions as the production of F-T diesel). Although F-T jet fuel can be made without added burdens, it is not possible to have a product slate of 100% F-T jet fuel (a value of 25% is taken as the preferred value, and a sensitivity study is used to assess the importance of this assumption). An F-T plant configured to produce 70% diesel and 30% naphtha should theoretically be able to undergo modifications such that it could yield 60% jet fuel and 40% naphtha (Gray et al., 2007). Sasol is developing the ability to produce a joint Battlefield-Use Fuel of the Future (BUFF) using F-T synthesis. This fuel could be used in place of JP-8 in military aircraft and they report a yield of ~30% that conforms to the freezing point standards of JP-8. The rest of the product slate is composed of "heavy" diesel and naphtha (Lamprecht, 2007).

6.2 Feedstock Profiles

The type of coal used, specifically the energy content and carbon fraction of the coal, have an appreciable impact on the life cycle GHG emissions of Fischer-Tropsch based pathways using coal as a feedstock (Wong, 2008). Sub-bituminous coal, bituminous coal and combinations thereof were used in defining the low, baseline and high emissions scenarios to capture the variability introduced by differing coal properties.[15] Details of coal used as feedstock to the F-T process are given in Section 6.2.1.

The biomass feedstocks examined include waste biomass (e.g. forest residue, agricultural residue) and non-food energy crops (e.g. herbaceous biomass) that were assumed to be grown on land that would not incur adverse direct or indirect land use change emissions (e.g. idle or abandoned cropland). Specifically, three types of biomass feedstocks were considered: switchgrass, corn

[15] Lignite coal can possibly be used as a feedstock to CBTL plants but lignite production in the US is much lower (~7% of total coal production in 2007, EIA 2008c) compared to bituminous and sub-bituminous coal production (46.7% and 46.3% of total coal production in 2007, respectively, EIA 2008c). Reliable data on methane emissions associated with the mining of lignite coal are not available. For these reasons, lignite coal is not analyzed in this work.

stover and forest residue. Switchgrass was considered as the primary biomass feedstock in all cases of the scenario analysis (low emissions, baseline and high emissions) because of its better yield and improved scalability relative to waste products. Furthermore, if waste products were used on a large scale then they would become a market commodity, as they are no longer waste. Such a change in classification leads to questions as to where system boundaries should be drawn with respect to the crop that initially produced the waste. Such issues were outside the scope of this work. Details of biomass used as feedstock to the F-T process are given in Section 6.2.2.

6.2.1 Coal

In 2007, almost 65% of bituminous coal production in the U.S. occurred via underground mining while the remainder was surface-mined. On the other hand, sub-bituminous coals are almost exclusively surface-mined. (EIA, 2008b) Underground mining results in substantially greater methane emissions compared to surface mining processes. Methane emissions arising from the production of underground-mined and surface-mined coals were estimated using aggregate coal mining methane emissions data (EIA, 2007; Bartis et al., 2008).[16] Default GREET assumptions were adopted regarding energy use for coal mining and cleaning.

The use of surface-mined sub-bituminous coal was assumed in the low emissions case; average US coal from 2007 (mix of underground-mined and surface-mined bituminous coal and surface-mined sub-bituminous coal[17]; anthracite or lignite coal is not considered) was assumed in the baseline case and underground-mined bituminous coal (from case 1 of Southern States Energy Board CTL study, SSEB, 2006) was assumed in the high case. The coal properties most important to this analysis are summarized in Table 3.

Table 3: Coal properties adopted for the analysis of coal and biomass to F-T jet fuel

	Low	**Baseline**	**High**
Coal Type	Surface-mined sub-bituminous	Average US mix	Underground-mined bituminous
Energy Content (MJ/kg)	18.4	22.5	26.4
Carbon Content	49.2%	57.2%	64.8%
Coal Mining Methane Emissions (gCO_2e/MJ_{Coal})	0.8	2.8	6.4

6.2.2 Switchgrass

Switchgrass is a perennial warm season grass native to North America, found in remnant prairies, native grass pastures, and naturalized along roadsides. Other forms of herbaceous biomass include mixed prairie grasses, wheat, hay and leaves, among others. As a replacement for annual crops, warm season grasses have also been shown to provide important habitat for wildlife, including game birds and other species threatened by the loss of tall grass prairie habitat (McLaughlin et al., 2002). The assumptions regarding the yield, energy and emissions associated with switchgrass cultivation were based on a survey of existing cultivation data from the literature. Also considered is the potential for long term changes in carbon contained within the soil on which the switchgrass is grown. The greatest potential for long-term soil carbon sequestration is in those situations where agricultural practices have led to a progressive and

[16] Bartis et al., 2008 estimated methane emissions of 338 pounds of carbon dioxide equivalent per ton of underground-mined coal and methane emissions of 42.4 pounds of carbon dioxide equivalent per ton of surface-mined coal based on EIA data (EIA, 2008b). The methane emissions per MJ of coal production were calculated from the lower heating values of bituminous coal and sub-bituminous coal.

[17] Compared to 2007, the coal production mix in 2017 is projected to comprise a larger proportion of surface-mined sub-bituminous coal from Western coal production, particularly the Powder River Basin. (EIA, 2008d)

historical decline in soil carbon stocks (McLaughlin el al., 2002). The properties (e.g. lower heating value, carbon content) of switchgrass used in this work are reported in Table 53.

6.2.2.1 Switchgrass Yield And Cultivation Trends

The approach used in this work is similar to that taken by the National Academies in their 2009 report on Liquid Fuels from Coal and Biomass. Figure 12 shows a distribution of annual switchgrass yields taken from Gunderson et al. (2008) that were used to establish predictive maps of potential yields across the continental United States. The data set comprises approximately 1400 observations with a mean of approximately 4.9 tons/acre/yr. For each data point, the specific cultivar, crop management information, ecotype, precipitation and temperature in the long-term climate record were documented. Using their model, Gunderson et al. (2008) predicted yields in excess of 8.9 tons/acre/yr for lowland ecotypes[18] in the Appalachian region and 5.4-6.2 tons/acre/yr in the Nebraska/South Dakota region. Similarly, yields for upland ecotypes in the Appalachian region were predicted to be greater than 6.2 tons/acre/yr and 3.1-4.5 tons/acre/yr in the Nebraska/South Dakota region. Gunderson et al. (2008) openly discuss that their model predicts the theoretical maximum yield for a given set of input conditions; hence, experimental yields for these regions will most likely be lower in practice.

Other studies have focused on establishing estimates for a national average yield. Heaton et al. (2004) found an average switchgrass yield of 4.6 tons/acre/yr (+/- 0.3 tons/acre/yr) and McLaughlin et al. (2002) projected a national average annual yield of 4.2 tons/acre/yr. Vadas et al. (2008) adopted a nominal yield of 4.0 tons/acre/yr and an optimistic yield of 5.8 tons/acre/yr based on data from large field plots in southern Wisconsin while Adler et al. (2007) simulated switchgrass production in Pennsylvania as 4.3 tons/acre/yr using DAYCENT.[19] Finally, the GREET herbaceous biomass production pathway assumes a yield of 6.0 tons/acre/yr.

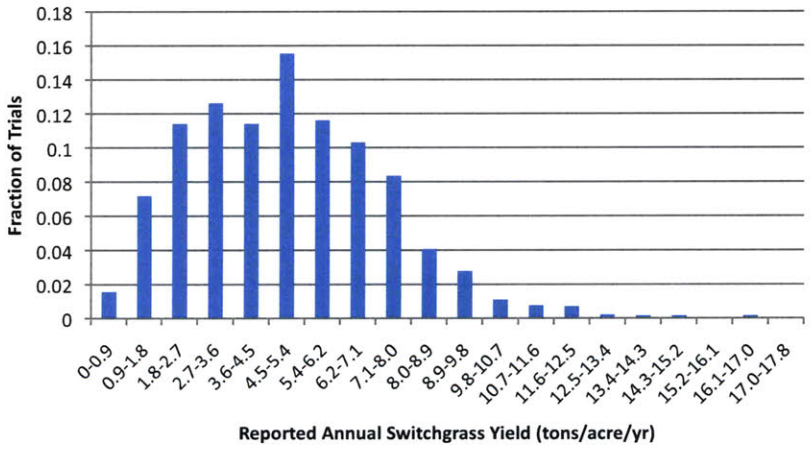

Figure 12: Distribution of reported switchgrass yields across the United States (data from Gunderson et al., 2008)

[18] Lowland and upland ecotypes are defined by position relative to the level where water flows or where flooding occurs

[19] DAYCENT is the daily time-step version of the CENTURY biogeochemical model. From weather (daily maximum and minimum air temperature, precipitation), soil-texture class, and land-use inputs, DAYCENT simulates fluxes of carbon (C) and nitrogen (N) between the atmosphere, vegetation, and soil while predicting crop production, soil organic-matter changes, and trace-gas fluxes.

While numerous studies have estimated the potential yield of switchgrass, many of these results are based on small plots (less than $5m^2$) and the results are not necessarily indicative of what can be expected of farm-scale production (National Academies, 2009). Schmer et al. (2008) managed switchgrass as a biomass energy crop in field trials of 7.4 to 22.2 acres on marginal cropland from 10 farms across a wide precipitation and temperature gradient in the mid-continental US. The actual farm-scale production resulted in harvested yields about 35 to 50 percent lower than those of small-scale plots. It is possible that the lower yields from large-scale production can be attributed to farmers' inexperience with the cropping system or differences in cropland quality; however, farmers worked closely with the researchers in collecting this data and the land had been in active crop production before being converted to switchgrass production (National Academies, 2009). Actual yield data from Schmer et al. (2008) ranged from 2.3 to 5.0 tons/acre/yr with a mean of 3.2 tons/acre/yr.

In their analysis, Gunderson et al. (2008) concluded that switchgrass yield is most influenced by ecotype (upland or lowland) and the relationship of precipitation and temperature. Lower yields were attributed to factors that were not quantified across the data set, such as soil pH, inherent soil fertility, total solar radiation (vs. long periods of cloud cover) and others that are artifacts of each individual growing site and cannot be aggregated for a generalized result. The specific rate of nitrogen application was found not to have a significant influence on yield. Very high levels of fertilization certainly did not guarantee increased biomass production, and in many cases, cases the zero fertilizer plantings did as well as any fertilized stands. Based on these conclusions, the yields adopted for the low emissions, baseline and high emissions scenarios (as shown in Table 4) were assumed to be independent input parameters from other cultivation inputs (on a per ton basis).

Table 4: Switchgrass yields assumed in the low, baseline and high emissions scenarios

	Low[1]	**Baseline**[2]	**High**[3]
Yield (tons/acre/yr)	5.8	4.6	3.2
Notes: 1) Optimistic yield from Vadas et al. (2008) based on large field plots in southern Wisconsin 2) Projected national average from McLaughlin et al. (2002) 3) Average farm-scale yield from Schmer et al. (2008) based on mid-continental US			

6.2.2.2 Cultivation and Transportation of Switchgrass

The key inputs for switchgrass production are the process fuels and electricity used in farming, fertilizer inputs and herbicide usage. These parameters have been identified in several studies but are the subject of much uncertainty. Although it was determined that these inputs do not have a substantial impact on yield, they are essential for estimating the GHG emissions associated with switchgrass production. A summary of the available data is given in Table 5.

These data show considerable variation in the application rates of non-nitrogen fertilizers and herbicides. The phosphorous and potassium application rates quoted by Vadas et al. (2008) are an order of magnitude larger than those given by Adler, which are in turn an order of magnitude larger than the GREET default values.

Using the same arguments, which were previously made in considering yield as an independent parameter, the process fuel usage, nitrogen fertilizer application and other fertilizer and herbicide application were decoupled from their respective data sets. Hence, they were also considered as independent parameters for the purposes of the scenario analysis. The input parameters used for

the low emissions, baseline and high emissions scenario are outlined in Table 6. The GREET default parameters were not used at all in this work because they are a decade older than the other results and they are not consistent with the 2015 timeframe of this study.

Default GREET transportation and distribution assumptions were adopted for switchgrass. Specifically that bailed switchgrass is transported 40 miles by truck from the field to an F-T processing facility in loads of 24 tons.

Table 5: Reported cultivation inputs for switchgrass

	Adler et al. (2007)[1]	**Vadas et al. (2008)**[2]	**Schmer et al. (2008)**[3]	**GREET (2008)**[4]
Process Fuels (Btu/ton)				
Diesel	82874	113046	107533	201589
Gasoline	0	22609	0	0
Electricity	0	7536	0	15641
Crop Management (g/ton)				
Nitrogen	5218	11348	7701	10635
P_2O_5	1236	10387	0	142
K_2O	2488	24607	0	226
Limestone	9491	0	0	0
Herbicides	6.4	0	185	28

Notes:
1) Actual fertilizer application rates were only given for nitrogen. All others were given in terms of CO_2e with application rates calculated using production emissions from GREET 1.8b.
2) Actual phosphorous and potassium usage was given in terms of elemental weight and converted to P_2O_5 and K_2O using molar mass fractions. Lube oil consumed is expressed in terms of diesel equivalent on an energy basis.
3) Data is the average of 10 field scale plots in Nebraska, North Dakota and South Dakota.
4) From Oak Ridge National Laboratory in 1998.

Table 6: Cultivation inputs for switchgrass in the low, baseline and high emissions scenarios

	Low	**Baseline**	**High**
Process Fuels (Btu/ton)			
Diesel	82874	107533	113046
Gasoline	0	0	22609
Electricity	0	0	7536
Nitrogen Fertilizer (g/ton)	5218	7701	11348
Other Fertilizers (g/ton)			
P_2O_5	0	1236	10387
K_2O	0	2488	24607
Limestone	0	9491	0
Herbicides	185	6.4	0

6.2.2.3 Nitrous Oxide Emissions

Nitrous oxide emissions can either be estimated using specialty software or through simple IPCC emissions factors. Estimates from Adler et al. (2007) using DAYCENT included both direct emissions of N_2O through nitrification and denitrification processes in the soil and indirect emissions of N_2O through soil nitrogen losses in forms other than N_2O (e.g. NO_X, NH_3, NO_3), which were subsequently converted to N_2O elsewhere. Conversely, the GREET method employs

the IPCC 2006 conversion factor for direct and indirect N_2O emissions from switchgrass production, as shown in using Equation 5.

$$N_2O\ \text{Emissions}\left(\frac{g_{N_2O}}{\text{ton}}\right) = \left(\frac{g_{\text{nitrogen fertilizer}}}{\text{ton}}\right) \cdot 0.01325 \cdot \left(\frac{44 g_{N_2O}}{28 g_N}\right) \qquad \text{Equation 5}$$

The N_2O emissions from Adler et al. (2007) were found to be 43% higher than those predicted by Equation 5 from the same application rate. The principle reason for this discrepancy is that annual nitrogen in crop residues (above-ground and below-ground) was not included. Estimates of the nitrogen deposited on the soil in the form of crop residues was obtained using the IPCC Tier 1 methodology for perennial grasses (De Klein et al., 2006) and implemented through Equation 6.

$$N_2O\ \text{Emissions}\left(\frac{g_{N_2O}}{\text{ton}}\right) = \left(\left(\frac{g_{\text{nitrogen fertilizer}}}{\text{ton}} + 6025\right) \cdot 0.01_{\text{direct}} + \left(\frac{g_{\text{nitrogen fertilizer}}}{\text{ton}}\right) \cdot 0.001_{\text{indirect}}\right) \cdot \left(\frac{44 g_{N_2O}}{28 g_N}\right) \qquad \text{Equation 6}$$

where 6025 is the nitrogen in crop residues, 0.01_{direct} is the emissions factor for N_2O from nitrogen and 0.001_{indirect} is the emissions factor for volatilized NH_3 and NO_x from synthetic nitrogen converted to N_2O. The N_2O emissions as calculated using the new IPCC methodology are within 2% of those estimated by Adler et al. (2007) for the same nitrogen application rate. As such, Equation 6 was used for all N_2O calculations within the switchgrass production pathway.

6.2.2.4 Long Term Soil Carbon Sequestration from Switchgrass

Soil carbon sequestration is a potential strategy for offsetting CO_2 emissions to the atmosphere. The capacity of perennial energy crops to offset CO_2 emissions through soil carbon sequestration depends on the rate of soil carbon additions, the long-term capacity of soil for carbon storage, and the stability of sequestered soil carbon over time. The greatest potential for long-term soil carbon sequestration is in those situations where agricultural practices have led to a progressive and historical decline in soil carbon stocks (McLaughlin el al., 2002). Two land use change scenarios were considered for switchgrass production. The first is switchgrass grown on Conservation Reserve Program (CRP) land and second is switchgrass grown on carbon-depleted soils. The carbon contained within soil can become depleted over time as a result of farming traditional row crops with conventional tilling practices. The CRP compensates farmers for removing lands from crop production for environmental and economic reasons (National Academies, 2009). After stopping crop production, the land naturally re-establishes its carbon content due to the growth of native perennial grasses; hence, switchgrass grown on CRP land was assumed to cause no net change of carbon in the soil. The change in soil carbon resulting from switchgrass grown on carbon-depleted soils was based on results from McLaughlin et al. (2002) and Adler et al. (2007).

McLaughlin et al. (2002) developed an empirically derived soil carbon dynamics model that estimates soil carbon accumulation rates for contrasting soil types and climates. After accounting for regional soil carbon gains by prior cropping history and climatic region, they found the average soil carbon sequestration level of traditional cropland converted to switchgrass production to be 0.21 Mg of C/acre/yr over a 30-year period. These sequestration rates are based on annual rates of aboveground production over a 6-year period, ranging from 5.3 to 7.9 tons/acre/yr. The variation between individual sites in the fist decade ranged from a minimum of -0.2 Mg of C/acre/yr for southeastern pastures to a maximum of 0.57 Mg of C/acre/yr for south-central croplands (McLaughlin et al., 2002). Therefore, increased soil carbon from switchgrass cultivation is not guaranteed and in some cases a carbon release could occur.

Adler et al. (2007) also estimated the net change in soil carbon associated with the cultivation of switchgrass. As was the case with McLaughlin et al. (2002), the land use change estimates made

by Adler et al. (2007) were sensitive to initial soil carbon levels, which are influenced by previous vegetation cover and land management. To acquire realistic modern soil carbon levels, 1800 years of native vegetation followed by tree clearing, plowing, and 200 years of cropping were simulated. The consequence of this effort is that the initial conditions included legacy effects of 215 years of conventional tillage cropping. The result of 15-year switchgrass cycle in DAYCENT was an average carbon sequestration of approximately 0.17 Mg of C/acre/yr (Adler et al., 2007).

Changes in soil carbon arising from changes in land use can constitute a major component of the life cycle GHG emissions; however, their quantification involves high levels of uncertainty. Therefore, a single value was chosen to illustrate the potential impact of land use change emissions on this pathway. Specifically, the estimate of 0.17 Mg of C/acre/year presented by Adler et al. (2007) was adopted as it represents a conservative value with respect the work of McLaughlin et al. (2008).

6.2.3 Corn Stover and Forest Residue

Input assumptions on the energy and emissions associated with the recovery and transportation of corn stover and forest residues were based on default GREET assumptions (GREET, 2008). Default GREET assumptions were also adopted for the energy and carbon content of corn stover and forest residues[20] (see Table 53). While forest residues require no fertilizer and their removal is assumed to have negligible impact on the surrounding environment, corn stover is usually left on the field to replenish soil nutrients and mitigate erosion; however, there is little consensus regarding the quantification of the impacts on productivity, soil structure, and nutrient cycling of removing stover from the field. In addition to maintaining soil carbon levels, stover is a source of nitrogen; hence, synthetic fertilizer would be needed to supply the incremental amount of nutrients needed for corn cultivation when stover is removed (GREET, 2007).

The yield attainable for corn stover is directly proportional to the fraction of stover that must be left on the field to mitigate these aforementioned negative impacts. The quantity of available stover can then be calculated as the difference between the total stover yield and quantity left on the field. The National Academies reported an average yield of corn stover across the United States in 2007 of 151 bu/acre/yr[21], or 4.24 tons/acre/yr. This yield is based on the assumption of a 1:1 ratio of dry weight of corn grain to stover (National Academies, 2009). Results from Wilhelm et al. (2007) have shown that the stover needed to maintain soil carbon, and thus productivity, is a greater constraint to an environmentally sustainable harvest than that needed to control water and wind erosion. They predicted that 3.4 tons/acre/yr are required to mitigate erosion and soil carbon loss with moldboard plowing while only 2.3 tons/acre/yr are required if no-till practices were employed. Sheehan et al. (2004) considered the USDA's regional tolerable soil-loss limits as the constraint for leaving stover on the field. They found that 2.2 tons/acre/yr are required with conventional tillage while only 1.1 tons/acre/yr are required if no-till practices are employed.

The corn stover yield adopted in this work was based on the total yield from the National Academies (2009) and the constraints for soil carbon and erosion under no-till practices from Wilhelm et al. (2007). These resulted in a yield of 1.65 dry tons/acre/yr (equivalent to 1.94 tons/acre/yr at 15% moisture). The key input assumptions for the recovery and transportation of corn stover and forest residues are shown in Table 7 and Table 8, respectively.

[20] A significant variation of forest residue properties can be found in the literature, due to different assumptions of the type of biomass (e.g. hard wood vs. soft wood), which constitute the forest residues.
[21] A bushel of corn or corn stover is defined as 56 lbs at 15.5% moisture content by mass.

Table 7: Input parameters for the recovery and transportation of corn stover

Input parameter[1]	Value
Yield	1.65 dry ton/acre
Collection Energy	254,190 Btu/dry ton (100% diesel fuel use)
Fertilizer Use Nitrogen Phosphorus Potassium	 4.50 kg/dry ton 1.63 kg/dry ton 8.35 kg/dry ton
N_2O emissions[2]	13.3 g/dry ton
Transportation distance	30 miles
Truck payload	24 ton
Notes: 1) All input parameters were based on GREET 1.8b (GREET, 2008) simulation year of 2015. 2) Includes N_2O emissions from nitrification and denitrification in the soil, as well as N_2O credit from corn stover removal based on GREET defaults.[22]	

Table 8: Input parameters for the collection and transportation of forest residue.

Input parameter[1]	Value
Diesel fuel consumption	3.4 gal/dry ton
Collection energy	459,200 Btu/dry ton
Transportation distance	75 miles
Truck payload	17 ton
Note: 1) These input parameters were based on GREET 1.8b (GREET, 2008)	

Although the corn stover yields adopted in this work were chosen to prevent a reduction of the natural carbon stock of the soil, an examination of the magnitude of potential land use change emissions from improperly harvested corn stover is still relevant. The analysis from Sheehan et al. (2004) imposed no constraint on maintaining soil carbon levels and the evolution of carbon stored in the soil was a central part of their results. Under maximum stover removal conditions subject to maintaining USDA's tolerable soil constraints, an average emissions rate of 13 kg of C/acre/yr was calculated over the first 30 years. The emissions profile over that time period is strongly positive for the first 10 years but becomes negative after year 20 as the soil begins to approach a new equilibrium state.

6.3 Carbon Capture and Sequestration with Fischer-Tropsch Facilities

By comparison to conventional power plants, F-T plants are well suited for the implementation of carbon capture and sequestration (CCS). This opportunity occurs because the F-T process results in a relatively pure stream of CO_2 upstream of the F-T synthesis step, whereas coal power plants produce flue gas, which must be scrubbed to obtain a pure CO_2 stream.

The use of CCS was assumed for coal and biomass-to-liquids plants; however, a configuration without CCS was examined as a case study. Carbon dioxide is already captured within F-T plants as part of the process; therefore, the only difference for standard CCS implementation is the addition of CO_2 compression, transport and storage capital and operating costs (Tarka, 2009). It

[22] Incremental fertilizer use (including nitrogen fertilizer) is accounted for to make up for the loss in soil nutrients from the removal of corn stover from the field. On the other hand, if left on the field, a fraction of the nitrogen in corn stover will be converted to N_2O and emitted from the soil. This N_2O emission is avoided when corn stover is removed from the field. In this case, the N_2O credit from the removal of corn stover slightly outweighs the N_2O emissions resulting from the incremental application of nitrogen fertilizers, resulting in net negative N_2O emissions.

was assumed that the energy needed for CO_2 compression was provided by electricity internally generated within the F-T process. This results in a reduction of the overall process efficiency because some of the energy from the feedstock is used to generate this additional energy. The electrical energy needed to compress the captured carbon dioxide to a pipeline ready pressure of about 15 MPa was assumed to be 250 kWh/ton carbon[23] (GREET, 2008; Kreutz et al., 2008). The transportation of compressed carbon dioxide and the energy required for sequestration in a storage site were not considered.

The amount of carbon available for capture is equal to the difference between the carbon present in the feedstock and the carbon present in the final products. The term carbon capture efficiency is used to define the percentage of available carbon that is actually captured. Capture efficiencies of 80% (Kreutz et al., 2008), 85% (SSEB, 2006) and 90% (Bartis et al., 2008; Deutch and Moniz, 2007; Tarka, 2009) were assumed for the high emissions, baseline and low emissions cases, respectively. Recent analyses at National Energy and Technology Laboratory (NETL) have indicated that capital expenditures associated with systems designed to capture CO_2 at the 80% level would not vary significantly from those capturing at the 90% level (Dilmore and Skone, 2009). A capture efficiency of 85% was chosen for the baseline case in this work to reflect the lack of commercial experience surrounding widespread implementation of CCS. Carbon emitted from the combustion of process fuels is not captured.

6.4 CBTL Processing Configuration

Both biomass and coal could be used as feedstock to a single F-T plant because they are processed into an F-T fuel using similar technology. The coal and biomass can be gasified either in parallel with the syngas streams being mixed afterwards, or in the same unit (co-gasification). Since the parallel configuration is a superposition of CTL and BTL results from Wong (2008), co-gasification is the primary focus. Parallel processing also requires additional infrastructure, as separate gasifiers are needed for each feedstock. Co-gasification was assumed to occur in an entrained flow gasifier. Such technology is already commercially available for large scale processing of coal and biomass (van der Drift et al., 2004). Before entering the gasifier, biomass must be milled down to particles of diameter 1mm or less. Currently, the most energy efficient method of milling the biomass is via torrefaction pre-treatment, which is a mild thermal treatment where the biomass is heated to ~250°C yielding a solid uniform product with lower moisture content and higher energy content. Studies have shown that torrified wood can be milled to the required size using only 10-20 $kW_{electricity}/MW_{biomass}$ and that capacity expansion factors between 2 and 6.5 can be achieved (van der Drift et al., 2004; Bergman et al., 2005). Moreover, torrified particles can be pneumatically transportable, which is considered impossible for a bed of untreated biomass particles. Efficiencies for torrefaction range from 85% to 97%, with 90% assumed in the baseline case (Bergman et al., 2005).

Because of the pre-processing of biomass, the overall F-T plant efficiency depends on the weight percent of biomass that is being co-gasified. This study explored a range from 10% to 40% biomass feed with 40%, 25% and 10% chosen for the low, baseline and high emissions cases, respectively. CTL plant efficiencies were modified to account for the extra power consumption of pre-processing the biomass; hence, the reduction of the CTL plant efficiency, η_{CTL}, depends on both the fraction of biomass feed and the torrefaction efficiency. The plant is assumed to be self sufficient in terms of electricity production with no extra power exported to the grid. The implementation for CCS comes at the cost of 250kWh per ton of carbon captured, as discussed in

[23] Kreutz et al. assume 90.5 kWh per tonne of CO_2, which converts to 300 kWh per ton of carbon. GREET default value in 2010 is 300 kWh per ton of carbon but an improved efficiency of 250 kWh per ton of carbon is assumed for 2015.

Section 6.3. This energy requirement is also accounted for in the CBTL process efficiency. Overall, the CBTL plant efficiency was examined as a function of CTL efficiency, biomass weight percentage, torrefaction efficiency, biomass grinding energy and CCS efficiency, as expressed in Equation 7.

$$\eta_{CBTL} = f\left(\eta_{CTL}, \text{biomass wt\%}, \eta_{torrefaction}, \text{biomass grinding energy}, \eta_{CCS}\right) \quad \text{Equation 7}$$

Input assumptions for the combined coal and biomass pathway are summarized in Table 9.

Table 9: Input assumptions for the production of F-T jet fuel from coal and biomass (with carbon capture) for low emissions, baseline and high emissions cases

	Low	**Baseline**	**High**
CTL Process Efficiency (LHV)	53%	50%	47%
Biomass Weight Fraction	40%	25%	10%
Carbon Capture Efficiency	90%	85%	80%
Carbon Compression Energy	250 kWh/ton C	250 kWh/ton C	250 kWh/ton C
Torrefaction Efficiency	97%	90%	85%
Coal Input Type	Surface-mined sub-bituminous	Average US mix	Underground-mined bituminous
Biomass Input Type	Switchgrass	Switchgrass	Switchgrass

6.5 Allocation Methodology

As previously stated, an F-T facility can produce a wide product slate. For example, the study carried out by NETL on F-T diesel from CBTL assumed an output of 70% diesel and 30% naphtha (Tarka, 2009). In this analysis, F-T jet fuel is the product of interest but does not consist of more than roughly a third of the total plant output to prevent excessive naphtha production. Since other F-T fuels are made as a result of producing F-T jet fuel, the emissions from processing and all other upstream activities must be allocated among the fuels being produced. Even when configured to make jet fuel, diesel fuel will likely be the primary output of the F-T facility due to economic drivers. For this reason, it is sensible to allocate emissions among the liquid products (i.e., jet fuel, diesel fuel, and naphtha) on the basis of their respective energy content.

Figure 13 demonstrates problems that could result from using the displacement method to assign emissions 'credits' to a fuel that is not the primary product. When the yield of jet fuel is 25% by volume, there are 3 liters of other F-T fuels produced for every 1 liter of jet fuel. When the yield of jet fuel is reduced to 5% by volume, there are 19 liters of other F-T fuels produced for every 1 liter of jet fuel. In the limit where the yield of jet fuel approaches zero, the quantity of other F-T fuels, relative to jet fuel, asymptotically approaches infinity. If the other F-T fuels represent a reduction in emissions as compared to their petroleum equivalents then the displacement method attributes these emissions reductions to the jet fuel; therefore, the displacement methodology results in a jet fuel which appears to have life cycle emissions that approach negative infinity as the yield of jet fuel is reduced towards zero. The results from Figure 13 show that an energy allocation scheme prevents a product that is responsible for a third, or less, of total output from the facility receiving the emissions 'credit' from the entire product slate.

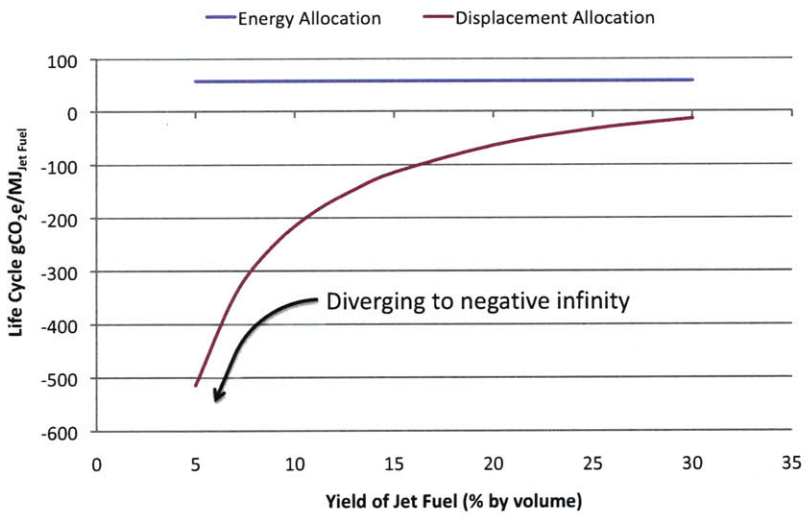

Figure 13: The effects of product slate composition on life cycle greenhouse gas emissions from F-T jet fuel

The diverging effect resulting from use of the displacement method is unavoidable because jet fuel is not the primary product from the F-T plant. This highlights the important conclusion that life cycle GHG emissions from a given fuel are as much a function of subjective choices of the analyst/operator regarding allocation methodologies, as they are of specific production characteristics and process inputs. In order to maintain consistent results, which cannot be skewed by choices such as the distribution of products leaving the F-T facility, energy allocation was chosen. This method comes with the caveat that all fuels produced in addition to jet fuel, such as diesel and naphtha, can also carry environmental benefits that are only captured when the entire system is considered as a whole. The specific product slate of this analysis was 25% F-T jet fuel, 55% F-T diesel and 20% F-T naphtha.

6.6 Results

Local sensitivity analysis was conducted on the feedstock type, the quantity of GHG emissions from land use change, CTL process efficiency, biomass weight percentage, torrefaction efficiency, CCS efficiency and CCS compression energy. Each parameter was varied with all others held at their baseline values with the impact on life cycle GHG emissions quantified as a percent change from the baseline value. Figure 14 presents this information in a manner that allows the magnitude of each change to be seen in comparison to the others. The biomass feed rate has the dominant influence. Since the biomass feed rate is a parameter that is chosen by the operator, the emissions from CBTL facilities will be dictated by practical, as opposed to technological, limitations. Overall, the choice of feedstock and the potential for soil carbon sequestration were found to have a larger impact on life cycle GHG emissions than the process efficiencies.

When examining the impacts of changing the plant efficiency (this can be achieved either directly or by changing the energy consumption for biomass pre-processing or carbon dioxide compression) it was found that lower efficiencies lead to lower net emissions. This counter-intuitive result occurs because the plants were chosen to be self-sufficient and CCS is used to capture emissions from gasifying additional biomass to supply syngas for process fuel. The

capture and sequestration of carbon contained in the biomass leads to a net carbon removal from the atmosphere and hence having less biomass converted to fuel results in more of the carbon in the biomass going to sequestration.

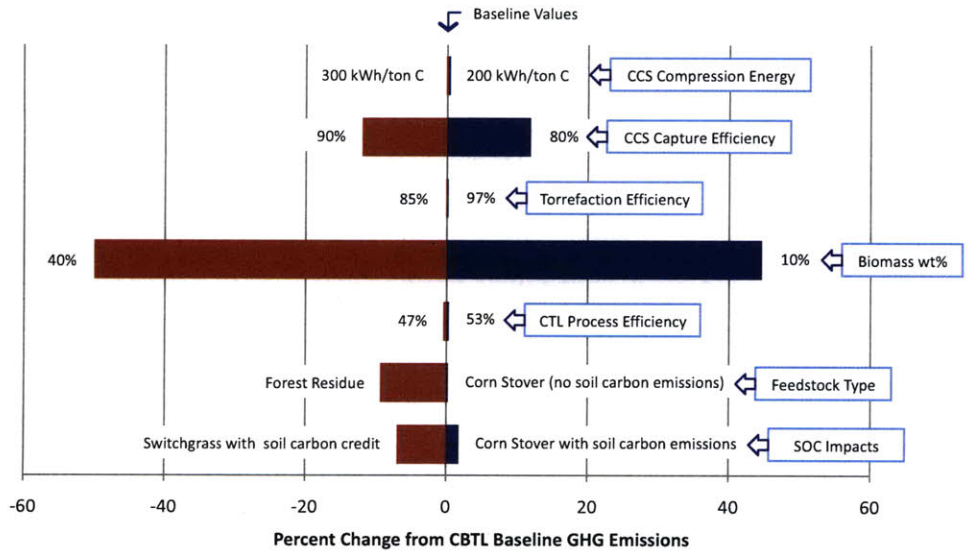

Figure 14: Sensitivity analysis of operational specifications and configurations of F-T jet fuel from coal and biomass

The results for the low emissions, baseline and high emissions scenarios for CBTL using switchgrass as the biomass feedstock are shown in Table 10 and Table 11. Table 10 gives the results when no soil carbon sequestration credit is given to the switchgrass while Table 11 gives the results when the soil carbon sequestration credit is included. The 'biomass credit' represents the CO_2 that is absorbed from the atmosphere during biomass growth. Increasing biomass credit reflects larger amounts of biomass being used as feedstock.

The life cycle GHG emissions of the CBTL pathway range from 0.14 to 1.14 times those of conventional jet fuel when no soil carbon sequestration credit is given. The emissions for this pathway range from 0.08 to 1.12 times those of conventional jet when the soil carbon sequestration credit is included. The large range of this pathway is primarily driven by the variation in biomass weight fraction of the feedstock.

In their assessment of F-T diesel production, Tarka (2009) used a displacement (system expansion) scheme instead of energy-based allocation to account for the benefit of making a reduced carbon, biomass-based F-T naphtha in addition to the F-T diesel. As such, their results differ from those given here. When a common allocation approach and productions assumptions are implemented, both analyses yield similar results.

Table 10: Summary of results for F-T jet fuel from coal and biomass without soil carbon sequestration credit

Land Use Change Scenario B0	**Low**	**Baseline**	**High**
Key Assumptions			
Biomass Weight Fraction	40%	25%	10%
Biomass Input	Switchgrass	Switchgrass	Switchgrass
Carbon Capture Efficiency	90%	85%	80%
CBTL Process Efficiency (LHV)	48.9% (53% without CCS or biomass processing)	46.0% (50% without CCS or biomass processing)	44.1% (47% without CCS or biomass processing)
Life Cycle CO_2 Emissions by Stage			
Biomass Credit (gCO_2/MJ)	-78.6	-44.3	-15.3
Recovery of feedstock (gCO_2/MJ)	1.2	1.2	1.1
Transportation of feedstock (gCO_2/MJ)	0.3	0.2	0.1
Processing of feedstock to fuel (gCO_2/MJ)	14.7	21.9	28.6
Transportation of jet fuel (gCO_2/MJ)	0.5	0.5	0.5
Combustion CO_2 (gCO_2/MJ)	70.4	70.4	70.4
WTT GHG Emissions by Species			
WTT CO_2 emissions (gCO_2/MJ)	-62.0	-20.5	14.9
WTT CH_4 emissions (gCO_2e/MJ)	1.1	4.9	13.6
WTT N_2O emissions (gCO_2e/MJ)	2.9	2.0	0.9
Total WTW GHG emissions (gCO_2e/MJ)	12.4	56.9	99.8
Life Cycle GHG Emissions Relative to Baseline Conventional Jet Fuel	**0.14**	**0.65**	**1.14**

Table 11: Summary of results for F-T jet fuel from coal and switchgrass with soil carbon sequestration credit

Land Use Change Scenario B1	**Low**[1]	**Baseline**[1]	**High**[1]
Land use change emissions (gCO_2/MJ)	-5.5	-3.9	-2.0
WTW CO_2 emissions (gCO_2/MJ)	2.9	46.0	83.4
Total WTW GHG emissions (gCO_2e/MJ)	6.9	53.0	97.8
Life Cycle GHG Emissions Relative to Baseline Conventional Jet Fuel	**0.08**	**0.61**	**1.12**

Notes:
1) All other input assumptions (cultivation of switchgrass, F-T processing and carbon capture efficiency) are based on those in the B0 emissions case of the corresponding scenario.

Figure 15 presents the implication of varying biomass weight over a range of 5% to 45%. Life cycle GHG emissions can be reduced to a fraction of conventional jet fuel with considerable biomass usage. For example, provided sufficient CCS is available, a CBTL jet fuel created from 45% biomass could have life cycle GHG emissions that are only 20% of conventional jet fuel; however, roughly 245 railroad cars of biomass would be needed every day to create sufficient CBTL jet fuel to power the aircraft at Boston Logan airport.[24] This large amount of biomass highlights the importance of considering GHG reductions for high biomass weight percentages in conjunction with biomass feeding requirements; it also points to lower biomass percentages being more realistic. Ongoing research is considering the economics of CBTL fuels.

[24] 6,500 tonnes of biomass would be needed per day to provide 25,000 barrels per day of jet fuel at a biomass feed rate of 45% (this is roughly the consumption of Boston Logan Airport). A typical railroad car can carry 26.5 tonnes of biomass (Mahmudi, 2006).

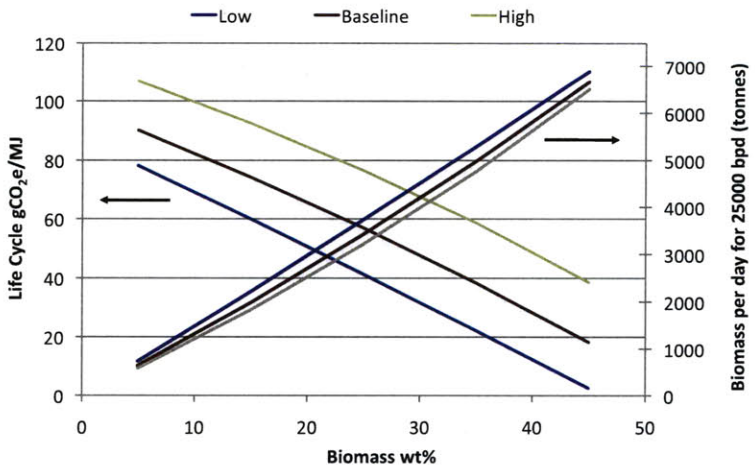

Figure 15: Dependence of cumulative life cycle emissions and biomass requirements for varied biomass utilization within CBTL

6.6.1 Case Study: Impact of Carbon Capture on GHG Emissions from CBTL Facilities

The analysis presented above assumed the use of CCS to reduce GHG emissions. Two additional cases were examined to emphasize the importance of using CCS to reduce GHG emissions from CBTL facilities. The first is the baseline CBTL case without CCS and without soil carbon sequestration. The second is the baseline CBTL case without CCS where the biomass feed rate has been adjusted such that the life cycle GHG emissions are on parity with conventional jet fuel.

A comparison of results from the baseline scenario with and without CCS is given in Table 12. Not having CCS leads to an increase in GHG emissions of 106.1 gCO_2/MJ, such that the WTW emissions from the CBTL pathway become 186% of conventional jet fuel. Without CCS, one needs to use 70% biomass, by weight, for F-T fuel from coal and switchgrass to reach GHG parity with conventional jet fuel. This understates the importance of CCS to getting reduced GHG emissions from CBTL fuels.

Table 12: Life cycle GHG emissions from F-T jet fuel from coal and switchgrass with and without CCS

	Baseline	**Baseline (w/o CCS)**	**Biomass for GHG Parity (w/o CCS)**
Key Assumptions			
Biomass Weight Fraction	25%	25%	70%
Biomass Input	Switchgrass	Switchgrass	Switchgrass
Carbon capture efficiency	85%	0%	0%
Life Cycle CO_2 Emissions by Stage			
Biomass credit (gCO_2/MJ)	-44.3	-42.0	-141.1
Recovery of feedstock (gCO_2/MJ)	1.2	1.2	1.9
Transportation of feedstock (gCO_2/MJ)	0.2	0.2	0.4
Processing of feedstock to fuel (gCO_2/MJ)	21.9	126.1	146.5
Transportation of jet fuel (gCO_2/MJ)	0.5	0.5	0.5
Combustion CO_2 (gCO_2/MJ)	70.4	70.4	70.4
WTT GHG Emissions by Species			
WTT CO_2 emissions (gCO_2/MJ)	-20.5	86.0	8.3
WTT CH_4 emissions (gCO_2e/MJ)	4.9	4.7	2.3
WTT N_2O emissions (gCO_2e/MJ)	2.0	1.9	6.5
Total WTW GHG emissions (gCO_2e/MJ)	56.9	163.0	87.5
Life Cycle GHG Emissions Relative to Baseline Conventional Jet Fuel	0.65	1.86	1.00

Chapter 7: Hydroprocessed Renewable Jet Fuel from Renewable Oils

Renewable oils can be processed into a fuel that has properties similar to those of F-T fuels. The processing involves hydrotreatment to deoxygenate the oil with subsequent hydrocracking to create hydrocarbons that fill the distillation range of jet fuel (Hileman et al., 2009). Wong (2008) developed life cycle GHG inventories for Hydroprocessed Renewable Jet fuel (HRJ) from soy oil and palm oil using Hydroprocessed Renewable Diesel (HRD) as a surrogate for HRJ. This thesis updated these results, as described in section 7.2, and subsequently examined the life cycle GHG emissions from the production and use of HRJ from rapeseed oil, algae oil, jatropha oil and salicornia oil. Soy and palm oil were examined using GREET version 1.8a whereas all other HRJ pathways used GREET version 1.8b.

As of the writing of this thesis, the production of hydroprocessed jet fuel from any oil feedstock is still limited to quantities suitable for flight-testing. Numerous flight tests have been successfully conducted of fuel composed of 50% HRJ from mixes of jatropha, algae and camelina blended with conventional jet fuel. In all cases, HRJ will have to compete with hydroprocessed renewable diesel (HRD) and biodiesel for feedstock availability. Biodiesel is currently the only biofuel produced at commercial scales from renewable oils; however, facilities to hydroprocess renewable oils are being built worldwide with an expected production capacity of nearly 60,000 bbl/day (Hileman et al., 2009). While biodiesel is not appropriate for use in gas turbines at any blending ratio, biodiesel production can be used to understand the resource potential of renewable oils for biofuel because it is made from the same feedstock.

Soybean oil is of interest as it is used extensively in the US and Europe for biodiesel production. The US and Europe used a total of 48,700 bbl/day (2.6 million metric tons per year) of soy oil in 2009 for biodiesel, which represents only 20% of total soy oil use in these regions. Similarly, rapeseed oil is the main feedstock used for biodiesel production in Europe. Approximately 35% of all rapeseed oil used in Europe went to biodiesel, amounting to 58,000 bbl/day (3.1 million metric tons per year). Palm oil, on the other hand, has grown to become the most produced oil in the world. Its production has increased rapidly in the past 20 years and the production of palm oil surpassed soy oil for the first time in 2006. Almost 90% of global palm oil production occurs in Indonesia and Malaysia (FAPRI, 2009). Biodiesel production is expanding based on the palm oil resources in this area. Malaysia has issued approval of 91 companies to build domestic palm oil based biodiesel plants; however, total planned capacity of the entire region is still less than 30,000 bbl/day (1.5 million metric tons per year) (Virki, 2007; Forbes.com, 2007; Mission Biofuels Limited, 2007).

Soybeans, palm and rapeseed are edible food crops requiring fertile cropland for cultivation. The use of these crops in fuel production could result in direct or indirect land use change emissions. As previously noted, large uncertainties exist in estimating the GHG emissions from both direct and indirect land use change. This work only quantifies direct land use change because the economic models required to analyze indirect effects are beyond the scope of this effort. Similar to the treatment of switchgrass in Section 6.2.2.4, the following sections consider a range of direct land use change scenarios using multiple land conversion scenarios to establish upper and lower bounds for these values. These scenarios were created based upon existing data from the literature. Since indirect land use change emissions are the integrated impact of direct land use change resulting from increased crop prices, the range of direct land use change emissions

presented herein should bracket any potential indirect land use change emissions occurring because of these feedstocks.

Jatropha curcus is a small tree or large shrub, up to 5-7 meters tall, which can grow without irrigation in a broad spectrum of rainfall regimes. All subsequent references to jatropha are with regard to *jatropha curcas*. Under normal conditions, the jatropha plant flowers only once a year during the rainy season; however, in permanently humid regions or under irrigated conditions it can be made to flower almost all year round (Achten et al., 2008). The resulting fruit is composed of an outer capsule containing two or three seeds. Each seed has a shell and a kernel, which contains oil. Jatropha plants have higher oil yields than many other oil yielding crops; however, the husk and the seed shells result in more co-product per unit mass of jatropha oil than both algae and palm fresh fruit bunches.

The potential for jatropha was recently demonstrated by successful gas turbine test flights using a hydroprocessed mix of jatropha and other oils. Jatropha cultivation is ideal for regions of the world with the highest rates of poverty and much hot, dry land because it is well adapted to the tropics and subtropics. India has been recently pushing to expand biodiesel production from jatropha oil; the government has announced plans to subsidize an intensive program to plant jatropha for biofuels on 27 million acres of "wastelands". Despite these recent efforts, global production in 2008 was limited to 242 cultivation projects, amounting to only 2.2 million acres. Furthermore, most jatropha grown for biofuels is cultivated locally on plots of less than 12 acres (Luoma, 2009). The major limitations to expanding from local cultivation to large scale production is that farmers are in poverty and only allow jatropha to grow on their land because of its ability to grow in the arid conditions. In areas where jatropha is not naturally occurring, farmers do not wish to take the initiative to restructure their farms to prevent other revenue generating species from dominating the natural growth of jatropha. New plantations takes 3-5 years for jatropha production to mature such that it can be grown commercially and farmers don't have the capital to invest in projects where the potential for revenue is several years away. Due to the general poverty of the regions where jatropha is considered promising, there is little to no loan availability or presence of long term contracts to guarantee a return on their investment (Mani, 2010). While it appears that jatropha may be an appropriate solution to provide fuel to the villages in which it is grown, without changes in investment structures it remains to be seen how jatropha will expand beyond the village level to become an energy resource on the global scale.

Algae were first examined as a biofuel feedstock by the Department of Energy during the Aquatic Species Program (ASP) from 1978 to 1996. The ASP focused most of its attention on identifying a specific factor that would stimulate the algae to have a high lipid weight fraction (Sheehan et al., 1998b). Much discussion still surrounds the possibility of genetically modifying certain strains of algae to produce more oils; however, the present analysis focuses only on previously documented strains that currently exist. Furthermore, it is important to differentiate between micro-algae and macro-algae. Microalgae, as the name suggests, are tiny organisms which grow in water with concentrations of ~0.2-0.4g/L that have the appearance of tinting the water green; these are the algae considered in this work. Macro algae are the classical long strands that grow on the bottom of ponds and lakes, (a.k.a. seaweed). While some research has been conducted using macro-algae as a fuel source, it is not considered further in this work; hereafter, algae will refer to microalgae.

No company is currently producing commercial quantities of algal oil for use as a transportation fuel; instead they are producing quantities that are appropriate for various stages of research and development. Furthermore, the industry is not sufficiently defined to have well defined best practices for cultivating and extracting the oil from the algal cells. This report examines relatively

conventional methods of oil extraction wherein the algae are dried prior to chemical treatment; however, several research efforts are ongoing to evaluate whether the oil could be extracted via electrical pulses or if the algae can be genetically modified to naturally excrete oil. Although no commercial scale production of algae currently exists, significant investments are being made into developing it as a feedstock for alternative fuels. For example, the Department of Defense recently ordered 20,000 gallons of algae fuel from Solazyme at a cost of $8.5 million USD ($425 per gallon) for advanced testing as F-76 Naval Distillate (Green Car Congress, 2009). This is a relatively small sum compared to the 600 million US$ that Exxon Mobil has invested in research and development of algal transportation fuels (Mouawad, 2009).

Halophytes are considered an oil seed crop for fuel production because they prosper in sea or brackish water on marginal lands. Other benefits of halophyte agriculture include freeing up arable land for freshwater resources, cleansing the environment, decontaminating soils, desalinating brackish waters and soil carbon sequestration. Considering that 43% of the earth's landmass is arid or semi arid and 97% of the earth's water is seawater (Hendricks and Bushnell, 2008), halophytes are an attractive option for large-scale production. From the halophyte family, *Salicornia bigelovii* emerged as an oilseed crop from a screening of wild halophytes and was selected for seawater trials due to its seed yield and oil fraction (Anwar et al., 2002). All further references to halophyte or salicornia refer specifically to *Salicornia bigelovii.*

The development of salicornia for fuel production is still in the experimental stage; no fuel testing has been conducted on fuel produced from the salicornia plant. Despite our inexperience, a major UNFCCC project in the Sonoran desert has been cultivating salicornia on 30 hectares of coastal land since 1996 with the goal of developing cost-effective cultivation processes on a commercial basis, and optimizing agronomic methods for irrigation and harvesting (UNFCCC, 1998). The GCC (Cooperation Council for the Arab States of the Gulf) countries have also established research programs for halophytes in the form of an experimental 200-hectare integrated seawater agricultural system near Abu Dhabi. The Masdar Institute of Science and Technology (MIST) is collaborating with UOP, Boeing and Etihad Airways to realize this project (Green Car Congress, 2010).

7.1 Energy Requirements for HRJ from Renewable Oils

The hydrotreatment process for the production of HRJ from renewable oils was based on the UOP hydrodeoxygenation process, which primarily produces "green diesel" (Marker et al., 2005; Huo et al., 2008). Other techniques are available to produce hydrocarbon fuels from renewable oils beyond the approach developed by UOP; however, the UOP process is currently the most established for jet fuel production. Similar to F-T fuels, additional hydroprocessing is needed for the production of jet fuel instead of diesel, resulting in increased hydrogen and power requirements. The assumption that additional processing requirements for F-T jet fuel relative to diesel are negligible is justified in the literature (Gray et al., 2007); however, in the case of HRJ, using diesel as a surrogate for jet is only appropriate for crude estimates.

The UOP process used for the creation of Hydroprocessed Renewable Diesel (HRD) is described by the following chemical reaction:

$$C_nH_{2n+1}COOH + 3H_2 \rightarrow C_{n+1}H_{2n+4} + 2H_2O \qquad \text{Equation 8}$$

where n is the carbon chain length of the fatty acids within the triglyceride molecules used as a feedstock for the process. Triglycerides are formed from a single molecule of glycerol, combined with three fatty acids. This simplified analysis assumed that all renewable oils, regardless of type (soy, palm, rapeseed, jatropha, algae or salicornia) are identical and contain only fatty acids with

a carbon chain length of 18. The error introduced by this assumption is likely small compared to the uncertainty in quantifying cultivation inputs for each feedstock; however, not all oils are chemically equal and this analysis does not reflect the physical properties of any single oil type.

Table 13 presents the actual distributions of fatty acid carbon chain lengths for most of the oils considered in this work.[25] An example of a shortcoming of the assumption used in this analysis is the treatment of oils containing unsaturated carbon chains. The presence of double bonds within a carbon chain would lead to additional hydrogen consumption during the deoxygenation process in order to saturate the molecule, however, such effects are ignored herein.

Table 13: Component fatty acid profiles for renewable oils considered in this work

Fatty Acid Components (weight %)	Caprylic (8:0)	Capric (10:0)	Lauric (12:0)	Myristic (14:0)	Palmitic (16:0)	Palmitoleic (16:1)	Stearic (18:0)	Oleic (18:1)	Linoleic (18:2)	Linolenic (18:3)	Arachidic (20:0)	Gadoleic (20:1)	Behenic (22:0)	Erucic (22:1)
Soybean	—	—	—	—	11	—	4	22	53	8	—	—	—	—
Palm	—	—	—	—	44	—	4	39	11	—	—	—	—	—
Palm Kernel	3	7	47	14	9	—	1	19	1	—	—	—	—	—
Rapeseed (B. campestris)	—	—	—	—	4	—	2	33	18	9	—	12	—	22
Rapeseed (B. napus)	—	—	—	—	3	—	1	17	14	9	—	11	—	45
Jatropha *curcas*[3]	—	—	—	—	13	—	8	45	34	—	—	—	—	1
Salicornia *bigevolii*[4]	—	—	—	—	7	—	3	18	73	—	—	—	—	—

Notes:
1) Unless otherwise indicated, this information comes from: DeMan et al. (1999)
2) Additional data for fatty acid components of coconut oil, canola oil, sunflower oil, cottonseed oil, peanut oil, olive oil, mustard seed, lard, yellow grease is also available from DeMan et al. (1999)
3) From Shweta et al. (2004)
4) Salicornia oil is similar to safflower oil in fatty acid composition (Glenn et al., 1998). This profile uses averaged values for safflower oil from: Coşge et al. (2007)

Equation 8 can be re-written in a mass balance form for easier comparison to experimental data.

1.12 lb Oil + **0.024** lb Hydrogen → **1.00** lb HRD + **0.14** lb Water

The feedstock, key products and process energy needed per pound of HRD are summarized in Table 14; however, further refinement of HRD is required for the creation of HRJ. The strategy to estimate the process requirements of HRJ was to use the experimental data for the creation of HRD and subsequently estimate the additional requirements to convert the HRD into HRJ. For this analysis, HRD and HRJ are assumed to be symmetrical distributions of straight chains hydrocarbons centered on C_{12} and C_{18} respectively. As shown schematically in Figure 16, the cracking from diesel fuel to jet fuel was assumed to occur via the addition of gaseous hydrogen.

[25] The notation for denoting carbon chain length and number of double bonds is (chain length):(number of double bonds). For example, a chain length of 18 with 2 double bonds is expressed as 18:2.

Table 14: Experimental and theoretical requirements for the creation of renewable diesel

Feedstock (lb)	Experimental			Theoretical
	Low	Baseline	High	
Oil	100	100	100	100
H_2 (51586 Btu/lb)	1.5	2.72	3.8	2.14
Key Products (lb)				
HRD (18908 Btu/lb)	83.0	84.19	86	89.28
Propane Mix Gas (18568 Btu/lb)	2.0	4.75	5	0.00
Process Energy (Btu)				
Electricity	5785	6942	8099	--
Natural Gas	8950	8950	8950	--

Notes:
1) Steam is assumed to be produced from natural gas at 80% efficiency
2) Energy contents are taken from GREET (2008)
3) Experimental data taken from Appendix 2 of Huo et al. (2008) with modifications per recommendations from UOP (Kalnes, 2009)

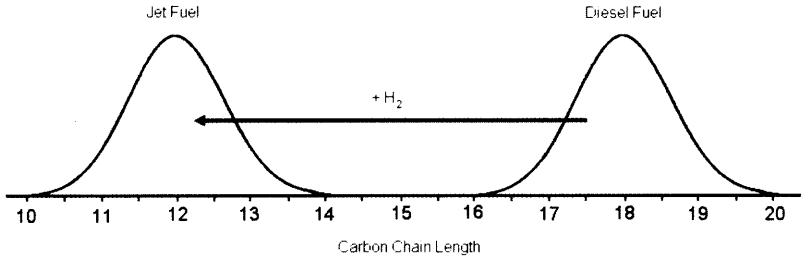

Figure 16: Schematic showing the change in hydrocarbon composition between HRD and HRJ fuels that results from additional hydroprocessing

The mechanism by which hydrocarbon chains crack is through smaller molecules, (e.g., pentane (C_5H_{12}) and hexane (C_6H_{14})) breaking off the end. The dominant effect that takes place is the reduction of C_{18} to C_{13} by cracking pentane and C_{12} by cracking hexane (Kalnes, 2009). Other reactions are also occurring where molecules from the distribution about C_{18} crack to those from the distribution about C_{12}. To account fully for this effect would entail including the statistical nature by which chemical reactions are more likely to take place. In keeping with the level of detail required of this analysis, the aforementioned effects were assumed to cancel out if the two distributions have the same shape about their mean.

Making use of these arguments simplifies the analysis to two chemical reactions converting diesel fuel to jet fuel:

$$\begin{array}{r} C_{18}H_{38} + H_2 \rightarrow C_{12}H_{26} + C_6H_{14} \\ C_{18}H_{38} + H_2 \rightarrow C_{13}H_{28} + C_5H_{12} \\ \hline C_{18}H_{38} + 2H_2 \rightarrow C_{12}H_{26} + C_{13}H_{28} + C_5H_{12} + C_6H_{14} \end{array} \qquad \text{Equation 9}$$

Written in mass balance form and normalized for one lb of HRD, the overall equation governing the formation of HRJ from renewable oil can be expressed as:

1.00 lb HRD + **0.0079** lb Hydrogen → **0.697** lb HRJ + **0.311** lb Naphtha

Although variations in carbon chain length are not captured in this analysis, fatty acids with carbon chain length distributions around 12 are better suited for use as feedstock for jet fuel because higher blending percentages can be used without the need for hydrocracking. Furthermore, carbon chain lengths closer to 12 would result in a higher yield of jet fuel per unit mass of oil input.

Naphtha in this case is a combination of 46 percent C_5H_{12} and 54 percent C_6H_{14} by mass. Using these ratios of HRD to HRJ, the process energies from Table 14 were modified to reflect the energy requirements to create HRJ as shown in Table 15. Based on discussions with experts at UOP (Kalnes, 2009), it is assumed that total process energies (natural gas and electricity) will increase by 10 to 30 percent per pound of renewable feedstock when including the hydrocracking required for the formation of HRJ. The total hydrogen consumption is the sum of that needed to first make HRD and then to crack it to HRJ. In all cases where renewable oils are processed into finished fuel products, energy and emissions were allocated based on energy content.

Table 15: Energy requirements for the creation of HRJ

	Emissions Scenarios		
Feedstock (lb)	**Low**	**Baseline**	**High**
Oil	100	100	100
H_2 (51586 Btu/lb)	2.15	3.38	4.48
Key Products (lb)			
HRJ (18950 Btu/lb)	57.8	58.7	59.9
Naphtha (19215 Btu/lb)	25.8	26.2	26.8
Propane Mix Gas (18568 Btu/lb)	2.0	4.8	5.0
Process Energy (Btu)			
Electricity	6364	8330	10529
Natural Gas	9845	10740	11635

The hydroprocessing step of converting renewable oil into HRD has a mass yield of 84% and results in 8.7 gCO_2/MJ. After making the aforementioned changes, hydroprocessing renewable oil into HRJ has a mass yield below 60% and results in 10.3 gCO_2/MJ. The emissions associated with hydrogen production in this work are representative of steam reforming natural gas and are consistent with default GREET assumptions. While these results provide a first approximation of mass and energy inputs, they do not reflect the impact of oil composition on process inputs or differences in real world production scenarios.

The decrease in yield is accompanied by an increase in naphtha production. Although naphtha is used as a blending stock in gasoline, it has a lower economic value than HRD, which is a high performance diesel fuel. Because petroleum refineries have on-site hydrogen production to meet internal demands that could be expanded to supply the hydrogen for hydroprocessing renewable oils, hydroprocessing facilities would likely have lower emissions if they were integrated into existing petroleum refineries. With such a configuration, excess naphtha resulting from HRJ production can be integrated into the refinery naphtha stream and catalytically reformed to high value hydrocarbons or steam reformed to supplement the internal hydrogen needs of the process. However, if the value of the HRJ and naphtha stream is less than the HRD stream, a fuel producer would likely focus on HRD production unless they could charge a premium for HRJ fuel. Under such a situation, the aviation community could consider using HRD as a dilute blend stock in gas turbine engines (~10%). This option would require further research to ensure viability with the

current fleet of aircraft. Further research is being devoted within PARTNER Project 28 to understand the tradeoffs among HRD, HRJ, and FAME production.

7.2 HRJ from Soybean Oil and Palm Oil

The GHG inventories of HRJ from soy oil and palm oil developed by Wong (2008) were updated to reflect the energy and emissions associated with HRJ production derived in section 7.1. A new methodology was also applied in the treatment of land use change emissions from these pathways. Land use changes can have a substantial effect on the life-cycle emissions of a biofuel, even when amortized over an extended time period. To allow for easier examination of this aspect of biofuel production, the analysis of soy and palm oil pathways were each expanded from individual pathways that have different land use change scenarios for each of the low, baseline and high emissions cases to three and four unique pathways, respectively, that represent various land use change scenarios. These pathways are summarized in Table 16. This approach was developed to explore the range of magnitudes of potential GHG emissions due to land use change. The goal is to provide the reader an understanding of how land use change emissions compare to the emissions from the other five life cycle stages. It is not intended to explicitly quantify the specific land use change emissions that would result from expanded soy or palm oil production.

The low, baseline and high emissions cases for each of these pathways are based on historical and projected variations in crop yield. For all of the pathways, the land use change emissions were amortized over a 30-year period with no discounting. This is consistent with the time frame adopted by the EPA in the Renewable Fuels Standard (EPA, 2010).

Table 16: Land use change scenarios explored for HRJ pathways

Land use change scenarios explored for HRJ pathways		**Land use change scenarios explored for HRJ pathways**	
LUC-S0	No land use change	LUC-P0	No land use change
LUC-S1	Grassland conversion to soybean field	LUC-P1	Logged over forest conversion to palm plantation field
LUC-S2	Tropical rainforest conversion to soybean field	LUC-P2	Tropical rainforest conversion to palm plantation field
n/a	n/a	LUC-P3	Peatland rainforest conversion to palm plantation field

An updated description of the soy and palm oil to HRJ pathways is given in Stratton et al. (2010). The results are included in the results section of this thesis in order to demonstrate how HRJ from soy oil and palm oil compare to other alternative jet fuel production pathways.

7.3 HRJ from Rapeseed Oil

The production of HRJ from rapeseed oil was analyzed with the GREET framework using cultivation and processing data from the literature.[26] Rapeseed has been grown for the production of animal feed and vegetable oils for both human consumption and biofuel production. The leading producers of rapeseed are currently China, Canada, India and the European Union (FAO, 2010). The use of rapeseed oil as a feedstock for biofuels is of particular interest in Europe, where Rapeseed Methyl Ester is one of the two main biofuels under consideration (CONCAWE, 2002). This analysis assumes that rapeseed oil is produced in Europe and subsequently imported to the

[26] Rapeseed oil is not a preexisting pathway within GREET. As such, a new pathway was built within the GREET framework using the soy oil to renewable diesel pathway as a guide.

United States to be hydroprocessed into HRJ. The key parameters used to form the low, baseline and high emissions scenario were the rapeseed yield, oil content, farming energy, fertilizer application, transportation distance and oilseed drying energy requirements. In addition to a scenario where land use change emissions were assumed zero, a scenario where rapeseed is grown on set-aside land[27] was examined; the aforementioned key parameters were varied within each land use change scenario.

7.3.1 Cultivation of Rapeseed

Rapeseed cultivation was assumed to take place predominantly in the United Kingdom (UK) and France based on data from Mortimer and Elsayed (2006), Edwards et al. (2007), Richards (2000) and Prieur et al. (2008). The analysis was supplemented by additional data from Sweden and Denmark from Bernesson et al. (2004) and Schmidt (2007). This was deemed appropriate due to the relative similarity in climate among southern Sweden, Denmark, France and the UK.

Rapeseed yield was estimated using data for the UK and France from 1999 through 2009. The baseline scenario adopted a projected rapeseed yield in 2015 of 3.35 Mg/ha (Eurostat, 2010) using linear regression on the historical data. The low and high emissions scenarios were developed using the same method employed to estimate soybean and palm yields. Specifically, based on historical rapeseed yield data from 1999 through 2009 (Eurostat, 2010), the variation between the lowest yield and the line of best fit was -16.8% (UK in 2001) while that between the highest yield and the line of best fit was +15.7% (France in 2009). Based on these historical data, it was assumed that yield fluctuations in some future year could be 16.8% lower than in the baseline case, corresponding to the high emissions case of 2.79 Mg/ha. Similarly, a yield in some future ideal growing year could be 15.7% higher than in the baseline case, corresponding to the low emissions case of 3.89 Mg/acre.

Yearly data from both France and the UK are shown in Figure 17. The weighted average corresponds to the ratio of total harvested weight to total planted area from both countries. Although there is substantial fluctuation in yield from year to year, the underlying trend is increasing over time at a rate of 23.7 kg/ha/year.

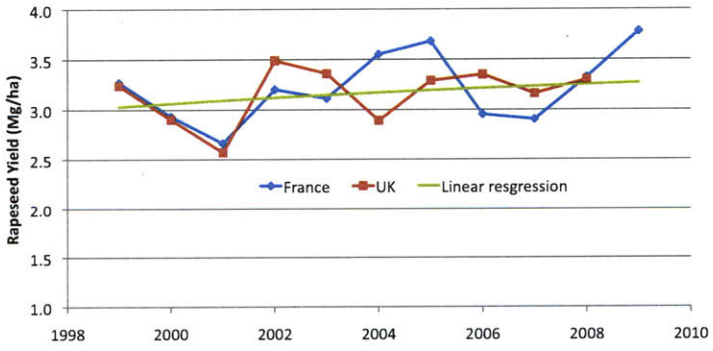

Figure 17: Yearly rapeseed yield for France and the UK between 1999 and 2009

The oil fraction of rapeseed ranges from 40% to 45% by mass based on the sources used to model cultivation. The oil yield per kilogram of rapeseed is higher than any other renewable oil

[27] From 1988 through 2009, the EU government compensated farmers to remove 10%-15% of their land from production to deliver some environmental benefits following considerable damage to agricultural ecosystems and wildlife as a result of the intensification of agriculture. The program has since changed such that the set aside system is on a voluntary basis with no compensation. Land that was set aside by farmers could be available for increased rapeseed cultivation (Gray, 2009).

feedstock considered in this work. In this analysis, oil fractions of 45% (Prieur et al., 2008; Bernesson et al., 2004), 44% (Schmidt, 2007) and 41% (Richards, 2000; Mortimer and Elsayed, 2006) were assumed in the low, baseline and high emissions scenarios.

Inputs to rapeseed cultivation are fuels for farming operations, nitrogen fertilizers, phosphate, potash and herbicides. The energy consumption of seed crop growth and processing of seeds is less than 1% of all energy used in cultivation and harvesting and was considered negligible for the purposes of this analysis (Richards, 2000). The usage per hectare of each of these resources in the low, baseline and high emissions scenario is given in Table 17. Nitrogen fertilizer application was assumed to occur in the form of 50% ammonia and nitrogen solutions and 50% ammonium nitrate and ammonium sulfate. Default GREET assumptions for soybeans were adopted regarding the types of herbicides applied during rapeseed cultivation. The largest variation was found in the use of diesel fuel on the farm. The low emissions scenario was based on data from Mortimer and Elsayed (2006) whose estimate for North East England was by far the most optimistic. The baseline scenario was based on French data from Prieur et al. (2008), although Bernesson (2004) gave a similar estimate in his analysis of rapeseed production in Sweden. The high emissions scenario employs data from Richards (2000) for arable lands in England, which is confirmed by Schmidt (2007) with his farming energy estimates of rapeseed production in Denmark.

The corresponding production inputs per Mg of rapeseed for each scenario were calculated by combining the production inputs and yields per hectare. The production of rapeseed oil results in straw biomass production. The average ratio of oilseed production to straw is approximately 0.96:1.[28] This analysis assumed that the straw was ploughed back into the fields after harvest. This leads to minimized depletion of soil nutrients and fertilizer savings, which were accounted for in the cultivation inputs (Prieur et al., 2008). Where there is a nearby heat or power generation facility that is outfitted to accommodate biomass feedstocks, the straw represents a potential energy source (Richards, 2000); however, straw from rapeseed is rarely harvested because of burning problems with the newer varieties and lower yields than grasses or wheat. Lower yield makes rapeseed straw more expensive to harvest so it is simply tilled back into the soil by most farmers (Bernesson et al., 2004).

Emissions from N_2O were estimated using IPCC Tier 1 methodology (De Klein et al., 2006). Nitrogen in above and below ground crop residues was estimated by applying the aforementioned crop residue production ratio to estimate the amount of straw tilled back into the soil. Rapeseed straw has been characterized as 0.75% nitrogen by mass (Karaosmanoglu et al., 1999) leading to 7125 g of nitrogen reapplied to the field in the form of straw biomass per megagram of oilseed production. The IPCC Tier 1 methodology estimates the combined direct and indirect conversion rate for nitrogen from synthetic fertilizers as 1.325% and nitrogen from crop residues as 1.225%. These rates include the atmospheric deposition of nitrogen volatilized from managed soils as well as nitrogen from leaching and runoff. The formula for calculating N_2O emissions from rapeseed cultivation is given by:

$$N_2O\ \text{Emissions}\left(\frac{g_{N_2O}}{Mg}\right) = \left(\left(\frac{g_{\text{nitrogen fertilizer}}}{Mg}\right)\cdot 0.01325 + \left(7125\frac{g_{\text{N-crop residue}}}{Mg}\right)\cdot 0.01225\right)\cdot\left(\frac{44g_{N_2O}}{28g_N}\right) \quad \text{Equation 10}$$

[28] The straw and oilseed production from Richards (2000) were 4 Mg/ha and 4.08 Mg/ha, respectively (ratio of 0.98:1). The straw and oilseed production from Schmidt (2007) were 2.93 Mg/ha and 3.13 Mg/ha, respectively (ratio of 0.94:1).

Table 17: Farming energy, fertilizer and herbicide usage for the production of rapeseed in the low emissions, baseline and high emissions scenarios

	Low	Baseline	High
Rapeseed Yield (Mg/ha)	2.79	3.35	3.89
Rapeseed Oil Fraction (mass)	45%	44%	41%
Fuel Usage			
Diesel (MJ/ha)[1]	1857	2310	3934
Fertilizer Usage			
Nitrogen(kg-N/ha)[2]	140	164	180
Phosphate (kg-P_2O_5/ha)[3]	34	47	56
Potash (kg-K_2O/ha)[4]	35	43	82
Herbicides[5]	1.8	2.3	2.8

Notes:

1) Mortimer and Elsayed (2006) – Low Case; Prieur et al. (2008) – Baseline Case; Richards (2000) –High Case
2) Bernesson et al. (2004) and Schmidt (2007) – Low Case; Prieur et al. (2008) – Baseline Case; Edwards et al. (2007) – High Case
3) Bernesson et al. (2004) – Low Case; Prieur et al. (2008) – Baseline Case; Mortimer and Elsayed (2006) and Schmidt (2007) – High Case
4) Prieur et al. (2008) – Low Case; Richards (2000) and Bernesson et al. (2004) – Baseline Case; Mortimer and Elsayed (2006) and Schmidt (2007) – High Case
5) Richards (2000) – Low Case; Prieur et al. (2008) – Baseline Case; Mortimer and Elsayed (2006) – High Case

The least defined aspects of rapeseed production are the drying and storage practices. In practice, there is little consensus on the oilseed moisture content at harvest, which has implications for energy consumption during drying. A recent survey of current harvesting, drying and storage practices of oilseed rape in the UK found that most farmers harvest above 12% moisture content, which is the threshold for Ochratoxin B production (Armitage et al., 2005).[29] After harvest the rapeseed must be dried to a moisture content of 9% for storage (Prieur et al., 2008; Richards, 2000; Schmidt, 2007). Most rapeseed is stored for about 3 months before being sold. This tendency is driven mainly by market strategy and cash flow. Longer storage periods may require lower moisture contents to minimize mite infestation and deterioration through rancidity. Mites are the greatest problem faced by rapeseed famers and were observed on more than 25% of sites. From the perspective of seed crushers, moisture content (high or low) and admixture of stores were the most common reason for rejection or price reductions (Armitage et al., 2005). This analysis assumed moisture contents of 13%, 14% and 15% at harvest and 9% after drying in the low emissions, baseline and high emissions scenario, respectively. Losses due to mites, rancidity and admixture were neglected due to lack of quantitative data but these could become important for ill-maintained rapeseed stored over long periods of time.

Approximately one third of farmers surveyed in the UK use ambient air drying to reduce the moisture content of their seed from the value at harvest to that required for storage. Drying using ambient air can take from 2 to 4 weeks, although 2 weeks is the most common. The other two thirds of farmers use hot air dryers to reduce drying times at the expense of increased energy consumption (Armitage et al., 2005). This work assumed the use of hot air drying according to energy consumption estimates from Mortimer and Elsayed (2006), Bernesson et al. (2004) and

[29] Ochratoxin B is the most abundant food contaminating mycotoxin in the world. Human exposure occurs primarily through consumption of improperly stored food products (Armitage et al., 2005)

Schmidt (2007) in the low, baseline and high emissions scenarios, respectively. The assumptions regarding the drying and storage of rapeseed used in this work are summarized in Table 18.

Table 18: Rapeseed drying and storage assumptions in the low emissions, baseline and high emissions scenario

	Low	Baseline	High
Moisture Content			
Harvest[1]	13%	14%	15%
Storage[2]	9%	9%	9%
Drying Energy Consumption[3]			
Diesel ($MJ/L_{evaporated}$)	n/a	4.7652	6
Grid Electricity ($MJ/L_{evaporated}$)	n/a	0	3.6
Diesel (MJ/Mg)	165.0	277.0	423.5
Grid Electricity (MJ/Mg)	0.0	0.0	254.1

Notes:
1) Mortimer and Elsayed (2006) – Low Case; Average of low and high cases – Baseline case; Bernesson et al. (2004) – High Case
2) Prieur et al. (2008), Richards (2000), Mortimer and Elsayed (2006), Schmidt (2007)
3) Mortimer and Elsayed (2006) – Low Case; Bernesson et al. (2004) – Baseline case; Schmidt (2007) – High Case

7.3.2 Extraction of Oil from Rapeseed

A modified version of the process for oil extraction from soybeans established by Sheehan et al. (1998a), including only the processes relevant to rapeseed in an N-hexane extraction facility, was used to model the process inputs to extracting oil from rapeseed. Ozata et al. (2009) also used this approach in their analysis of biodiesel from rapeseed. The changes to the data from Sheehan et al. (1998a) were limited to removing the energy demands for drying as this has been explicitly quantified for rapeseed in Table 18. The process energies were converted from energy per unit mass of oilseed to energy per unit mass of oil using the oil fractions from the low emissions, baseline and high emissions scenarios. The outputs and energy consumption assumed in the extraction of oil from rapeseed are shown in Table 19.

7.3.3 Co-Product Usage and Allocation Methodology

In the extraction of oil from rapeseed, rapeseed meal is produced in large quantities as a co-product (1.22-1.44 kg of meal per kg of oil). This is similar to the extraction of oil from soybeans; hence, the same challenges with respect to allocation arise. Rapeseed meal is primarily used as an animal feed and could potentially displace barley, corn, and soybean meal. One kg of rapeseed meal is equivalent to 0.87 kg of soybean meal on a protein basis (Prieur et al., 2008).

Based on the results for soy oil from Stratton et al. (2010), the displacement method, as applied here, is not appropriate because of the large variation in life cycle GHG emissions that will result from the choice of feedstocks (i.e., barley, corn, and soybean meal) displaced by rapeseed meal. The mass or energy allocation method may not be most appropriate as rapeseed meal is not valued based on its mass, or sold as a commercial energy product. The commercial value of the protein in rapeseed meal for animal feed resulted in market value allocation being adopted in this work. This is internally consistent with the other pathways considered in this work as well as with Prieur et al. (2008), Mortimer and Elsayed (2006) and Ozata et al. (2009).

Table 19: Process inputs for extracting oil from rapeseeds

	Low[1]	Baseline[1]	High[1]
Receiving and Storage			
Electricity	18.60	19.02	20.41
Rapeseed Preparation			
Electricity	68.76	70.32	75.46
Steam	153.35	156.83	168.31
Oil Extraction			
Electricity	11.46	11.73	12.58
N-hexane	94.15	96.29	103.34
Meal Processing			
Electricity	63.56	65.01	69.77
Steam	492.54	503.74	540.59
Oil Recovery			
Electricity	1.21	1.24	1.33
Steam	77.04	78.79	84.55
Solvent Recovery			
Electricity	1.66	1.69	1.82
Steam	0.00	0.00	0.00
Oil Degumming			
Electricity	5.38	5.50	5.91
Steam	60.53	61.91	66.44
Waste Treatment			
Electricity	1.82	1.86	1.99
Steam	32.56	33.30	35.74
Totals			
Electricity	172.45	176.37	189.27
Natural Gas[2]	1020.03	1043.21	1119.54
N-hexane[3]	94.15	96.29	103.34

Notes:
1) All values are in Btu per pound of oil
2) Steam is generated from natural gas with an efficiency of 80%.
3) GREET uses Liquefied Petroleum Gas (LPG) as a surrogate for N-hexane when calculating emissions

7.3.4 Transportation of Rapeseed Oil to HRJ Production Facilities

Rapeseed cultivation, harvesting and oil extraction were assumed to occur primarily in France and the UK. The one-way distance from the farm to the oil extraction facility was assumed to be 115 km (Prieur et al., 2008).[30] It was then assumed that the United States imports this oil to a domestic hydroprocessing facility where it is converted to jet fuel. This transportation profile is not available in GREET and was created using the data from Table 20. Default GREET assumptions were used for the details of each transportation mode.

[30] Richards (2000) and Mortimer and Elsayed (2006) estimated one-way transport distances of 90 km and 130 km, respectively.

Table 20: Transportation profile of Rapeseed Oil from Europe to the United States

Transportation of Rapeseed Oil to European Shipping Ports[1]	
Mode (%)	
Truck	100
Distance (kilometers)	150
Transportation of Rapeseed Oil from European Ports to U.S. ports[2]	
Mode (%)	
Ocean tanker	100
Distance (kilometers)	
Western UK to Eastern US (50%)	5520
Western France to Eastern US (25%)	5780
Southern France to Western US (25%)	7170
Average	6000
Transportation of Rapeseed Oil from U.S. ports to HRJ production facilities[1]	
Mode (%)	
Truck	50
Rail	50
Distance (miles)	
By truck	160
By rail	800
Notes:	
1) Author's own estimates	
2) Shipping distances from http://www.searates.com/reference/portdistance/	

7.3.5 Land Use Change Emissions from Rapeseed Oil Production

Two scenarios of land usage were considered for the cultivation of rapeseed in France and the UK. Rapeseed is an established crop in these areas where over 2 million hectares were harvested in 2008 (Eurostat, 2010). The first scenario represents established rapeseed production with an assumption that land use change emissions were zero. A second scenario resulting in positive GHG emissions was envisioned where rapeseed production is expanded for biofuel production on set aside land thus resulting in land use change emissions. Set aside land is land that was removed from agricultural production as a result of government mandates to re-establish some environmental benefits to agricultural ecosystems and wildlife. This is similar to the Conservation Reserve Program (CRP) in the United States. While removed from production, the natural carbon and nitrogen stocks of the land are replenished. Participation by farmers in the set aside system has recently changed to voluntary and these lands could be available for rapeseed cultivation (Gray, 2009). A return to crop production would cause the accumulated carbon and nitrogen in the soils to be depleted over time. The goal of this section is to provide an understanding for the reader of how land use change emissions compare to emissions from the other five life cycle stages. It is not intended to explicitly quantify the specific land use change emissions that would result from expanded palm oil production.

The estimate of GHG emissions resulting from the conversion of set aside land to rapeseed cultivation was based on Schmidt (2007). The total land use change emissions were amortized over 30 years with no discounting. The corresponding land use change emissions per Mg of rapeseed were calculated by combining the GHG estimate with the yield per hectare; this is presented in Table 21.

Table 21: Land use change emissions from rapeseed cultivation on set aside lands in Europe

Scenario	Land use change Emissions (Mg CO_2e/ha)	Assumed Rapeseed yield (Mg/ha)	Land use change emissions (g CO_2e/Mg)[1]
Conversion of set-aside land[2]	94.6	2.79 3.35 3.89	1,129,700 940,800 810,200
Notes: 1) Assumed to be amortized over 30 years with no discounting 2) Estimate from Schmidt (2007)			

7.3.6 Results

The life cycle GHG emissions from the production and use of HRJ fuel from rapeseed oil are given in Table 22 and Table 23. When no land use change emissions are present, the life cycle GHG emissions range from 0.45 to 0.87 times those of conventional jet fuel; however, nitrous oxide emissions represent between 39% and 44% of the total. Edwards et al. (2007) found nitrous oxide emissions from rapeseed production to be of similar magnitude using an independent, well-validated soil chemistry model (DNDC, version 82N). When rapeseed is grown on set aside land, the life cycle GHG emissions range from 0.87 to 1.47 times those of conventional jet fuel. The variation in the biomass credit is due to minor changes in the allocation scheme through the pathway. The transportation of oil across the Atlantic is responsible for only 0.6 g CO_2e/MJ; these emissions would not have been incurred had the fuel been processed and used within Europe.

Nitrous oxide emissions represent more than approximately 40% of the total life cycle GHG emissions from the rapeseed to HRJ pathway. As such, the consequences of the uncertainty associated with IPCC correlations are more important for this pathway. Although the magnitude of N_2O emissions in this work compare favorably with the detailed model used by Edwards et al. (2007), the reader should be aware of these inherent uncertainties when comparing different pathways for GHG reduction potential in sections 10.1 and 10.2.

Table 22: Summary of results from renewable jet fuel production and use from rapeseed

Land Use Change Scenario R0	Low	Baseline	High
Key Assumptions			
Total Biomass Yield (Mg/ha/yr)	2.79	3.35	3.89
Seed Oil Fraction	45%	44%	41%
Life Cycle CO_2 Emissions by Stage			
Biomass Credit (gCO_2/MJ)	-73.7	-70.5	-68.9
Recovery of feedstock (gCO_2/MJ)	13.6	17.2	26.4
Transportation of feedstock (gCO_2/MJ)	3.2	3.1	3.1
Processing of feedstock to fuel (gCO_2/MJ)	7.1	10.3	13.2
Transportation of jet fuel (gCO_2/MJ)	0.6	0.6	0.6
Combustion CO_2 (gCO_2/MJ)	70.4	70.4	70.4
WTT GHG Emissions by Species			
WTT CO_2 emissions (gCO_2/MJ)	-49.2	-39.2	-25.7
WTT CH_4 emissions (gCO_2e/MJ)	1.0	1.3	1.7
WTT N_2O emissions (gCO_2e/MJ)	17.6	22.4	29.5
Total WTW GHG emissions (gCO_2e/MJ)	39.8	54.9	75.9
Life Cycle GHG Emissions Relative to Baseline Conventional Jet Fuel	0.45	0.63	0.87

Table 23: Life cycle GHG emissions for production and use of renewable jet fuel from rapeseed assuming cultivation on set-aside land

Land Use Change Scenario R1	**Low**[1]	**Baseline**[1]	**High**[1]
Land use change emissions (gCO_2/MJ)	38.4	43.0	52.6
WTW CO_2 emissions (gCO_2/MJ)	35.8	40.0	48.9
WTW N_2O emissions (gCO_2e/MJ)	2.7	3.0	3.6
Total WTW GHG emissions (gCO_2e/MJ)	78.2	97.9	128.5
Life Cycle GHG Emissions Relative to Baseline Conventional Jet Fuel	0.89	1.12	1.47
Notes: 1) All other input assumptions (rapeseed cultivation, extraction of oil, processing of oil to HRJ) are based on those in the R0 emissions case of the corresponding scenario.			

7.4 HRJ from Jatropha Oil

The creation of HRJ from jatropha oil is not a pathway available in GREET; hence, supporting information was obtained from the literature and a pathway was constructed within the GREET framework. The jatropha fruit is composed of an outer capsule containing two or three seeds. Each seed has a shell and a kernel, which contains oil. This structure differs from other oil seed crops because additional co-products beyond meal result from the oil extraction process.

There are also concerns with jatropha cultivation for biofuels that do not apply to soy, palm, or rapeseed. An overarching concern of jatropha cultivation for fuel production is that the biomass co-products are toxic to both humans and animals. Further, there are questions regarding the introduction of a non-native invasive species to the North American ecosystem. The toxicology of jatropha oil is discussed later in this section while more details on the impacts of invasive species within the North American ecosystem are provided in Section 7.4.3.

7.4.1 Yield and Plant Characterization

Jatropha plants are well adapted to semi-arid conditions, although more humid environments are shown to result in higher crop yields. The plant can tolerate high temperatures but it does not tolerate frost, which causes immediate damage. Upon removal of the outer capsule, the primary products are seeds and the co-products are husks; at this stage, the seeds can be processed directly or the shells can be removed through decortication.[31] If the seeds are left intact, oil is extracted leaving de-oiled cake as the co-product. If the shells are removed before oil extraction, oil and meal are created from the kernel and the shells are considered a separate co-product. The parts of the jatropha fruit are characterized in Table 24.

Upon examination of 28 growth sites worldwide, a correlation of 0.22 was found between the quantity of precipitation and seed yield (Achten et al., 2008). This means that although more precipitation is moderately connected to higher seed yields, there are many cases where excellent yields have been realized in dry conditions and poor yields realized in wet conditions. The majority of data used in this work came from cultivation details and physical characterization of jatropha by Reinhardt et al. (2008) and Achten et al (2008).

Based on these data, it was concluded that an average yield of 2500kg/ha/yr of dry seeds is a representative estimate while 5000kg/ha/yr could be realized under optimal management practices; 1000kg/ha/yr appears to be a reasonable lower bound (Achten et al., 2008; Reinhardt et al., 2008). These values provide the bounds on yield for the low and high emissions cases. Note

[31] Decortication is a procedure involving the removal of a surface layer, membrane or fibrous cover. In the case of jatropha, this refers to the removal of the shells from the kernels.

that yields are quoted in terms of seed weight. To fully characterize the fruit, mass ratios of oil to seed, husk to seed and kernel to seed were developed for the low emissions, baseline and high emissions cases. These are shown Table 25 in conjunction with yield assumptions.

Table 24: Parts of the jatropha fruit including processed states

Product	Energy Content (MJ/kg)	Sub-fractions	Description
Capsule	--	Husk + seeds	Entire fruit
Husk	15.5	--	Outer core of fruit, surrounding seeds; green and 'fleshy' in fresh state, later brown and dry
Seed	--	Shell + kernel	Compact unit inside fruit, consists of shell and kernel, usually 2-3 per capsule
Shell	19.0	--	Brown or black shell surrounding the kernel
Kernel	--	--	White compact nucleus of seed, actual oil-containing part of the fruit
Oily cake	19.5	Seeds (processed)	Leftovers from the mechanical oil extraction from seeds (incl. shells), contains residual oils
De-oiled cake	17.5	Seeds (processed)	Leftovers from the mechanical and solvent-aided oil extraction from seeds
Meal	18.0	Kernels (processed)	Leftovers from the mechanical and solvent-aided oil extraction from seeds
Notes: 1) Reinhardt et al (2007 and 2008)			

Table 25: Yields and mass fractions characterizing the jatropha fruit

	Low	Baseline	High
Jatropha Yield (kg_{seed}/ha/yr)	5000	2500	1000
Oil Ratio (kg_{oil}/kg_{seed})	0.37	0.35	0.34
Husk Ratio (kg_{husk}/kg_{seed})	0.48	0.60	0.60
Kernel Ratio (kg_{kernel}/kg_{seed})	0.67	0.63	0.63

7.4.2 Cultivation of Jatropha Fruit

The input assumptions surrounding jatropha cultivation are based on a 30-hectare test plot in India documented by Reinhardt et al. (2008). The inputs required for growth are seedlings, irrigation water (first three years only), diesel fuel (for tractor and irrigation pump) and mineral fertilizers in the form of nitrogen, phosphorous pentoxide (P_2O_5) and potassium oxide (K_2O). Since irrigation water is needed for only the first three years of growth, this analysis does not include the diesel fuel required for pumping irrigation water in calculating life cycle GHG emissions of HRJ from jatropha. The cultivation assumptions adopted in this work are listed in Table 26.

Table 26: Cultivation inputs for the growth of jatropha

	Low	Baseline	High
Cultivation Diesel (Btu/kg_{seed})	1163	1320	1419
Pesticides (g/kg_{seed})	0	0	0
Nitrogen (g/kg_{seed})	31.8	34.0	35.3
P_2O_5 (g/kg_{seed})	12.6	13.0	13.4
K_2O (g/kg_{seed})	31.3	37.4	37.4

Nitrous oxide emissions from jatropha cultivation were estimated using the IPCC Tier 1 methodology (De Klein et al., 2006). Due to the lack of data, N_2O emissions from nitrogen in above and below ground crop residues were not accounted for in this analysis. The IPCC Tier 1 methodology estimates the combined direct and indirect conversion rate of nitrogen from synthetic fertilizers to N_2O emissions as 1.1%. These rates include the atmospheric deposition of nitrogen volatilized from managed soils; however, nitrogen from leaching and runoff was assumed to be negligible, in terms of N_2O conversion, as jatropha is ideally grown in well-drained or gravelly soils[32] (Achten et al., 2008). The formula used for calculating N_2O emissions from jatropha cultivation is given by:

$$N_2O\ \text{Emissions}\left(\frac{g_{N_2O}}{kg_{seed}}\right) = \left(\frac{g_{\text{nitrogen fertilizer}}}{kg_{seed}}\right) \cdot 0.011 \cdot \left(\frac{44g_{N_2O}}{28g_N}\right) \qquad \text{Equation 11}$$

7.4.3 Toxicity of Jatropha Fruit and Oil

Due to the toxicity of jatropha fruit and oils, attention is warranted to the impacts on human health and work environment. The fruits contain irritants affecting pickers and manual dehuskers. In addition, accidental consumption of the seeds or oils can lead to severe digestion problems. For these reasons, intercropping edible crops with jatropha is only recommended during the period before any fruit is borne (Achten et al., 2008). Gandhi et al. (1995) evaluated the crude oil in vivo and in vitro for toxicity, skin irritation and haemolytic activity. The toxic fraction containing phorbol esters was subsequently isolated from the oil. Locals use the oil as a cathartic purgative and for treating skin ailments. The seeds are also used for the treatment of dropsy, gout, paralysis and rheumatism. Upon administering tests on mice, rats and rabbits, jatropha oil was found to be acutely toxic after oral administration, leading to diarrhea, bloodshot eyes and inflammation of the gastro-intestinal tract. Topical application not only had an irritant effect but also caused diarrhea and mortality in the animals. Gandhi et al. (1995) summarize the impacts of ingestion and contact with jatropha oil as a severe health hazard to livestock and humans. The phorbol esters in the oil are irritants of skin and mucous membranes produce haemolysis of red blood cells and are reported to be tumor promoters (Gandhi et al., 1995). These results lead to the conclusion that complete removal of toxins is essential before any industrial applications are considered for jatropha oil. The removal of toxins was not modeled as a source of GHG emissions within this analysis.

7.4.4 Transportation of Jatropha Fruit to Production Facilities

Even though there are questions regarding the wisdom of introducing potentially invasive species such as jatropha to non-native environments, the production of jatropha in this analysis is assumed to take place in the southwestern United States. If the oil were produced overseas, then there would be an increase in the GHG emissions from transportation, comparable to that discussed in regards to rapeseed oil (see Section 7.3.4). After harvesting, assumptions of the transportation mechanisms and distances are consistent with GREET defaults for the soybeans to HRJ pathway. Specifically, the transportation of capsules is by truck to a local storage area and subsequently to a local oil extraction facility. The capsule processing, oil extraction and hydroprocessing of oil to HRJ are assumed to occur at the same location with on site capabilities for power generation using biomass co-products. As was the case in other HRJ pathways, transportation elements of the life cycle GHG emissions are sufficiently small to be within the margin of error; therefore, assumptions in this area carry little consequence.

[32] Nitrous oxide emissions from leaching and run off only apply to soils where the soil water-holding capacity is exceeded (IPCC, 2006)

7.4.5 Extraction of Oil from Jatropha Fruit

Extracting oil from the jatropha fruit has a large influence on the life cycle emissions. Before beginning oil extraction, a dehusker must remove the husks and obtain the seeds. In small-scale production facilities, the seeds are then crushed in a screw press to extract the oil. This method can only obtain up to 80% of the oil so larger production facilities mill the seeds into small particles and N-hexane chemical solvent is used to obtain up to 99% of the oils (Achten et al., 2008). The deterministic factor of this life cycle is how the co-products are used (husks, shells, meal). It is not necessary to remove the shells from the kernels before the solvent treatment, but it is more energy efficient to do so because the additional burden of processing the added material from the shells through the chemical solvent is more than the burden of removing the shells beforehand. If the shells are removed prior to milling, they are obtained independently of the meal and the oil. If the shells were not removed, the seeds could be split into a de-oiled cake and the oil itself. Regardless of whether the shells are removed, the resultant product is not suitable for animal and human consumption because of its toxicity (see Section 7.4.3).

The co-products from oil extraction can be used in a multitude of capacities. Figure 18 shows the products resulting from this process and potential uses for each.

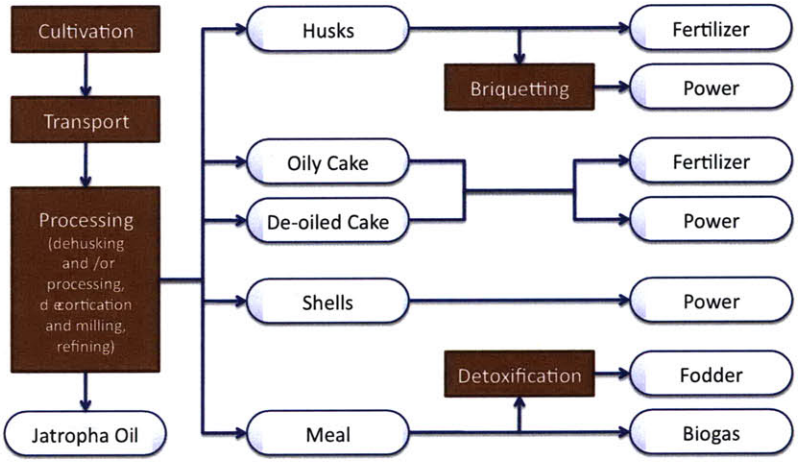

Figure 18: Utilization of by-products from jatropha cultivation and oil extraction (adapted from Reinhardt, 2007)

When using the co-products from jatropha, caution must be maintained due to its toxicity. For example, the use of shells and meal as fertilizer in edible crop production raises bio-safety questions and warnings have been issued to the serious lack of information surrounding the health effects of burning the oil in closed quarters (Achten et al., 2008).

To estimate the emissions from oil extraction, this work combined the process inputs from Reinhardt et al. (2008) with modified processes for oil extraction from soybeans established by Sheehan et al. (1998a) to model oil extraction from jatropha fruit in an N-hexane extraction facility. The assumed process energies are summarized Table 27.

Table 27: Process inputs for extracting oil from jatropha fruit

	Low[1,3]	Baseline[1]	High[1]
Receiving and Storage			
Electricity	33.5	38.3	39.4
Jatropha Preparation			
Electricity (briquetting)	93.2	122.8	126.6
Electricity (decorticator)	23.2	24.6	25.3
Electricity (dehusking)	51.6	59.0	60.7
Electricity (cleaning)	3.0	2.9	3.0
Steam (cleaning)	125.9	123.2	127.0
Oil Extraction			
Electricity	9.4	9.2	9.5
N-hexane[4]	77.3	75.7	77.9
Meal Processing			
Electricity	38.1	37.3	38.4
Steam	368.7	361.0	371.9
Oil Recovery			
Electricity	1.0	1.0	1.0
Steam	63.2	61.9	63.8
Solvent Recovery			
Electricity	1.4	1.3	1.4
Steam	0.0	0.0	0.0
Oil Degumming			
Electricity	4.4	4.3	4.5
Steam	49.7	48.6	50.1
Waste Treatment			
Electricity	1.5	1.5	1.5
Steam	26.7	26.2	27.0
Totals			
Electricity	260.3	302.1	311.2
Natural Gas[2]	792.8	776.3	799.6
N-hexane[4]	77.3	75.7	77.9

Notes:
1) All values are in Btu per pound of oil
2) Steam is generated from natural gas with an efficiency of 80%.
3) The low emissions case appears to have higher process energy than the baseline; however, this arises due a larger fraction of the seed weight going through the extraction processes (see Table 71) and is counteracted in the fuel production stage.
4) GREET uses Liquefied Petroleum Gas (LPG) as a surrogate for N-hexane when calculating emissions

7.4.6 Co-Product Usage and Allocation Methodology

To understand the influence of co-product type and usage on the life cycle emissions of the fuel, four scenarios, outlined in Table 28, were considered. These scenarios examined how the life cycle GHG emissions of HRJ from jatropha oil change depending on the use of co-products for animal feed, fertilizer or electricity production. The electricity production was further broken down to examine displacement of US average grid electricity and energy allocation between oil and electricity. The life cycle GHG emissions resulting from each scenario are summarized in Figure 19.

As explained below, Scenario 1 was chosen for this analysis. Using the products for power generation seems a more logical choice for the biomass co-product because the displacement of

fertilizer on large scales with a product that is toxic to humans was deemed undesirable due to the potential for ground water contamination (this eliminates Scenario 2). Energy allocation was chosen over displacement due to the large quantities of co-product generated per unit of oil production (this eliminates Scenarios 3 and 4). As shown in Figure 19, the displacement of fossil based electricity results in the unrealistic result of negative life cycle GHG emissions for the fuel. It is important to understand that the allocation method used in scenario 4 attributes energy and emissions based on the electricity produced from the biomass co-products and the energy contained in the oil. This is equivalent to expanding the system boundary of the oil extraction stage to include the power generation unit. Assumptions regarding the generation of renewable electricity from biomass are outlined in Table 29.

Table 28: Co-product creation and allocation scenarios from the oil extraction process for jatropha capsules. The corresponding life cycle emissions for each scenario are shown in **Figure 19**

Scenario	Co-Product	Use	Emissions Allocation Method
1	Husks, shells and meal	Burned for electricity	Energy allocation via energy of electricity produced and energy contained in the oil
2	Husks, shells and meal	Fertilizer	Displacement method (system expansion) where fertilizers are displaced in subsequent cultivation practices
3	Husks and shells	Burned for electricity	Displacement method (system expansion) where electricity from US grid is displaced
	Meal	Detoxified and sold for animal feed	Market value allocation between oil and meal.
4	Husks, shells and meal	Burned for electricity	Displacement method (system expansion) where electricity from US grid is displaced

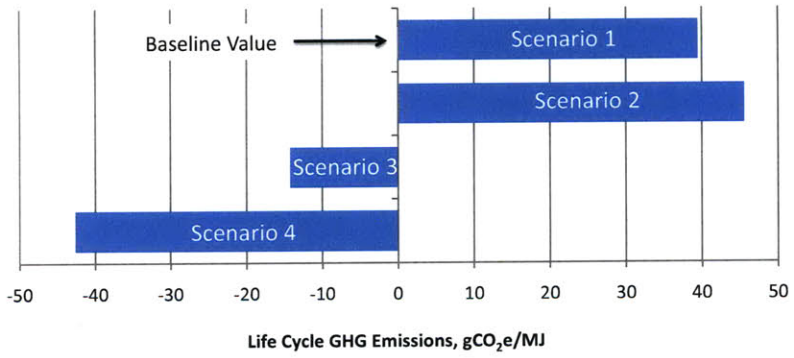

Figure 19: Sensitivity of life cycle emissions of HRJ from jatropha to co-product utilization and allocation scheme. Scenarios are described in **Table 28**

Table 29: Assumptions used in establishing average US biomass conversion efficiency to electricity

Generation Method	Production Share	Generation Efficiency
Biomass Utility Boiler	99%	32.1%
Biomass IGCC	1%	43.0%
Note: 1) Transmission losses of 8% were also included in the overall efficiency of generation		

7.4.7 Results

The life cycle emissions from the production and use of HRJ fuel from jatropha oil are given in Table 30. The life cycle GHG emissions resulting from the production and use of jatropha HRJ range from 0.36 to 0.52 times those from conventional jet fuel. The variation in the biomass credit is due to minor changes in the allocation scheme through the pathway. Because marginal land was assumed and no estimates of root carbon sequestration from jatropha were available, the GHG emissions from land use change were assumed to be zero and no other land use change scenarios were created.

Table 30: Life cycle emissions from the jatropha oil to HRJ pathway

	Low	Baseline	High
Key Assumptions			
Jatropha Seed Yield (kg/ha/yr)	1000	2500	5000
Jatropha Seed Oil Fraction	0.34	0.35	0.37
Life Cycle CO_2 Emissions by Stage			
Biomass Credit (gCO_2/MJ)	-73.7	-70.5	-68.9
Recovery of feedstock (gCO_2/MJ)	16.1	16.7	17.6
Transportation of feedstock (gCO_2/MJ)	1.5	1.5	1.5
Processing of feedstock to fuel (gCO_2/MJ)	7.1	10.3	13.2
Transportation of jet fuel (gCO_2/MJ)	0.6	0.6	0.6
Combustion CO_2 (gCO_2/MJ)	70.4	70.4	70.4
WTT GHG Emissions by Species			
WTT CO_2 emissions (gCO_2/MJ)	-48.5	-41.3	-36.1
WTT CH_4 emissions (gCO_2e/MJ)	1.0	1.2	1.4
WTT N_2O emissions (gCO_2e/MJ)	8.9	9.1	9.4
Total WTW GHG emissions (gCO_2e/MJ)	31.8	39.4	45.1
Life Cycle GHG Emissions Relative to Baseline Conventional Jet Fuel	0.36	0.45	0.52

Nitrous oxide emissions represent more than 20% of the total life cycle GHG emissions from the jatropha to HRJ pathway. As such, the consequences of the uncertainty associated with IPCC correlations are more pronounced for this pathway. The reader should be aware of these inherent uncertainties when comparing different pathways for GHG reduction potential in sections 10.1 and 10.2.

7.5 HRJ from Algae Oil

The creation of HRJ from algae oil is not a pathway available in GREET; hence, supporting information was obtained from the literature.[33] Algae can be grown in an open pond, a controlled bioreactor, or a combination of both. A typical open pond approach consists of a raceway (oval) shaped pond using a paddlewheel to circulate the water and mix the algae for even light exposure and growth. In bioreactors, the algae are grown in sheets or tubes, allowing for much higher growth rates per unit area than open ponds. Bioreactors shield the algae from weather variations and facilitate growth in vertical geometries thereby reducing land requirements; however, these designs are cost intensive relative to open ponds. Only open pond technologies were examined in this analysis because of their reduced capital costs, the relative abundance of experimental documentation, and their increased technological readiness (relative to bioreactors). Given time, the capital costs of bioreactors could decrease as technological advances are made; these concepts will be examined further as a part of this continuing research effort. Furthermore, only conventional means of oil extraction using chemical solvents were considered in this report. As was discussed in the introduction of this chapter, there is currently much research devoted to other methods of oil extraction including genetic modification of the algae such that they naturally excrete oil and using electric shocks to open the algal cells. Such methods were not considered here.

7.5.1 Algal Yield and Lipid Content

The two defining characteristics for algae as a biofuel are its growth rate (generally given in grams/m^2/day) and lipid content (generally given as a weight percent of total biomass). Both quantities vary greatly within the literature as they depend on variables including algae type and weather conditions, among many others. Generally higher algal growth rates reported in the literature represent bioreactor technology and not open ponds. Some recent presentations have employed yields equivalent to 140g/m^2/day at 25% lipids content; an estimate over 550% of the yields adopted in this study (Daggett, 2007). The current analysis is based on the engineering judgment of the authors gained from their literature review of open ponds. During peak periods of growth, 50g/m^2/day could be achieved, but a yearly average of 20 g/m^2/day appears to be more reasonable (Ben-Amotz, 2008; Sheehan et al., 1998b). A survey of algal strains also returned a range of lipid contents up to 40% (Becker, 2007). Assuming that technology will improve by the simulation year of 2015, 50 g/m^2/day and 40% lipids by weight was adopted for the low emissions case, 25 g/m^2/day and 25% lipids by weight was adopted for the baseline case and 20 g/m^2/day at 15% lipids by weight was adopted for the high emissions case.

7.5.2 System Expansion (Displacement) for Electricity Emissions

While much of the methodology for the analysis of algal HRJ is similar to that discussed for other HRJ pathways, the life cycle is complicated by the need to feed CO_2 to the algae to sustain acceptable growth rates. As schematically shown in Figure 20, system expansion (displacement method) was used instead of energy allocation when apportioning emissions between the fuel and any electricity generated in providing the CO_2 required for growth. Justification for this choice is rooted in the argument that electricity used for CO_2 production operates independently of the algae cultivation and hence, should be treated differently than co-products physically created from the cultivation itself. The system boundary was expanded to include both the electricity and emissions from a power plant producing equivalent electricity to that within the original system boundary. The expanded system had both HRJ and biomass co-products leaving the system boundary, but zero net electricity exiting the expanded system. Thus, the expanded system could be treated in a similar fashion as the other HRJ pathways.

[33] Algae oil is not a preexisting pathway within GREET. As such, a new pathway was built within the GREET framework using the soy oil to renewable diesel pathway as a guide.

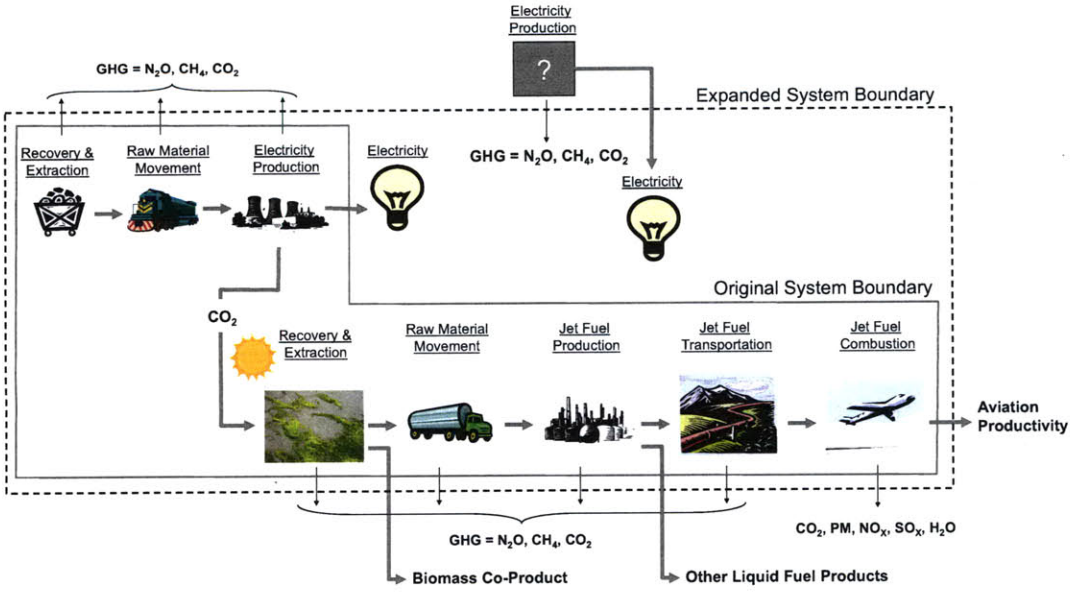

Figure 20: System boundary expansion of the algal HRJ fuel pathway

The life cycle GHG emissions from the type of electricity used to supply CO_2 for algal growth and the type of electricity being displaced both impact the life cycle emissions of the algal fuel. This is due to the variation that could exist in the emissions per kilowatt-hour of different power generation technologies (e.g. a coal utility boiler has higher emissions than an integrated gasification combined cycle which, in turn, has higher emissions than a nuclear power plant). The options in Table 31 outline the effects on the life cycle emissions that these choices could cause. When CO_2 created from 'dirty' electricity is used to feed algal growth, but 'clean' electricity is included in the expanded system then the CO_2 emissions credit is less than the CO_2 used to grow the algae; this results in a fuel that appears to be 'dirty' in terms of higher CO_2 emissions. When CO_2 created from 'clean' electricity is used to feed the algae but 'dirty' electricity is included in the expanded system then the CO_2 emissions credit is greater than the CO_2 used to grow the algae; this results in a fuel that appears to be 'clean' in terms of lower CO_2 emissions. In this analysis, the electricity used to provide the CO_2 was assumed to be the same as that in the expanded system. For this configuration, the CO_2 emissions credit was approximately equal to the biofuel combustion emissions, which is the assumption used for biofuels that have not been 'fed' CO_2 for enhanced growth.

Carbon dioxide usage in algae cultivation can vary depending on the lipid content and meal carbon content of the algae. A simpler approach was adopted in this analysis where data from the literature were used to conclude that algae as a whole is approximately 60% carbon (Weissman and Goebel, 1987; Kadam, 2001). The supporting literature indicates that CO_2 requirements range from 2.16-2.2 kg per kg of algae grown. Emissions factors for power plant technologies from GREET are listed in Table 32 (these are not the full life cycle GHG emissions from power generation, rather they are just the CO_2 available to be captured and used from the power plant itself). Depending on the power plant, between 0.23 and 0.5 kg of algae could ideally be grown from the CO_2 resulting from each kWh of electricity. This includes electricity generated from biomass.

Table 31: Impact of CO_2 source and electricity choice on the biomass credit given to algal HRJ

CO_2 Source for Algae Growth	**Electricity displaced in expanded system boundary**	**CO_2 "Biomass Credit" allocated to the algal fuel**
Conventional Coal Electricity	Conventional Coal	Biomass Credit ≈ Combustion CO_2
	US Average Grid	Biomass Credit < Combustion CO_2
	Nuclear (zero CO_2)	Biomass Credit ≈ 0
US Average Grid Electricity	Conventional Coal	Biomass Credit > Combustion CO_2
	US Average Grid	Biomass Credit ≈ Combustion CO_2
	Nuclear (zero CO_2)	Biomass Credit ≈ 0

Table 32: US power generation data as it relates to algae cultivation

Generation Technology	**Fraction of US Mix (%)**	**Power Plant Efficiency (%)**	**Power Plant Emissions (g_{CO2}/kWh)**	**Plant Capacity for Algae Cultivation (kg_{algae}/kWh)**
Oil-Fired	2.6	34.8	834	0.38
NG-Fired	22.5	43.5	495	0.23
Coal-Fired	48.7	36.1	1027	0.47
Biomass Fired	1.3	32.2	1084	0.50
Nuclear	17.6	--	0	0
Other (hydro, wind, etc.)	7.3	--	0	0

Notes:
1) All data from GREET (2008)
2) Based on 2.18 kg CO_2 being required per kg of algal growth

7.5.3 Algal Carbonation Options and Technologies

Algae cultivation using an open pond configuration can be supplied CO_2 as a part of flue gas either from an adjacent power plant or from a purified CO_2 stream. Flue gas is approximately 14% CO_2 (Kadam, 2001) but can be purified to more than 99% CO_2 using the recyclable solvent monoethanolamine (MEA). The process known as MEA extraction is specifically targeted to remove large amounts of CO_2 from flue gas. The greatest advantage of MEA extraction is its relatively high carrying capacity in terms of the amount of CO_2 absorbed per unit volume of solvent. Less solvent circulation is required for a given system performance specification, leading to lower capital and operating costs than other solvent extraction methods (Herzog et al., 1991).

Little data exists documenting the benefits, if any, of using pure CO_2 compared to flue gas as a carbon source for algae cultivation. The assumption here is that both methods result in the same algae yield. The disadvantage of flue gas manifests from the compression and transportation of over seven times more gas volume for the same quantity of CO_2. For this reason, flue gas usage is only considered an option for algae cultivation facilities co-located with their CO_2 source. The disadvantage of pure CO_2 is that flue gas must be scrubbed to remove all non-CO_2 elements and subsequently compressed for transportation; flue gas requires only a simple blower. Scrubbing flue gas using the MEA process requires substantial quantities of steam and energy intensive compression. The compression can represent between 13 and 30 percent of the total process energy consumption (Herzog et al., 1991). Table 33 compares the energy usage of direct flue gas injection with two studies estimating energy usage for the MEA process. In both MEA studies,

98% of the energy results from producing steam to strip CO_2 from the amine solution. The remainder of the MEA process energy, and all energy for direct injection, comes from electricity.

Table 33: Comparison of energy inputs of direct flue gas injection and MEA extraction

	Total Energy (MJ/t_{CO2})	Total Energy (MJ/kg_{algae})	Emissions (g_{CO2}/kg_{algae})
Direct Injection			
Kadam (2001)	80	0.18	35
MEA			
Kadam (2001)	6650	14.63	911
Herzog et al. (1991)	6097-10248	13.41-22.55	835-1404
Note: 1) Steam production is assumed to occur using an 80% efficient industrial boiler			

The emissions to create a pure CO_2 stream are over 25 times higher than those from using flue gas from a co-located source. For this reason, the low and baseline scenarios adopted the assumption that algae cultivation occurs adjacent to a power plant, thus using flue gas as the CO_2 source. The high emissions scenario assumed that CO_2 must be scrubbed from the flue gas using MEA extraction prior to compression for transportation and storage, according to the estimate by Kadam (2001). This assumption is appropriate for facilities that are not located in the immediate vicinity of a CO_2 source. Furthermore, transportation energy is not included in the estimates of Table 33 and would be a function of distance between the CO_2 source and algae cultivation facility.

7.5.4 Cultivation of Algae in Open Ponds

The process energy and nutrient requirements for algae cultivation were established from two sources: (1) a simulated open pond algae farm that was used to capture flue gas from an adjacent fossil power plant and (2) design specifications for an open pond system used for fuel production. The simulated open pond algae farm parameters were obtained for a 1000-hectare algal production system based on primary bench scale data and process modeling (Kadam, 2001). Weissman and Goebel generated the open pond design specifications for a 192-hectare system in 1987 (Weissman and Goebel, 1987). While Kadam presents all energy inputs of cultivation and harvesting as a single value, Weissman and Goebel show the inputs for the individual steps of mixing, pumping, primary harvesting and secondary harvesting. The data from both studies are in good agreement and were amalgamated to form the inputs to this analysis.

Since both studies quote similar electrical inputs, all electricity estimates were taken from Weissman and Goebel due to their higher degree of detail. In their design specifications, electric motors were assumed to operate with a drive efficiency of 70%. Drive efficiency encompassed the motor, an in-line speed reducer and a two-stage chain and sprocket reduction. This study considers a simulation year of 2015; hence, modern motors and gearing mechanisms could be incorporated. A modern three-phase (variable speed) electric motor meeting similar cost and performance requirements is rated as up to 92.4% efficient (Marathon Electric, 2009). The mechanical efficiency of a chain and sprocket has been found to reach 98.6% in ideal conditions and 81% in poor conditions (Spicer et al., 2001). Assuming both a motor and connection efficiency of 90%, the drive efficiency climbs to 81%, corresponding to an improvement of 15.7% above Weissman and Goebel's estimates. This efficiency improvement was applied to all process inputs related to electric motors or electric pumps.

The cultivation inputs used for the low, baseline and high emissions scenarios are shown in Table 34 (normalized per kilogram of algae) while harvesting and drying are dealt with in subsequent sections.

Table 34: Cultivation inputs per kilogram of algae for algae growth in an open pond

	Low	Baseline	High
Nutrients			
CO_2 (kg)	2.16	2.2	2.2
Nitrogen (kg)	0.044	0.053	0.053
Superphosphate (kg)	0.019	0.029	0.039
Potassium Sulfate (kg)	0.030	0.030	0.030
Process Energy			
Mixing (Btu)	281.8	281.8	281.8
Water Supply (Btu)	229.8	229.8	229.8
Nutrient Supply (Btu)	16.2	16.2	16.2

Nitrogen from fertilizer use was assumed to come only from ammonia. As a well-established fertilizer in the farming industry, ammonia has a production pathway within the GREET framework. The production pathways of superphosphate and potassium sulfate are not established within GREET. The process energies required for the production of superphosphate were adopted from Anderi Silva and Alexandre Kuley (2003). Specific inputs for potassium sulfate were not available in the literature. A final emissions inventory from potassium sulfate production was taken from Kadam (2001). The emissions resulting from the production of nitrogen fertilizer, superphosphate and potassium sulfate are summarized in Table 35.

Table 35: Life cycle GHG emissions from the production of nutrients used in algae cultivation

	Nitrogen	Superphosphate	Potassium Sulfate[1]
CO_2	2537	235	-370[1]
CH_4	62.5	7.5	1.5
N_2O	5.6	1.3	1.5
Total	2605	244	-367

Notes:
1) Negative process energy flows occur due to displacement allocation being used in their life cycle assessment
2) Units are g CO_2e/kg of nutrient

Nitrous oxide emissions from algae cultivation were estimated using IPCC Tier 1 methodology for flooded rice fields (De Klein et al., 2006). It was assumed that the conversion rate of nitrogen contained in a flooded rice field is similar to the conversion rate of nitrogen from an open pond. Open ponds were the only source of N_2O emissions from algae considered in this work. The IPCC Tier 1 methodology for flooded rice fields estimates the direct conversion rate of nitrogen from synthetic fertilizers as 0.3%. No mechanisms for indirect emissions were considered due to a lack of information. The formula used in this study for calculating N_2O emissions from algae cultivation is given by:

$$N_2O\ \text{Emissions}\left(\frac{g_{N_2O}}{kg}\right) = \left(\frac{g_{\text{nitrogen fertilizer}}}{kg}\right) \cdot 0.003 \cdot \left(\frac{44 g_{N_2O}}{28 g_N}\right) \qquad \text{Equation 12}$$

7.5.5 Nutrient Recycling via Anaerobic Digestion

Fertilizer production is a non-negligible GHG source in the algae to HRJ pathway. As can be seen from the data in Table 36, which were derived from Table 34 and Table 35, the nitrogen fertilizer emissions are comparable to those from the baseline soybean to HRJ pathway. High quantities of fertilizer in any algal effluent leaving the system can also lead to eutrophication of natural waters. The additional fertilizer can over-stimulate the production of organic compounds leading to negative environmental effects such as hypoxia and reductions in water quality, fish, and other animal populations. If not properly contained, the environmental impacts of this process include decreased biodiversity, changes in species composition and dominance, and toxicity. These considerations warrant an investigation into nutrient recycling systems to reduce fertilizer demand. The analysis that follows assumes that all nitrogen and phosphorous is contained in the meal after oil extraction.

Table 36: GHG emissions resulting from fertilizer production within the algae to HRJ pathway for the three emissions cases

	Low	Baseline	High
Nitrogen (gCO_2e/kg_{algae})	114.6	130.3	138.1
Superphosphate (gCO_2e/kg_{algae})	4.6	7.1	9.5
Potassium Sulfate (gCO_2e/kg_{algae})	-11.0	-11.0	-11.0

One means of nutrient recycling is anaerobic digestion, wherein microorganisms break down carbon-based matter in the absence of oxygen. It is widely used as a renewable energy source because the process produces a methane-rich biogas. Other products of anaerobic digestion are a liquid effluent and a solid digestate. Of interest here is the nutrient-rich liquid effluent that can be used to supplement fertilizers. A conventional reactor is maintained at an operating temperature of approximately 35°C. Retention times for conversion range from 20 to 30 days where about 60% of organic carbon is converted to biogas. The biogas composition is typically 60% methane and 40% CO_2 with traces of hydrogen sulfide and water vapor (Chynoweth et al, 2001). By using the algal meal co-products to feed a digester, a substantial nutrient fraction could be recovered. Such systems would also allow for the recycle of carbon contained in the meal, thus reducing the demand on an external CO_2 source.

Several factors affect the rate of digestion and biogas production. The most important is temperature. Anaerobic bacteria communities can endure temperatures ranging from below freezing to above 57°C, but they thrive best at temperatures between 37°C and 54°C. Bacteria activity, and thus biogas production, falls off gradually from 35°C to 0°C (DOE, 2008). In some cases, the conventional design discussed above is being replaced by more innovative designs influenced primarily by the suspended solids content of the feed. Designs for feed with intermediate solids contents (such as sewage sludge or aquatic plants) involve recycling the solids following settling within the digester. Such designs have increased loading rates 20-fold and improved process stability. Furthermore, the biodegradability of certain feedstocks has been seen to exceed 90% (Chynoweth et al., 2001).

The process flows for an algae system that includes an anaerobic digester are shown in Figure 21. It is assumed that the algae are being grown in areas with sufficient heat and sunshine to sustain the required temperature of 35°C and the energy required to maintain a suitable temperature is negligible from the life cycle analysis standpoint. Furthermore, any additional heating requirements would be low-grade and could be met using flue gas before injection into the pond or exhaust gas from the drying facility.

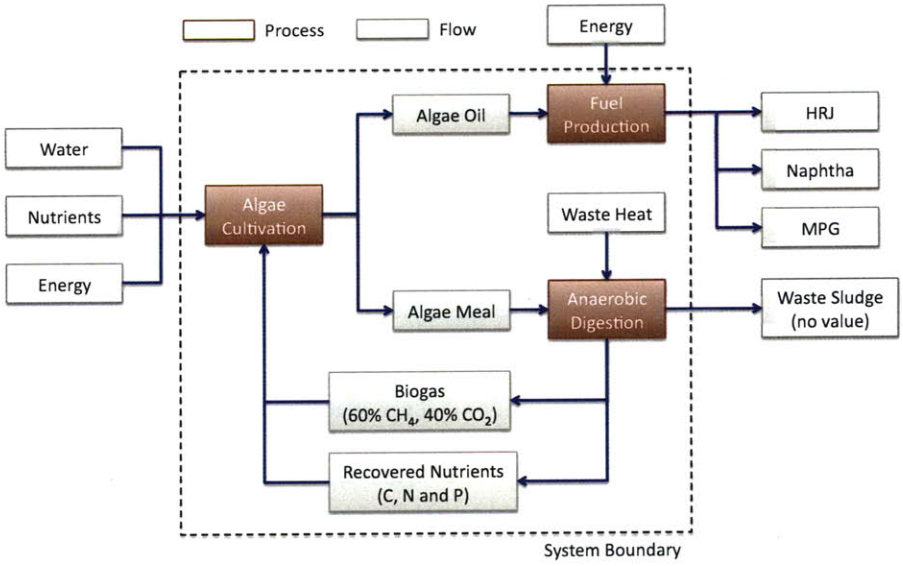

Figure 21: Process flows for algae oil HRJ using anaerobic digestion to recover nutrients from algae meal

Weissman and Goebel explored the potential for nutrient recovery from algae meal using anaerobic digestion. They projected that 50% of carbon not converted to biogas, 75% of all nitrogen and 50% of all phosphorous could be recovered in the liquid effluent. The remainders would be contained in the digestate, which is considered a waste of zero value.

The carbon content of algae meal can vary depending on the total carbon content and lipid faction of the algae. It is also directly proportional to the methane production potential from anaerobic digestion. Algae was assumed to have a constant carbon content of 60% while lipids were assumed to have a constant carbon content of 76.1% (based on their molecular formula). Under these assumptions, the carbon content of meal, and thus the methane production potential, is a function of lipid fraction.[34]

When digested, the resulting biogas can be used directly to meet internal heat demands or to fuel any other heat engine. Methane within the biogas can be upgraded to the same standards as fossil natural gas. If allowed, the biogas may be utilized within the local gas distribution networks. Gas must be cleaned to reach pipeline quality, and be of the correct composition for the local distribution network to accept it. These restrictions on raw biogas usage outside the system lead to the conclusion that on-site usage is the most practical use for biogas produced from anaerobic digestion.

7.5.6 Dewatering and Drying

After cultivation, algae can represent as little as 1 part in 2000 in water (Kadam, 2001; Weissman and Goebel, 1987). Conventional chemical oil extraction technologies require a feedstock that is approximately 90% dry. The task of extracting and drying the solid algae is the most energy intensive step of the cultivation process. As shown schematically in Figure 22, the algae must first be harvested, then dewatered and finally dried to reach the desired concentration. The applicability of algae as an environmentally beneficial biofuel when using conventional oil

[34] This assumption is most likely only valid for lipid contents between 0 and 50%; however, that is irrelevant because algae strains considered in this work do not exceed 50% lipids.

extraction facilities can be highly dependent on the extent of dewatering and the method of drying.

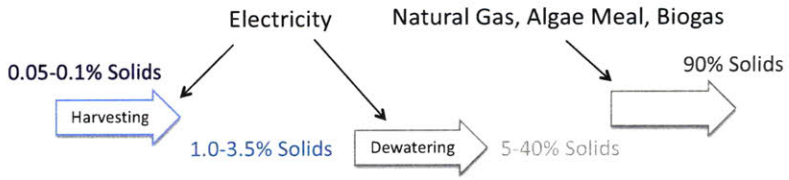

Figure 22: Flow chart showing the steps involved in dewatering and drying of algae

Generally, harvesting and initial dewatering is performed by mechanical or gravitational force while drying relies on direct heating to evaporate the remaining water. Due to the high latent heat of water, dewatering and drying have considerable impact on the life cycle GHG emissions of the pathway. Additional dewatering and less drying generally lead to reduced emissions. Solar, natural gas, algae meal and biogas from the anaerobic digestion of algae meal were considered as options for providing the drying energy. Common types of dewatering procedures are flocculation[35] or settling, filtering with a vacuum or press and centrifugation. The performance of each method is characterized by the total suspended solids (TSS) of the initial feed (given as a percentage by mass), the concentration factor,[36] energy usage per m^3 of throughput and energy usage per kg of processed solids. The initial TSS relates the energy usage per kg of processed solids to the energy usage per m^3 of throughout.

Weissman and Goebel consider three different two-stage harvesting and dewatering configurations. Each begins with a solids concentration of 0.075% and is comprised of primary harvesting using a micro strainer, vacuum belt filter or settling pond followed by secondary dewatering using a centrifuge to achieve 10% solids. The centrifuge dominates energy consumption from this step; hence, a higher concentration factor in the primary harvesting step reduces energy consumption in the centrifuge. Specifications for a belt-filter, micro-strainer and settling pond are given in Table 37 (Shelef et al., 1984). Notice that the concentration factor of the belt filter and settling pond are higher than that of the micro-strainer. In all cases, flocculent must be used to aid in the harvesting process; however, the environmental impacts of the flocculent were assumed to be negligible in terms of the life cycle GHG emissions.

Table 37: Energy consumption and performance specifications for primary algae harvesting mechanisms

Micro-strainer		**Vacuum Belt Filter**		**Settling pond**	
Electricity (Btu/kg)	Concentration Factor	Electricity (Btu/kg)	Concentration Factor	Electricity (Btu/kg)	Concentration Factor
23.8	10	47.6	70	46.9	50

It is desirable to extend the centrifuge energy consumption estimates to explore the impacts of varying the %TSS after dewatering. The result of combining the energy consumed per m^3 of throughput with the initial TSS is the energy consumed per kg of processed solids. The relationship between the energy consumed per kg of processed solids and concentration factor is plotted in Figure 23 and was subsequently used to define a continuous function for the centrifuge energy consumption. Data points originate from the three configurations described by Weissman

[35] Flocculation is a process where particles come out of suspension in the form of floc or flakes. The action differs from precipitation in that, prior to flocculation, the particles are merely suspended in a liquid and not actually dissolved in a solution.

[36] Concentration factor is defined as the ratio of initial feed volume to concentrated volume after separation.

and Goebel and independent average data for a solids ejecting disc centrifuge from Shelef et al. (1984). The advantage of this type of centrifuge for algae harvesting is its ability to reliably dewater to 12-25% solids, although, solids finer than algae may be retained in the overflow stream. Based on a review of the technology survey conducted by Molina Grima et al. (2003) and the conclusions of Shelef et al. (1984), even the best centrifuges appear to have a concentration limit of 25% TSS. More common results place the final TSS level around 15 percent. While following the energy consumption mapped in Figure 23, this analysis assumed that dewatering can occur to a maximum of 25% TSS.

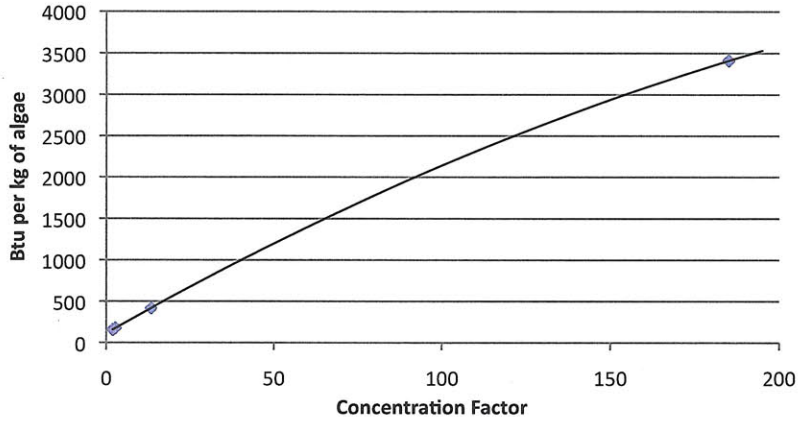

Figure 23: Energy consumption of a centrifuge secondary harvesting mechanism. Line is a fit through four data points

The values in Figure 23 are based on historical studies and may be pessimistic for a simulation year of 2015. As such, the efficiency improvement of 15.7% discussed with regards to cultivation was applied to all electrical inputs of harvesting and dewatering.

Each method must be considered within the context of reliability and scalability. The advantages of micro-strainers are their operation, low energy consumption, and high filtration ratios. Their problems include incomplete solids removal and the buildup of bacterial and algae slime on the micro fabric (Shelef et al., 1984). Regardless of their merits, micro-strainers result in high-energy consumption at the centrifugation stage due to their low concentration factor, making them an undesirable choice. Belt filters and settling ponds are both promising from the perspective of energy consumption and they have been assessed as a reliable method for harvesting (given the use of a flocculent). Furthermore, the concentration factors estimated by Weissman and Goebel are reasonable when compared to data from Shelef at al. (1984). Because some experiments have indicated that belt filters may be less successful at harvesting small algae such as *Chlorella* (Weissman and Goebel, 1987), settling ponds were chosen for the low, baseline and high emissions scenarios.

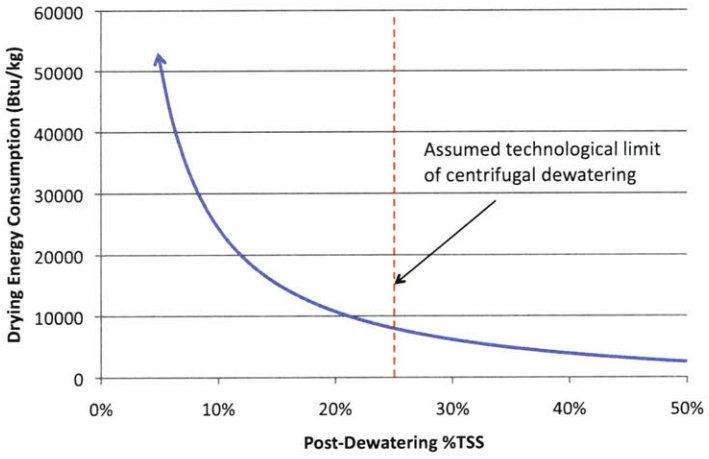

Figure 24: An examination of the post-dewatering moisture content impact on energy consumption of drying algae to 90% total suspended solids

The impacts of dewatering on drying energy requirements are demonstrated in Figure 24. As the extent of dewatering increases, there is a sharp reduction in the energy required for drying to 90% TSS. Drying energy must be in the form of direct heat in order to evaporate water from the algae slurry. Solar drying is considered to be an optimistic choice but is not out of the realm of possibility, with some reports estimating a drying area only 12% of that required for growing (Shelef et al., 1984). The low emissions scenario therefore adopted solar drying while the baseline and high emissions scenarios require the combustion of a process fuel for heat. The process fuel may be natural gas, algae meal or biogas from the anaerobic digestion of algae meal.

As discussed in the previous section, an opportunity for system integration is available by using energy contained in the algae meal to supply internal energy demands. This energy can be obtained by burning the meal directly in a boiler or by combusting the biogas produced from anaerobic digestion. Depending on the quantity of meal produced per kg of algae, some or all of the drying energy can be supplied by these methods. This threshold point, where all drying energy is supplied by the meal, is fundamentally related to the lipid content and the post-dewatering %TSS content. Designing a sustainable drying technique that does not rely on the combustion of non-renewable fuels is essential in creating a sustainable fuel.

The threshold lipid content is also dependent on whether the meal is burned directly or whether anaerobic digestion is used to obtain biogas. These relationships are explored in Figure 25 where two different biomass conversion factors from anaerobic digestion are compared to directly burning the meal in a boiler. While both methods result in zero net GHG emissions from the drying process, nutrient recovery is not possible with meal combustion. The opportunity to recover nutrients leads to the conclusion that an algae cultivation facility concerned with minimizing GHG emissions would be equipped with an anaerobic digester. Therefore, the low and baseline emissions scenario assumed the use of an anaerobic digestion system with biomass conversion factors of 80% and 70% respectively. The high emissions scenario assumed the meal is sold as animal feed.

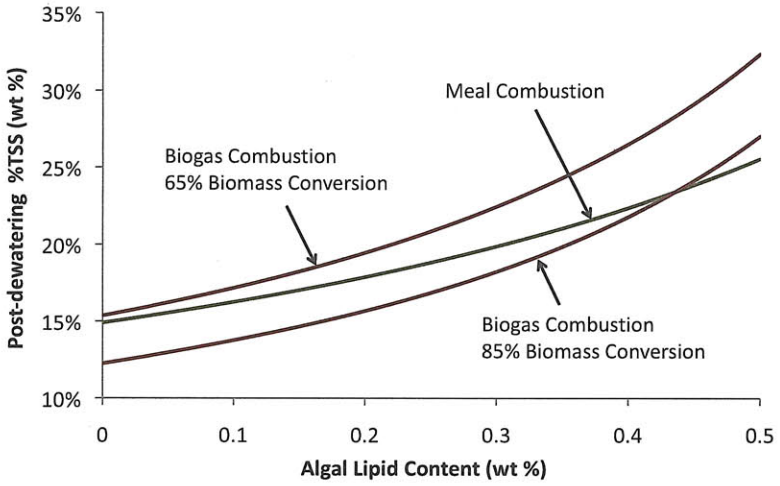

Figure 25: Algal lipid content and post-dewatering moisture content that result in a sustainable drying process. Points above each line require additional energy to be added (e.g. from natural gas)

For an algae strain comprised of 25% oil by mass, sufficient meal is produced to supply the energy to dry other algae from a post-dewatering %TSS content of 19% via direct burning and from 17% to 21% via anaerobic digestion (depending on anaerobic digester efficiency). If the post-dewatering %TSS content were above these threshold values then the algae meal would need to be supplemented by natural gas to supply sufficient energy for drying to 90% TSS.

The decision to use algae meal or natural gas as a drying fuel must be made in the context of the economic, technological and energy usage limitations of dewatering. The trade-offs between these factors and other system parameters can only be understood by considering the entire algal production system.

7.5.7 Transportation of Algae to Production Facilities

The production of algae in this analysis is assumed to take place in the southwestern United States. After harvesting, assumptions about the transportation mechanisms and distances have been modified from GREET defaults for the soybeans to HRJ pathway. When meal is used as an energy source, oil extraction must be collocated with the cultivation facility to enable the recycling and integration of energy flows. In these configurations, only the oil is transported from the cultivation site to a hydroprocessing facility. Specifically, the transportation is by tanker truck in 25-ton shipments; raw algae transportation would occur in truckloads of only 15 tons. In cases where meal is sold as a supplement to animal feed, standard GREET transportation assumptions were adopted. As was the case in every other pathway considered, the contribution from transportation elements in the life cycle analysis are sufficiently small to be within the margin of error; therefore, the importance of these assumptions is minimal. As such, the geographic location of the facility is of secondary importance to the overall results. However, as was discussed in Section 7.5.3, the relative location of the algae facility to its CO_2 source is very important to the life cycle GHG emissions.

7.5.8 Extraction of Oil from Algae

The extraction of oil from algae is currently an area of considerable research. This analysis used a modified version of the process for oil extraction from soybeans established by Sheehan et al.

(1998a) that includes only the processes relevant to algae in an N-hexane extraction facility. The process energies from Sheehan et al. were converted from energy per unit mass of biomass to energy per unit mass of oil using the oil fractions from the low emissions, baseline and high emissions scenarios. The outputs and energy consumption assumed in the extraction of oil from algae are shown in Table 38.

Table 38: Outputs and process energy for N-hexane oil extraction from algae

	Low[1]	Baseline[1]	High[1]
Algae Lipid Content	40%	25%	15%
Meal Produced (lb_{meal}/lb_{oil})	1.5	3	5.67
Receiving and Storage			
Electricity	20.9	33.5	55.8
Algae Preparation			
Electricity	4.0	6.5	10.8
Steam	172.5	276.0	460.0
Oil Extraction			
Electricity	12.9	20.6	34.4
N-hexane[3]	105.9	169.5	282.5
Meal Processing			
Electricity	52.2	83.5	139.1
Steam	505.4	808.6	1347.7
Oil Recovery			
Electricity	1.4	2.2	3.6
Steam	86.7	138.7	231.1
Solvent Recovery			
Electricity	1.9	3.0	5.0
Steam	0.0	0.0	0.0
Oil Degumming			
Electricity	6.1	9.7	16.1
Steam	68.1	109.0	181.6
Waste Treatment			
Electricity	2.0	3.3	5.4
Steam	36.6	58.6	97.7
Total			
Electricity	101.4	162.2	270.3
Natural Gas[2]	1086.6	1738.6	2897.6
N-hexane[3]	105.9	169.5	282.5

Notes:
1) All values are in Btu per pound of oil
2) Steam is assumed to be generated from natural gas with an efficiency of 80%.
3) GREET uses Liquefied Petroleum Gas (LPG) as a surrogate for N-hexane when calculating emissions

As discussed previously, algae meal resulting from oil extraction can be burned in a utility boiler, used as a feed to an anaerobic digester or sold as a substitute product to soy meal consumed as animal feed. When burned in a boiler, the direct heat can be used to fuel the drying process. If there is excess meal after drying is completed, the rest is sold as animal feed; if meal is unable to provide all the drying energy then natural gas could be used to supply the difference. When digested, the resulting biogas can be used directly to fuel the drying process or any other heat engine. Methane within the biogas can be upgraded to the same standards as fossil natural gas. If allowed, the biogas may be utilized within the local gas distribution networks. Gas must be

cleaned to reach pipeline quality, and be of the correct composition for the local distribution network to accept it. These restrictions on raw biogas usage outside the system lead to the conclusion that on-site electricity generation is the most practical use for biogas not consumed for drying. Any electricity generated over and above the internal demand of cultivation is considered exportable to the grid and emissions from cultivation and oil extraction were allocated between oil and exported electricity based on energy. If insufficient biogas is produced to provide all the drying energy then natural gas could be used to supply the difference.

When sold as an independent product, market value allocation was used in partitioning emissions between algae oil and meal. As discussed with regards to soy oil to HRJ, using market value allocation captures temporal changes in the allocation fractions between products. Since no established market price exists for algae oil, or algae meal, they were assumed related to the prices of soy oil and soy meal. Prices assumed for soy oil and soybean meal are the 2015 projections made by FAPRI (FAPRI, 2009). Algae oil was assumed to have the same market price as soy oil, $1.05/kg, while algae meal was assumed to have a price related to that of soy meal based on protein equivalency. Protein content serves as a common denominator because both meals would be used as animal feed. Soybean meal was assumed to have a protein content of 48% (Ahmed et al., 1994) and algae meal to have an average protein content of 52% (Becker, 2007).[37] Based on these protein contents, a price of $0.31/kg was calculated for algae meal.

7.5.9 Sensitivity Analysis and System Design

For algal facilities yielding a fixed lipid content, the life cycle GHG emissions of fuel production are most sensitive to the extent of dewatering. Using the relationships and assumptions discussed in the previous section, life cycle GHG emissions were explored for a range of post-dewatering %TSS contents. Using assumptions consistent with the baseline case, the results are plotted in Figure 26 for three different system configurations. It can be seen that maximum dewatering is always optimum for minimizing life cycle GHG emissions, regardless of the source of drying energy and use of meal. If the post-dewatering %TSS content is less than 15%, algal HRJ results in higher GHG emissions on a life cycle basis than jet fuel from conventional petroleum. Recall that dewatering to 25% TSS content was assumed as the maximum dewatering achievable with current technology. By comparing the two natural gas drying cases, one can see the benefit of nutrient recycling as cases using fertilizer to meet all nutrient demands resulted in approximately twice the GHG emissions, for higher post-dewatering %TSS contents, as those where nutrients were recycled. The lowest life cycle GHG emissions were achieved by using biogas from the anaerobic digester and recycled nutrients.

The low emissions, baseline and high emissions scenarios assumed post-dewatering %TSS contents of 25%, 20% and 15% respectively. While the high emissions scenario assumed natural gas as the fuel used for drying, the baseline scenario was constructed with an anaerobic digester producing biogas configured to supply the drying energy. The low scenario assumed solar drying with an anaerobic digester producing biogas, which would then be used for on-site electricity generation to meet internal demands with excess power being exported to the gird.

Local sensitivity analysis was conducted on the anaerobic digestion biomass conversion efficiency, lipid content and CO_2 injection method. Each parameter was varied with all others held at their baseline values with the impacts quantified as a percent change from the baseline

[37] The meal is assumed to be the only oil-containing portion of algae. This hypothesis is verified by considering soybeans and soy meal. Soybeans have a protein content of 40% (GREET, 2008) and an oil fraction of 18.25% (Sheehan et al., 1998a) leading to a soy meal protein content of 48.9%. The average protein and lipid contents of the strains documented by Becker (2007) were 45.1% and 13.2%, respectively.

value. Figure 27 presents this information in a manner that allows the magnitude of each change to be seen in comparison to the others. Section 7.5.3 discussed the use of MEA extraction to create a pure CO_2 stream from flue gas. The importance of collocating the cultivation facility to its CO_2 source is further emphasized by these results. The unexpected result that life cycle GHG emissions are reduced by using algae with lower lipid contents can be understood by considering that additional meal, and hence more biogas and by extension more energy, is available per kg of oil if the algae have lower lipid contents. Finally, the conversion efficiency is directly proportional to the quantity of energy available from the meal, making it the second most sensitive operational specification of the system (second to post-dewatering %TSS content).

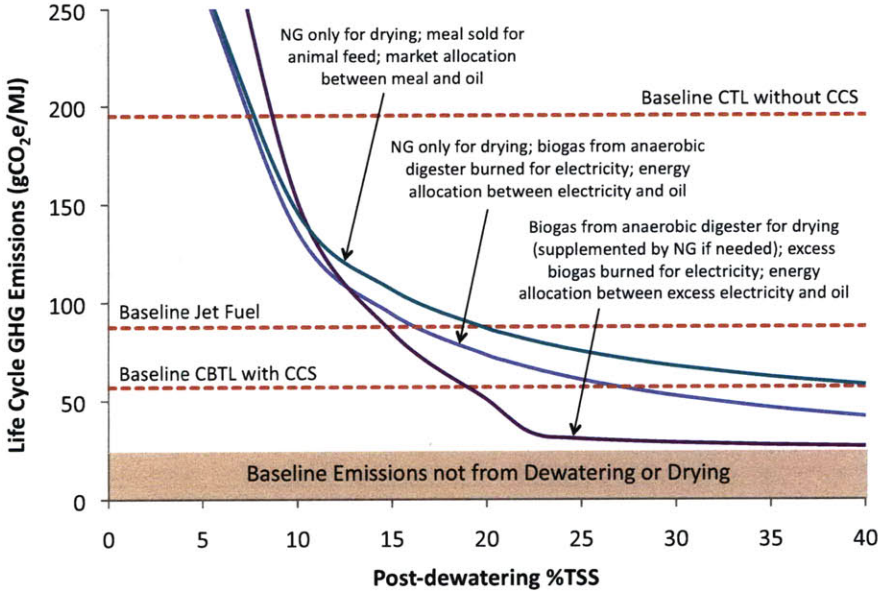

Figure 26: Life cycle GHG of HRJ production from algae as a function of the extent of dewatering. Three different system configurations were explored which are described more fully in the figure

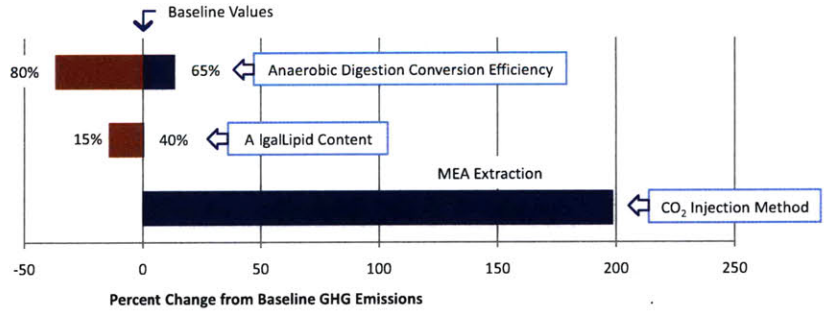

Figure 27: Sensitivity analysis of operational specifications and configurations of HRJ production from algae

7.5.10 Results

The key assumptions and corresponding life cycle GHG emissions in the production and use of HRJ from algae oil are outlined in Table 39. It should be noted that although water usage was not quantified in this section, it is a part of ongoing research efforts. The most notable differences between the cases lie in the recovery step and the WTT CH_4. The recovery step includes emissions from CO_2 injection, dewatering and drying. The dominant factors of each life cycle stage were described in previous sections and are the driving sources of variation between scenarios. The increased WTT CH_4 in the high emissions scenario is a result of natural gas usage for MEA extraction and drying.

The life cycle GHG emissions resulting from the production and use of HRJ from renewable algae oil range from 0.16 to 2.2 times those from conventional jet fuel. Variation in the biomass credit is due to minor changes in the allocation schemes used throughout the pathway.

Table 39: Life cycle emissions from the algae oil to HRJ pathway

	Low	Baseline	High
Key Assumptions			
Algae Yield ($g/m^2/day$)	40	25	20
Algal Lipid Content	40%	25%	15%
Anaerobic Conversion Efficiency	80%	70%	n/a
Life Cycle CO_2 Emissions by Stage			
Biomass Credit (gCO_2/MJ)	-73.7	-70.5	-68.9
Recovery of feedstock (gCO_2/MJ)	5.4	29.6	143.1
Transportation of feedstock (gCO_2/MJ)	0.3	0.3	1.2
Processing of feedstock to fuel (gCO_2/MJ)	7.1	10.3	13.2
Transportation of jet fuel (gCO_2/MJ)	0.6	0.6	0.6
Combustion CO_2 (gCO_2/MJ)	70.4	70.4	70.4
WTT GHG Emissions by Species			
WTT CO_2 emissions (gCO_2/MJ)	-60.3	-29.7	89.2
WTT CH_4 emissions (gCO_2e/MJ)	0.7	1.8	27.7
WTT N_2O emissions (gCO_2e/MJ)	3.3	8.1	5.8
Total WTW GHG emissions (gCO_2e/MJ)	14.1	50.7	193.2
Life Cycle GHG Emissions Relative to Baseline Conventional Jet Fuel	**0.16**	**0.58**	**2.21**

The uncertainty surrounding N_2O emissions from algae cultivation is larger that other pathways due to the assumption that algae ponds have the same emission factor as flooded rice fields. While there is little existing information on N_2O formation from algae ponds, the results from Table 39 indicate that N_2O represents less than 16% of the total life cycle GHG emissions. The reader should be aware of the additional uncertainty with respect to N_2O emissions from algae cultivation when comparing different pathways for GHG reduction potential in sections 10.1 and 10.2.

7.6 HRJ from Salicornia Oil

The creation of HRJ from salicornia oil is not a pathway available in GREET; hence, supporting information was obtained from the literature and a pathway was created within the GREET framework. Salicornia is both a wild and cultivated annual shrub that germinates, grows and reproduces in areas of high salinity such as coastal shorelines, marshes or inland lakes. The plant itself is leafless with green jointed and succulent stems that form terminal fruiting spikes in which seeds are borne. In subtropical regions, salicornia can grow up to 50cm in height with most of the

seed spikes on the upper one third of the plant (Anwar et al., 2002). Since oil containing seeds represent only a small fraction of the total plant, the deterministic factor in the life cycle analysis of jet fuel from Salicornia is the usage of non-oil containing biomass. The cultivation of halophytes on arid or semi-arid land, where there is little or no carbon stock naturally present in the soil, can lead to substantial net long-term carbon storage. Salicornia falls into the category of coastal halophytes because of its ability to grow in saltwater.

This work considers the production of HRJ from Salicornia oil while varying the crop productivity, oil yield, cultivation inputs and nutrient usage to establish the low emissions, baseline and high emissions scenarios. Due to the nature of Salicornia growth, the combination of either electricity generation or Fischer-Tropsch synthesis with an HRJ facility were explored. Long-term carbon sequestration potential is quantified through scenarios that vary the beneficial GHG credit from land use change.

7.6.1 Biomass, Seed and Oil Yield

In a similar manner to jatropha, additional products are created while growing seeds for oil production. When considering the yield of salicornia, three yield parameters define productivity: total biomass yield per hectare, seed yield per kilogram of total biomass and seed oil fraction. Total biomass is defined as seeds and straw biomass (similar to other forms of herbaceous biomass considered for BTL facilities). Data used to establish growth and oil yields was taken from field trials conducted at Puerto Penasco, Sonora, Mexico in an extreme coastal desert environment at the northern Gulf of California (Glenn et al., 1991). The ranges for the emissions scenarios were established using data from multiple plots taken from 1982 through 1988. The baseline total biomass yield and seed yield were defined by taking a weighted average (weighted by the number of plots) of the data from Glenn et al. (1991). The low emissions and high emissions data were defined as plus and minus one standard deviation from the weighted mean, respectively (standard deviation also weighted by the number of plots). The oil fractions adopted were taken directly from the range quoted by Glenn et al. (1991). The assumptions regarding total biomass yield, seed yield and oil fractions for Salicornia are given in Table 40.

The total biomass yield is almost an order of magnitude higher than the seed yield (per hectare). In the baseline case, this translates to 7.22 kg of straw biomass for every kilogram of seeds, 25.6 kg of straw biomass per kilogram of oil and 43.5 kg of straw biomass per kilogram of HRJ. The most important point highlighted by these numbers is that the production of salicornia will not be driven by the demand for its seeds, but rather the demand for its straw biomass. Were salicornia grown to use its straw biomass for either electricity production or as feedstock to a Fischer-Tropsch facility, the production of hydroprocessed renewable fuels from its oil seeds would be a high value co-product from the process.

Table 40: Salicornia yield and oil fraction assumptions

	Low	Baseline	High
Total Biomass Yield (kg/ha/yr)	17614	16247	14880
Seed production ($g_{seed}/kg_{total\ biomass}$)	142	122	101
Seed Yield (kg/ha/yr)	2506	1977	1504
Seed Oil Fraction	33%	28.2%	26%

In section 7.6.5.1, a system is considered where straw biomass is used for renewable power generation and seeds are used for HRJ production. The heating value of salicornia biomass varies with the species, the chief variable being the ash content, but in general salicornia biomass falls in the range of Lignite A or B coals (Glenn et al., 1992).

In section 7.6.5.2, a system is considered where straw biomass is used as a feedstock for a BTL facility and seeds are used for HRJ production. The BTL plant is similar to the CBTL configuration discussed in section 6.4; namely, that feedstock is used to meet internal process energy needs, with little or no excess electricity produced for export, and commercial quality middle distillate fuels such as diesel and jet fuel are produced.

7.6.2 Cultivation of Salicornia

The cultivation of salicornia is generally motivated by the opportunity to directly sequester carbon from the atmosphere. This occurs by reversing the trend towards desertification through cultivation of salicornia on saline lands and re-vegetation of degraded rangelands (Glenn et al., 1993). For this reason, process energy requirements for the cultivation of salicornia are sometimes presented in the form of fossil carbon emitted per carbon absorbed during growth. Glenn et al. (1992) calculated the carbon costs of salicornia assuming that all farm operations, from pumping water to planting, harvesting, baling and hauling the crop were performed using diesel fuel. They found that salicornia required 225kg to 300kg of fossil carbon for each 1000kg of atmospheric carbon fixed. The low emissions and high emissions case were defined as the lower and upper extremes, respectively, while the mean is assumed in the baseline case. All calculations assumed diesel fuel composed of 85.6% carbon and salicornia composed of 24.7% carbon (Glenn et al., 1992).

The use of fertilizers in the cultivation of salicornia is a subject of debate. The test plots created by Glenn et al. in the Sonoran Desert were irrigated solely with hyper saline seawater that had first been used in a shrimp aquaculture facility (O'Leary et al., 1985), which added nitrogen and other nutrients to the water. In later trials, fields irrigated with un-enriched seawater received fertilizer additions equivalent to 200kg of nitrogen per hectare as urea, di-ammonium phosphate or ammonium nitrate (Glenn et al., 1991). The degree to which fertilizer must be added is a function of the coupling between aquaculture farms and salicornia farms. Large-scale coastal shrimp farms have caused algal blooms and disease problems in rivers and basins that receive their nutrient-rich effluent. The same problems can be expected to occur from the large volume of highly saline drainage water containing unused fertilizer discharging from salicornia farms (Glenn et al. 1998). When coupled together, salicornia farms could help mitigate the problem if aquaculture effluent is recycled onto a salicornia farm instead of being discharged directly to the sea; hence, any assumptions made regarding fertilizer use carry a degree of uncertainty. The assumptions adopted in this work to establish a reasonable range deal with varying the fraction of irrigation water that comes from aquaculture facilities. The low emissions case assumed 100% of the irrigation water was pre-enriched from an aquaculture facility; the baseline case assumed 50% was pre-enriched, leading to 100kg of nitrogen usage per hectare, and the high emissions case assumed the full 200kg of nitrogen usage per hectare.

Irrigation is the single most expensive production cost in growing salicornia. In general, seawater irrigation requires copious and frequent, sometimes even daily, irrigation to prevent salt from building up in the root zone. Partially offsetting this effect is that increased salinity of irrigation water can lead to higher water usage efficiencies; therefore, higher salinity leads to less water being required to produce a kilogram of dry biomass (Glenn et al., 1992). During cultivation experiments in the Sonoran Desert, it was determined that salicornia can thrive when water salinity exceeds 100ppm (three times the normal ocean level); however, the volume of seawater required for irrigation is 35% more than the value that would be required if freshwater were being used. The additional volume is needed to control salt levels in the soil (Glenn et al., 1998). Although more volume is required for salicornia cultivation, seawater farms often require less water lifting than conventional farms, which may lift water from wells far deeper than 100 meters. This difference results in seawater farms using less energy for water pumping than

freshwater farms. The life cycle GHG emissions calculated in this work include the emissions from pumping irrigation water but secondary effects of salt-water irrigation were not quantified. Glenn et al. (1998) showed that normal farm and irrigation equipment could be modified such that it is protected from salt damage from seawater.

The input assumptions discussed above are summarized in Table 41.

Table 41: Input assumptions regarding the cultivation of salicornia

	Low	Baseline	High
Process Fuels			
Diesel ($kg/kg_{C\ Fixed}$)	225	262.5	300
Diesel (Btu/kg_{seed})[1]	18557	25316	34831
Fertilizer Use			
Nitrogen (kg/ha/yr)	0	100	200
Nitrogen (g/kg_{seed})[1]	0	50.6	133.0
Notes: 1) Calculated using the yield assumptions from Table 86			

Emissions from N_2O were estimated using IPCC Tier 1 methodology (De Klein et al., 2006). Due to the lack of data, N_2O emissions from nitrogen in above and below ground crop residues were not accounted for in this analysis. The IPCC Tier 1 methodology estimates the combined direct and indirect conversion rate for nitrogen from synthetic fertilizers as 1.325%. These rates include the atmospheric deposition of nitrogen volatilized from managed soils as well as nitrogen from leaching and runoff. The formula for calculating N_2O emissions from salicornia cultivation is given by:

$$N_2O\ \text{Emissions}\left(\frac{g_{N_2O}}{kg_{seed}}\right) = \left(\frac{g_{\text{nitrogen fertilizer}}}{kg_{seed}}\right) \cdot 0.01325 \cdot \left(\frac{44 g_{N_2O}}{28 g_N}\right) \qquad \text{Equation 13}$$

7.6.3 Transportation of Salicornia Biomass and Seeds to Production Facilities

The production of salicornia biomass and seeds was assumed to take place on the southwestern coast of the United States. After harvesting, GREET default values from the soybeans to HRJ pathway were assumed in regards to transportation mechanisms and distances travelled for the seeds. The assumptions of transportation mechanisms and distances for straw biomass are consistent with GREET defaults for herbaceous biomass in the BTL pathway. Specifically, the transportation of seeds is by truck to a local storage area and subsequently to a local oil extraction facility. The transportation of straw biomass is also by truck directly to an F-T or renewable power generation facility assumed to be the same distance as the HRJ facility. The difference between seed and straw biomass transportation is that seeds are loose and moved in loads of 15 short tons while straw biomass is baled and moved in loads of 24 short tons. Even after accounting for transportation of both seeds and straw biomass, the transportation elements of the life cycle GHG emissions are sufficiently small to be within the margin of error; therefore, assumptions in this area carry little consequence.

7.6.4 Oil Extraction from Salicornia Seeds

As there is no commercially available process for extracting oil from salicornia seeds, the extraction process was modeled with the soybean oil extraction process described by Sheehan et al. (1998a). Glenn et al. (1998) classify salicornia oil as highly poly-unsaturated and similar to safflower oil in fatty-acid composition (as presented in Table 13). They also conclude that it can be extracted from the seed and refined using conventional oilseed equipment. This same method was applied to both algae and jatropha oil extraction. Salicornia seeds more closely resemble soybeans than either algae or jatropha; hence, less modification to the soybean process was

required. Specifically, pre-drying of seeds was eliminated and seed shell removal energy was included. Field drying of the seeds, prior to harvest was assumed and the energy for removing shells from jatropha seeds was applied to salicornia seeds. The process inputs assumed in this analysis are summarized in Table 42.

Table 42: Process inputs for extracting oil from salicornia seeds. All values are in Btu/lb of oil

	Low[1]	Baseline[1]	High[1]
Receiving and Storage			
Electricity	20.9	33.5	55.8
Salicornia Preparation			
Electricity	4.0	6.5	10.8
Steam	172.5	276.0	460.0
Oil Extraction			
Electricity	12.9	20.6	34.4
N-hexane	105.9	169.5	282.5
Meal Processing			
Electricity	52.2	83.5	139.1
Steam[3]	505.4	808.6	1347.7
Oil Recovery			
Electricity	1.4	2.2	3.6
Steam	86.7	138.7	231.1
Solvent Recovery			
Electricity	1.9	3.0	5.0
Steam	0.0	0.0	0.0
Oil Degumming			
Electricity	6.1	9.7	16.1
Steam	68.1	109.0	181.6
Waste Treatment			
Electricity	2.0	3.3	5.4
Steam	36.6	58.6	97.7
Totals			
Electricity	101.4	162.2	270.3
Natural Gas[2]	1086.6	1738.6	2897.6
N-hexane[3]	105.9	169.5	282.5

Notes:
1) All values are in Btu per pound of oil
2) Steam is assumed to be generated from natural gas with an efficiency of 80%.
3) GREET uses Liquefied Petroleum Gas (LPG) as a surrogate for N-hexane when calculating emissions

7.6.5 Co-Product Usage and Allocation Methodology

Based on the yields adopted in the baseline case, 7.22 kg of straw biomass is produced for each kilogram of seed. Although salicornia could be grown for its seeds with the straw biomass tilled back into the field to facilitate higher rates of long-term carbon sequestration in the soil, it is doubtful that this would be done in practice. In an economy where 85% of all energy is derived from fossil carbon sources, the waste biomass could be used as a renewable energy source thus displacing fossil-based electricity or heat generation. Assuming the energy content of straw biomass is 16.3 MJ/kg, within the range of lignite A and B coals, the energy contained in straw biomass created per pound of oil is 10.5 times that contained in the oil itself.

7.6.5.1 Electricity Production from Biomass Co-products

The use of straw biomass co-product for electricity production was modeled with the assumption that to the electricity production occurred at the same location as the oil extraction and HRJ production. Three allocation methodologies were envisaged for this configuration. A summary of each is given in Table 43. The first methodology, which is the most straightforward, would displace average US grid electricity with the result being the lowest life cycle emissions for HRJ. The second methodology, system level energy allocation of recovery and feedstock transportation emissions, is the most complicated and is shown schematically in Figure 28. The unallocated cultivation and transportation emissions are first divided between HRJ production and electricity production based on the energy of the final products (39.9% and 60.1% respectively); the emissions associated to HRJ production are then allocated between oil and meal based on market value (61.5% and 39.5% respectively); both are then summed back together and allocated based on energy between HRJ and all other energy products from the system (15.4% and 84.6% respectively). The other energy products from the system are comprised of renewable naphtha, mixed propane gas and electricity. The third allocation methodology involves initially allocating only the cultivation emissions between the seeds and straw biomass based on market valuation (67.2% and 32.8% respectively).[38] The life cycle GHG emissions resulting from each of the aforementioned systems are compared in Figure 29.

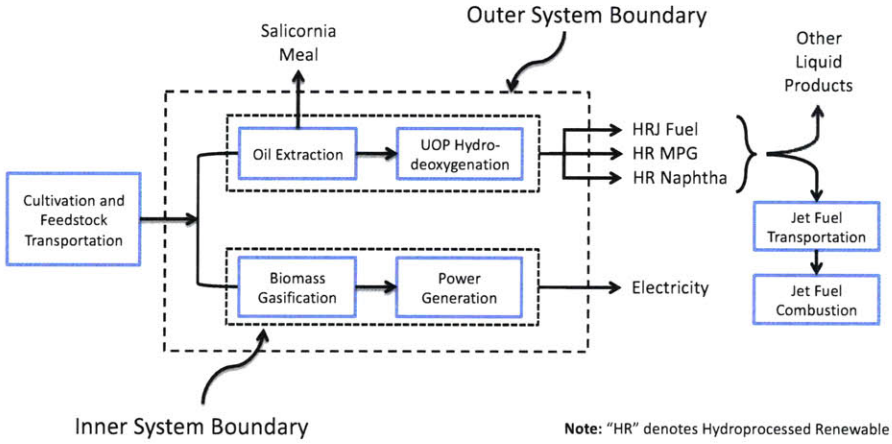

Figure 28: System boundary definitions for system level energy allocation between HRJ production from salicornia oilseeds and electricity generation from salicornia straw biomass

As was observed for other fuel pathways, different allocation schemes result in varied emissions within the same pathway. The most important point to realize from this configuration is that there are 5 MJ of electricity generated for each MJ of HRJ. Hence, giving a liquid fuel credit for this electricity will reduce its emissions considerably. Additionally, when only the oilseeds are used for fuel production, the yield of HRJ per hectare is small, being less than even soybeans. This underscores the importance of the straw biomass as the driving renewable energy resource from salicornia cultivation.

[38] Market value of seeds is the sum of market value of oil and meal individually. Value of salicornia oil was taken as equivalent to soy oil while the value of salicornia meal was found by scaling the value of soy meal by the ratio of protein contents. Soy meal has an average protein content of 48% (Ahmed et al., 1994) while salicornia meal has a protein content of 42% (Glenn et al., 1992). The market value of straw biomass was assumed to be proportional to the cost of coal based on energy value. The average cost of coal for electric utilities in 2008 was $2.07/mmBtu (EIA, 2009a).

Table 43: Allocation methodologies examined for the production of HRJ from salicornia oil when using the straw biomass co-product for electricity generation

Scenario	Co-Product	Use	Emissions Allocation Method
1	Straw biomass	Burned for electricity production	Displacement method (system expansion) where electricity from US grid is displaced. The corresponding emissions credits are given to the fuel production process.
2	Straw biomass	Burned for electricity production	Electricity production considered a parallel process to HRJ production. Cultivation and feedstock transportation emissions are allocated using a system level energy allocation scheme between all energy products from the system.
3	Straw biomass	Burned for electricity production	Cultivation and feedstock transportation emissions are allocated prior to any electricity production based on market valuation of the unprocessed seeds and straw biomass.

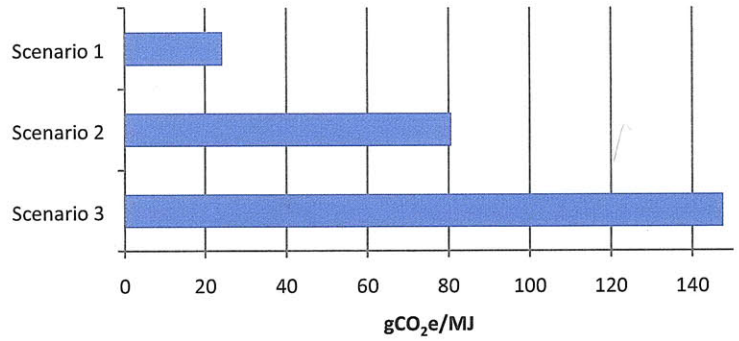

Figure 29: Comparison of life cycle GHG emissions from the allocation methodologies of **Table 43** based on the production of HRJ from salicornia oil when using the straw biomass co-product for electricity generation

7.6.5.2 Fischer-Tropsch Fuel Production from Biomass Co-products

If the straw biomass co-product from salicornia oilseeds is used for electricity production then jet fuel represents only 15% of the total energy products created. This is a smaller fraction than any other oilseed crops considered in this work and is not conducive to being a part of a large-scale biofuel production network. In Chapter 6, jet fuel from coal and solid terrestrial biomass via the Fischer-Tropsch process was discussed with switchgrass as the biomass feedstock. Any carbon containing matter could theoretically be used to create syngas, which contains primarily H_2, CO and CO_2. This section discusses the implementation of a fuel production configuration where salicornia oilseeds are processed through an HRJ facility and all of the straw biomass is used as feedstock to a BTL facility.

By incorporating a BTL facility producing 25% jet fuel, the total yield of jet fuel grows to be three times larger than that from HRJ alone for the same quantity of feedstock consumed. Furthermore, F-T diesel and naphtha are also created which contribute to GHG mitigation efforts in other energy consuming sectors. For these reasons, this work focused on a coupled HRJ and F-T facility. All assumptions discussed thus far were applied to the HRJ section, while input assumptions pertinent specifically to the BTL section are summarized in Table 44.

Table 44: Input assumptions relevant to a BTL facility using salicornia straw biomass as feedstock

	Low	Baseline	High
BTL Plant Efficiency	52%	45%	42%
F-T Jet Fuel Yield (fraction of all F-T fuel products)	30%	25%	20%
Straw Biomass Energy Content (MJ/kg)	17.4	16.3	15.1

As was the case when electricity was produced, the allocation methodology is an important choice in determining the final life cycle GHG emissions of the jet fuel. Figure 30 outlines how the coupling of an HRJ facility with an F-T facility was arranged for this analysis. Straight black lines correspond to emissions flows following one or more products. This methodology allocates energy and emissions common to both processes on a pseudo-system wide level by energy content and attributes energy and emissions coming from a specific process to the products from the process. The unallocated cultivation and transportation emissions are first divided between HRJ production and F-T fuel production based on the final energy products (allocation ratio 1); those associated to HRJ production are then allocated between oil and meal based on market value (allocation ratio 2); the HRJ and F-T emissions are then summed back together and allocated based on energy between jet fuel and all other energy products from the system (allocation ratio 3). The other energy products from the system are comprised of F-T diesel, F-T naphtha, hydroprocessed renewable naphtha and mixed propane gas. The allocation ratios and combined facility product slate resulting in the low emissions, baseline and high emissions scenarios are presented in Table 45.

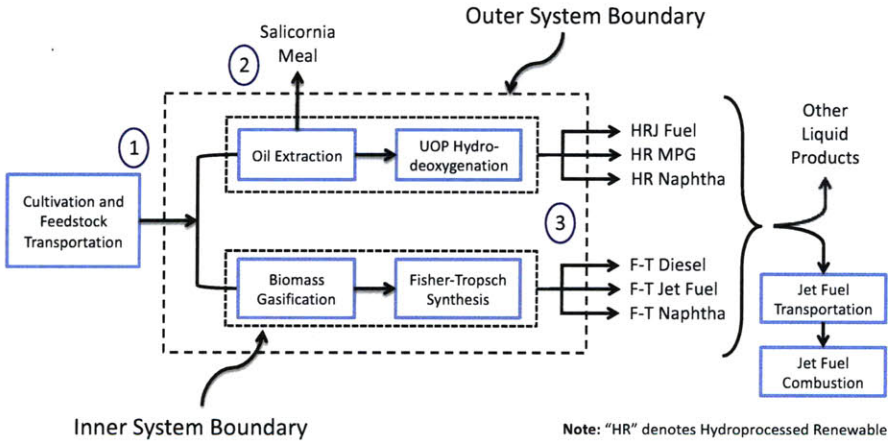

Figure 30: System boundary definitions for system level energy allocation of coupled HRJ and F-T fuel production from salicornia oilseeds and straw biomass

Table 45: Allocation ratios and product slates describing a coupled HRJ and F-T facility processing salicornia oilseeds and straw biomass

	Low	Baseline	High
Product Slate (MJ/MJ_{Jet})			
F-T Diesel	1.2	1.5	1.8
F-T Naphtha	0.30	0.49	0.75
Renewable Naphtha	0.16	0.16	0.16
Mixed Propane Gas	0.012	0.027	0.028
Salicornia Meal	0.52	0.64	0.71
Allocation Ratios			
Allocation Ratio 1	32.1% HRJ 67.9% F-T	30.9% HRJ 69.1% F-T	27.8% HRJ 72.2% F-T
Allocation Ratio 2	66.7% Oil 33.3% Meal	61.5% Oil 38.5% Meal	58.8% Oil 41.2% Meal
Allocation Ratio 3	37.1% Jet Fuel 62.9% Other Fuels	31.9% Jet Fuel 68.1% Other Fuels	26.6% Jet Fuel 73.4% Other Fuels

7.6.6 Land Use Change Emissions from Salicornia Cultivation

The degree to which carbon can be sequestered through salicornia cultivation depends on the initial state of the soil in which they are grown and the penetration of the roots in this soil. Dry land soils are typically low in organic carbon and could conceivably hold greater carbon under restored conditions (Glenn et al., 1993).

Estimates of soil organic carbon, root carbon and charcoal carbon storage of semi-permanent cultures conducted by Sommer et al. (2000) have been previously used to estimate potential carbon sequestration from halophyte cultivation (Hendricks, 2008; Hendricks and Bushnell, 2008). These estimates are for deep soils under small farmer land use systems in the Eastern Amazon region that contain conventional vegetation and crops, not salicornia. They were intended to quantify current carbon stock; hence, using the carbon storage values from Sommer et al. as a sequestration potential implicitly assumes similar soil carbon storage capacity and zero soil carbon prior to any halophyte cultivation. Soil carbon stored for semi-permanent secondary vegetation range in the Eastern Amazon region range from 146 to 167 tC ha^{-1}, where approximately 90% is soil organic carbon, 5% is root carbon and the remaining 5% is charcoal in the soil. Furthermore, although this range applies to the top 6m of soil, an average of 67% of the carbon is stored in the top 1.2 meters (Sommer et al., 2000).

A second independent analysis of carbon sequestration from salicornia was carried out for a joint project between the United States and Mexico. The project is called "Project Salicornia: Halophyte Cultivation in Sonora" and is operated under the United Nation Framework convention for Climate Change. Project developers have a preliminary estimate that the cultivation area would reach a steady state soil carbon content of 49 tC ha^{-1} after 100 years (UNFCCC, 1998). This value happens to correspond to half the carbon stock in the top 1.2 meters of soil as estimated by Sommer et al. (2000), namely 48.7 to 55.7 tC ha^{-1}. The UNFCCC estimate was adopted for this study as a land use change scenario.

Under the optimistic assumption that all of the soil carbon sequestration occurs in the first 30 years, the impact of long-term soil carbon sequestration on life cycle GHG emissions are given in Table 46. The sequestered carbon was amortized over 30 years with no discounting. The values are on the basis of carbon sequestered per MJ of jet fuel created from salicornia oil and straw biomass

Table 46: Long term soil, root and charcoal carbon sequestration from the cultivation of salicornia for fuel production

Long Term Carbon Sequestration ($tC\ ha^{-1}$)	Long Term Carbon Sequestration (gCO_2/MJ)		
	Low	**Baseline**	**High**
49	49.7	41.9	33.9
Note: 1) Since values represent carbon sequestration, larger values correspond to lower emissions.			

Soil carbon sequestration estimates lead to emissions credits ranging from 0.39 to 0.57 times the life cycle GHG emissions from the production and use of conventional jet fuel. Recall that these estimates assume that the carbon content of the soil used for cultivation is depleted prior to cultivation occurring. Were salicornia grown on land with non-depleted carbon stocks then it is unlikely that any long-term soil carbon sequestration would result.

7.6.7 Results

The life cycle GHG emissions resulting from the production and use of HRJ and F-T jet fuel from salicornia seeds and straw biomass are summarized in Table 47. Results incorporating long-term carbon sequestration are given in Table 48.

These results reflect the sum of emissions from HRJ production and F-T jet production for one total megajoule of jet fuel. Based on the input assumption adopted in this work and the allocation methodologies discussed above, the life cycle emissions of the salicornia to HRJ and F-T jet pathway range from 0.35 to 0.76 times those from the production and use of conventional jet fuel. If long-term carbon sequestration occurs because of the salicornia growth, the life cycle GHG emissions range between -0.2 to 0.37 times those from conventional jet fuel.

Table 47: Summary of results from renewable and F-T jet fuel production and use from salicornia

Land Use Change Scenario H0	**Low**	**Baseline**	**High**
Key Assumptions			
Total Biomass Yield (kg/ha/yr)	17614	16247	14880
Seed production ($g_{seed}/kg_{total\ biomass}$)	142	122	101
Seed Yield (kg/ha/yr)	2506	1977	1504
Seed Oil Fraction	33%	28.2%	26%
Life Cycle CO_2 Emissions by Stage			
Biomass Credit (gCO_2/MJ)	-90.9	-105.3	-116.9
Recovery of feedstock (gCO_2/MJ)	26.7	36.8	47.1
Transportation of feedstock (gCO_2/MJ)	1.0	1.1	1.2
Processing of feedstock to fuel (gCO_2/MJ)	21.6	38.3	51.5
Transportation of jet fuel (gCO_2/MJ)	0.5	0.5	0.5
Combustion CO_2 (gCO_2/MJ)	70.4	70.4	70.4
WTT GHG Emissions by Species			
WTT CO_2 emissions (gCO_2/MJ)	-41.0	-28.6	-16.5
WTT CH_4 emissions (gCO_2e/MJ)	1.0	1.3	1.7
WTT N_2O emissions (gCO_2e/MJ)	0.2	4.6	10.5
Total WTW GHG emissions (gCO_2e/MJ)	30.5	47.7	66.1
Life Cycle GHG Emissions Relative to Baseline Conventional Jet Fuel	**0.35**	**0.55**	**0.76**

Table 48: Life cycle GHG emissions for production and use of renewable and F-T jet fuel salicornia assuming long-term carbon sequestration

Land Use Change Scenario H1	**Low[1]**	**Baseline[1]**	**High[1]**
Land use change emissions (gCO_2/MJ)	-49.7	-41.9	-33.9
WTW CO_2 emissions (gCO_2/MJ)	-20.3	-0.1	20.0
Total WTW GHG emissions (gCO_2e/MJ)	-19.2	5.8	32.2
Life Cycle GHG Emissions Relative to Baseline Conventional Jet Fuel	**-0.22**	**0.07**	**0.37**
Notes: 1) All other input assumptions (salicornia cultivation, extraction of oil, processing of oil to HRJ and straw biomass to F-T jet) are based on those in the H0 emissions case of the corresponding scenario.			

Without the opportunity to obtain nutrients from the recycled streams of aquaculture farms, substantial increases in nitrous oxide emissions are likely to occur. An increase in N_2O emissions translates to more pronounced consequences from the uncertainty associated with the IPCC correlations. The reader should be aware of the potential for these inherent uncertainties when comparing different pathways for GHG reduction potential in sections 10.1 and 10.2.

Chapter 8: Land Use, Water Consumption and Invasiveness

The focus of this thesis thus far has been to establish well-to-tank GHG emissions inventories for a variety of alternative jet fuels. This present chapter extends the discussion of environmental sustainability beyond GHG emissions to include fuel yield, land use, fresh water use and the potential for the introduction of invasive species in an unprepared ecosystem.

8.1 Fuel Yield and Land Requirements

Figure 31 summarizes the fuel production potential for each of the biofuel pathways considered by Wong (2008) and in chapters 5, 6 and 7 of this thesis. The range in yields of fuel per kilogram of oilseed feedstock arises from both crop yield per acre of land and variation in oil fraction. Rapeseed seed yields the most oil per kilogram (44%) followed by jatropha seeds (35%), algae (25%), palm kernels (22%) and finally soybeans (18%). Recall that there can be considerable variability in biomass oil yields, (e.g., potential algal yields up to 390% of those used in this work have been quoted by stakeholders in the industry). The fuel production from salicornia is the result of the combined jet fuel production from HRJ and BTL facilities. When configured in this manner, each megajoule of jet fuel is composed of 65% F-T jet and 35% HRJ.

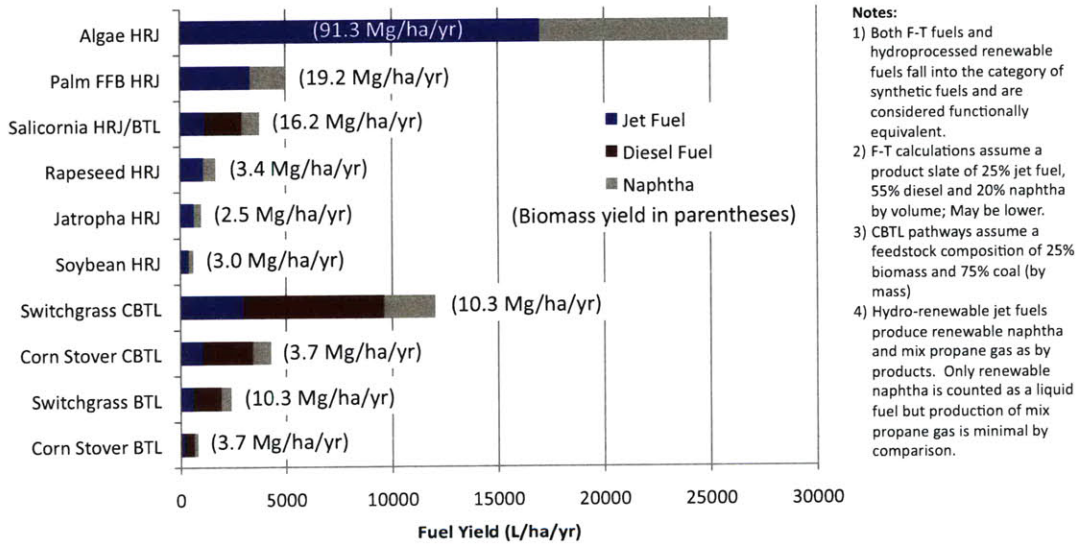

Figure 31: Fuel production potential for various alternative jet fuels that could be derived from biomass. This is not an all-encompassing list of alternative jet fuel options; it merely represents those examined as part of this research effort

A subtle but important point surrounding the F-T jet fuel results is that only 25% of the fuel output from the F-T fuel facility was assumed to be jet fuel. Using switchgrass CBTL as an example, there would be 12,000 (3000 × 4) liters of liquid hydrocarbons produced for every hectare of switchgrass, only 3,000 liters of which would be jet fuel (the rest could be fuels such as diesel, gasoline, and naphtha). All 12,000 liters of fuel produced carry an environmental benefit; therefore, all liquid fuel products must be considered to capture the total CO_2 mitigation. The switchgrass (or other biomass) used as feedstock for pure BTL plants have low energy densities. This causes a large quantity to be required in order to make a relatively small quantity of jet fuel

(which has a high energy density). Although the same feedstock could be used for both pure BTL and CBTL, when supplemented by coal, the same fuel output can be obtained from a smaller quantity of biomass. This increase is only due to supplementing the biomass feedstock with coal and not to an increase in biomass usage efficiency. Corn stover or forest residue can also be used as a feedstock.

Determining the scales at which the alternative fuels under consideration must be implemented to represent a meaningful contribution to the current jet fuel industry was included in the scopte of this thesis. This requires combining the analysis of fuel yield from Figure 31 with the production scales of the petroleum-based jet fuel industry discussed in Section 2.1. A graphical representation of the land requirements to supply the entire 2009 US jet fuel market with 100% SPK and a 50/50 blend of SPK and conventional jet fuel is shown in Figure 32.[39] Three representative fuel yields were chosen to span the relevant range from feedstocks considered in Figure 31. Most fuel options suffer from inconsistency between the fraction of total US land area required to meet a given production capacity and the fraction of US fuel demand satisfied by that production capacity. Recall that jet fuel is only 9% of total domestic petroleum consumption. As stated in Section 2.1, even small fractions of the petroleum industry translate to massive production scales when considered in absolute terms.

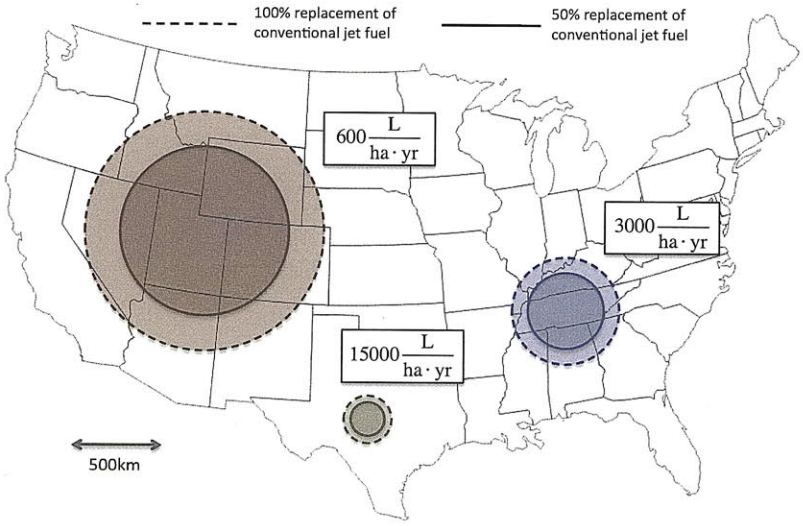

Figure 32: Land area requirements to replace conventional jet fuel use within the US with 100% SPK and 50/50 blend of SPK with conventional jet fuel. Average US conventional jet fuel consumption in 2009 was 1.4 million bbl/day

8.2 Biofuel Impact on Domestic Water Resources

Water plays an essential role in developing and utilizing energy resources. It is used in energy-resource extraction, refining and processing, and transportation. The dependence of biofuels on water extends even further to include water used for feedstock growth. This work has thus far only focused on life cycle GHG emissions and yield as the bounding factors to large-scale biofuel production. Water requirements and regional availability serve as a third bound to the trade space of biofuel development.

[39] Average US consumption of jet fuel in 2009 was been roughly 1.4 million barrels per day (EIA, 2009b)

It is important to distinguish between water withdrawal and water consumption. Water withdrawal involves withdrawing water from its source and subsequently returning it after use. The quality of the returned water may not be the same as when it was originally removed. Electricity generation is the best example where water use is dominated by withdrawn water used for cooling (some cooling water is lost to evaporation and this fraction is considered consumed). Water consumption involves withdrawing water from its source and not returning it after use. Crop irrigation represents the largest fraction of water consumption within the US. Figure 33 shows water withdrawals and water consumption by sector for the US in 2000 and 1995 respectively. Notice that the volume of consumed water is only 30% of that withdrawn.

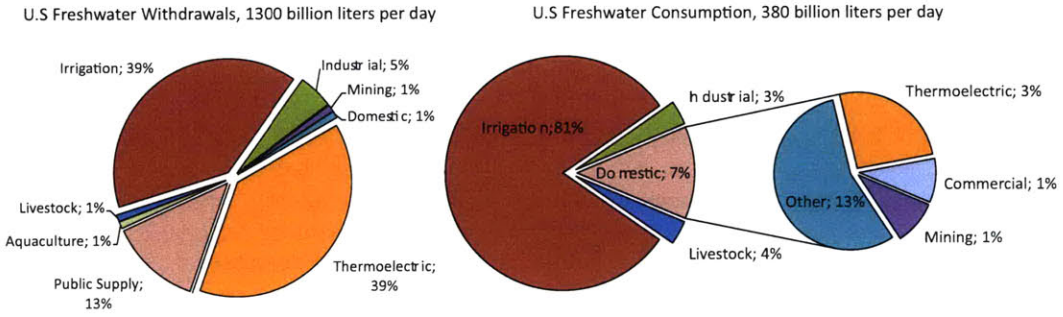

Figure 33: Water consumption and water withdrawals in the US by sector (data adapted from DOE, 2006)

The water required to refine one liter of petroleum fuels was found to be between 1 and 2.5 liters (King and Webber, 2008). Jet fuel consumption in the US is currently at 1.4 million barrels per day, or 222 million liters per day (EIA, 2009b). This means that the aviation industry alone is responsible for consuming between 222 and 556 million liters of water each day. Most alternative fuels will require at least the quantity of water that refineries currently consume and have the potential to consume several orders of magnitude more (DOE, 2006). This fact leads us to define the life cycle water consumption in fuel production using a similar metric to that used to quantify life cycle GHG emissions. The units of liters consumed per MJ of fuel energy delivered to the tank are used to encompass the water consumed during the recovery and transportation of the feedstock from the well, field, or mine to the production facility, processing of these materials into fuels, transportation and distribution of the fuel to the aircraft tank, and combustion of the fuel in the aircraft. Without considering any specific examples, water consumption from feedstock recovery and processing will dominate the life cycle water consumption while water consumption from feedstock and fuel transportation will be indirect through consuming fuels that required water for their production. Water consumption from the combustion stage is zero.

The primary focus of this thesis was on life cycle GHG emissions; hence no new data have been generated concerning water usage within fuel production pathways. This section makes use of a study concerning energy demand on water resources from the US Department of Energy (2006) and a study on the water intensity of transportation from King and Webber (2008). The relevant data from both papers is presented in Figure 34. Notice that corn and soybeans requiring irrigation consume 3 orders of magnitude more water than refining of conventional petroleum based fuels. The irrigation needed for crop production varies greatly depending on the region. For example, water use for irrigated soy production varies from 600,000 liters per hectare for Pennsylvania to about 4.3 million liters per hectare for Colorado, with a national average of 2.4 million liters per hectare (DOE, 2006). The overall average is deceiving because many areas use no irrigation while others have much higher demands.

Few new reservoirs have been built since 1980, and fresh surface-water withdrawals have peaked at about just over 1 trillion liters per day. Many regions depend on groundwater to meet increasing water demands, but declining groundwater tables could limit future water availability. Some regions have seen groundwater levels drop as much as 300 to 900 feet over the past 50 years from pumping water from aquifers at a rate faster than the natural rate of recharge (DOE, 2006). The expansion of biofuel production could exacerbate non-uniform regional water stresses between states; hence, the impact of biofuels on water consumption will be regionally dependent and cannot be summarized by a single value.

If feedstocks can be found that require no additional water above the status quo, their processing to jet fuel will still place additional strain on the current system. Converting natural gas and coal to F-T diesel are 5 and 7 times more water intensive than refining of conventional petroleum, respectively. Similarly, water consumption from steam reforming of natural gas to make hydrogen for hydroprocessing renewable oils to HRJ will be at least comparable to refining conventional petroleum.

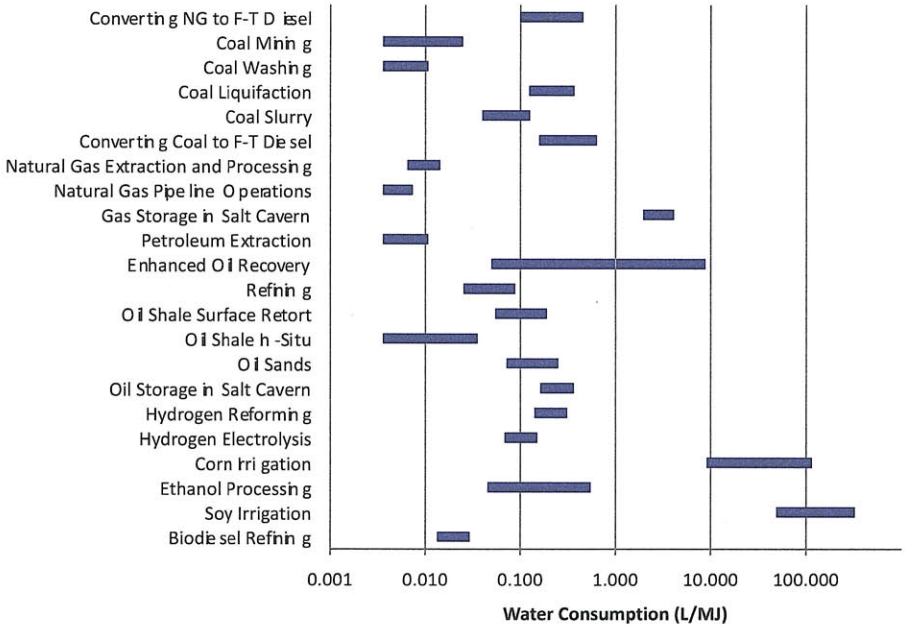

Figure 34: Water consumption for the production of various fuels (data adapted from DOE, 2006 and King and Webber, 2008)

Depending on the water quality needs for particular applications, freshwater supplies can be augmented with degraded or brackish water. This applies to the algae and salicornia pathways discussed in sections 7.6 and 7.7. Algae grown in open ponds have the additional complication of evaporation from the pond surface. Algae are most effectively grown in shallow, high surface area ponds. Assuming an evaporative rate of 1.5 cm/day (Weissman and Goebel, 1987), 100 liters of water per hectare need to be replenished each minute. This constraint will limit the location of algae farms to being adjacent to a plentiful source of degraded or brackish water.

As previously discussed, biofuel production would aggravate regional strains on freshwater supply and local infrastructure. Further insight as to where these strains will be felt can be gained by considering the data from DOE (2006) in conjunction with the regions within the US where

biofuel feedstock cultivation expansion is likely. In their 2006 report on the interdependency of energy and water, the US Department of Energy (DOE) showed that freshwater withdrawal in most regions of the US exceeds the available precipitation (precipitation minus evapotranspiration[40]). While the ratio of freshwater withdrawals to available precipitation is less than 30 for most of the Northeast, Midwest and Southeast, values between 100 and 500 are not uncommon for western states. The magnitude of this ratio indicates the degree to which current water demands are being met with groundwater pumping or transport of surface water from other regions (DOE, 2006).

Locations most conducive to next generation biofuel feedstock cultivation are the Southwest and Southeast for algae, Southwest for salicornia, and Midwest and Southeast for switchgrass. With the exception of Midwest and part of the Southeast, these are regions where groundwater withdrawal is well in excess of the available precipitation each year. The Southwest should receive particular attention when discussing the expansion of domestically produced biofuels because of existing water constraints.

These data demonstrate that water availability could be a limiting factor for biofuel production in certain regions of the US and the need for further research.

8.3 Invasive Species with Respect to Biofuels

Crops ideal for large-scale biofuel production are those with high yield that do not require fresh water irrigation and can maintain high yields when grown on marginal lands. These are also general traits that describe invasive species. More specifically, the National Invasive Species Information Center (NISIC) defines the following characteristics as some of the traits of species likely to be invaders (NISIC, 2006).

- Rapid growth and short life cycle: go from seed to producing seed very rapidly – sometimes within a few weeks.
- Able to grow in a wide range of habitats
- High number of seeds produced
- Long seed dormancy and staggered germination
- Efficient method of seed dispersal
- Benefit from allelopathy, which is the release of chemicals into the surrounding soil that prohibit the growth of other plants.

As defined by most government organizations, invasive species are non-indigenous and adversely affect the habitats they invade economically, environmentally or ecologically. There are approximately 50,000 non-indigenous species in the United States. Some of these are noninvasive and beneficial to society, such as corn, wheat and rice. Others have caused major economic losses in agriculture and forestry and have irreversibly damaged the ecosystems to which they were introduced (Pimentel et al., 2000).

Historically most plant introductions, with the exception of agricultural weeds, have been intentional while microbe introductions have been accidental. Regardless of initial rationale, an additional 700,000 hectares of US wildlife habitat are invaded each year by non-indigenous weeds. As an example, 4 million hectares of grassland in northern California have been lost to yellow star thistle (Campbell, 1994). These are lands that may otherwise have been used for energy crop cultivation such as switchgrass. Invaded lands can also become predisposed to fires.

[40] Describes the sum of evaporation and plant transpiration from the Earth's land surface to the atmosphere.

Cheatgrass growth in the Great Basin in Idaho has increased the frequency of fires by more than an order of magnitude (Whisenant, 1990).

The accidental introduction of weeds and microbes often occurs via crop seeds and other parts of host plants. The agriculture industry suffers an overall reduction of 12% in crop yields due to weeds with each 1% decrease in crop yield being accompanied by a 4.5% increase in crop cost to the farmer. Ecologists agree that non-indigenous weeds are a greater risk than native ones. Plant pathogens carried by foreign microbes result in crop losses of approximately 65% those of weeds. Similarly, pathogens of forest plants cause the loss of 9% of forest products each year (Pimentel et al., 1997).

The majority of the aforementioned impacts occurred because of intentional introduction of foreign plants to the North American ecosystem. Many of the feedstocks considered in this work have never before been grown at large scale and/or require deliberate introduction to an ecosystem. The financial burden of losses and control due to invasive plants and microbes has been estimated as several tens of billions of dollars each year (Pimentel et al., 2000). While the authors are not attempting to imply that the expansion of biofuels could result in such significant economic losses, it is important to understand that controlling invasive plants is not a negligible consideration in the decision making process. The awareness that invasive species can be a direct financial burden highlights the potentially negative economic consequences of introducing new species to the environment. Maintaining environmentally sustainable feedstock production that meets food and energy demands is essential to the economic success of meeting large-scale biofuel demands.

The expansion of biofuel consumption within the U.S. will require a significant increase in crop and feedstock production and this presents the possibility that non-indigenous species will be introduced into an unprepared ecosystem. Ironically, the impact of these invasives could be to inhibit crop production, which could hurt the industry that was responsible for their introduction.

Chapter 9: Tank-to-Wake Combustion Emissions

9.1 Aircraft Combustion Products and Effects

The combustion of hydrocarbon fuels results in the release of CO_2 and water. The CO_2 from combustion can be quantified with minimal uncertainty (Hileman et al., 2010) and was added to the GHG inventories from well-to-tank life cycle steps presented in Chapters 5 through 7. The combustion of jet fuel in aircraft also causes the formation of non-CO_2 products, namely, soot and sulfate aerosols, water vapor, greenhouse gas precursors (NO_x), contrails and contrail cirrus. In most life cycle analyses of bio-based fuels, the emissions from the combustion of the fuel are considered equal and opposite to the emissions absorbed from the atmosphere during growth of the feedstock (Edwards et al, 2007, Broch, 2009). However, this approach neglects non-CO_2 products of combustion. Such products will still exist even if the net GHG emissions from the fuel life cycle are zero. They are particularly important for aircraft where near-term impacts are dominated by the non-CO_2 effects while long-term impacts are driven by only the CO_2 and other long lived greenhouse gases (Marais et al., 2008).

Figure 35 schematically demonstrates the impacts pathway of aviation related climate change starting with direct emissions from the engine and culminating in societal consequences. Some species cause warming while others cause cooling. Mahashabde (2009) developed an analytical framework to characterize the full impact pathway for each species and this work builds upon that existing modeling capacity as described in Section 4.3.2.

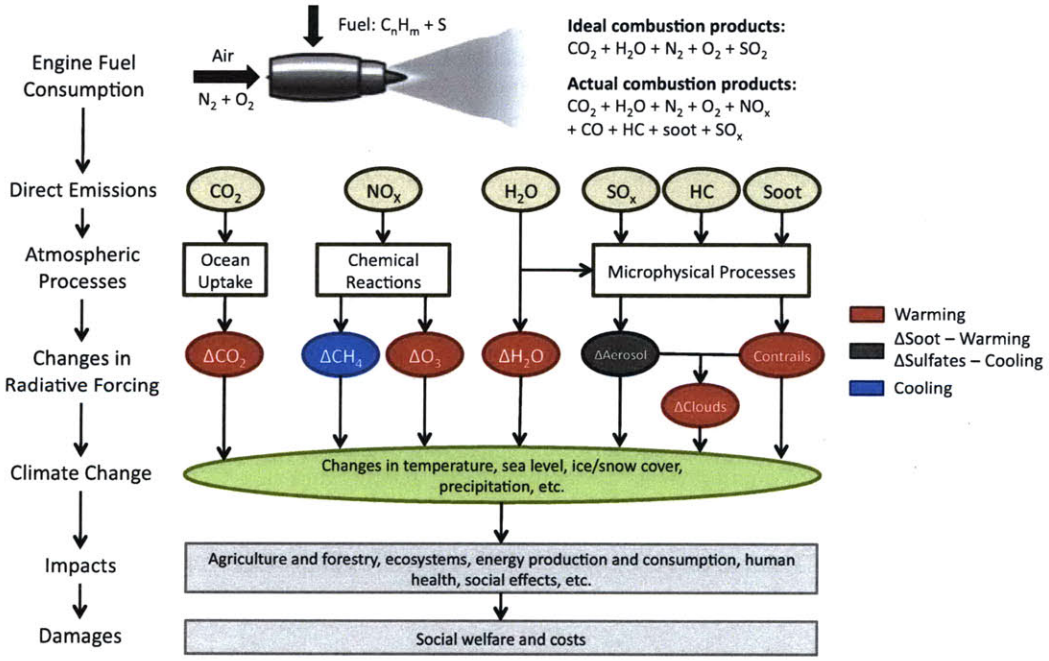

Figure 35: Aviation climate change impacts pathway (adapted from Wuebbles et al., 2007)

9.2 Including non-CO_2 Effects in the Fuel Life Cycle

The challenge in treating non-CO_2 combustion effects lies in reconciling the wide range of atmospheric residence times. Carbon dioxide has a warming effect on the atmosphere and a long atmospheric residence time (on the order of 100 years). Soot and sulfate aerosols generate atmospheric warming and cooling, respectively, and have residence times on the order of weeks (EPA, 2009). Contrails and contrail cirrus sustain only for hours to days and cause atmospheric warming (Minnis et al., 2003). NO_x has several different effects, which result in both warming and cooling. In the months following a pulse of NO_x in the upper atmosphere, ozone production is stimulated causing a short term warming. The NO_x also stimulates the production of additional OH, acting as a sink for methane. The corresponding reduction in methane, which is an important ozone precursor, leads to a long-term reduction in ozone. Both the long-term reduction in methane and ozone are cooling and decay with a lifetime of approximately 11 years (Stevenson et al., 2004; Mahashabde, 2009). Long lived gases become well mixed in the atmosphere; however; short lived emissions can remain concentrated near flight routes, mainly in the northern mid-latitudes; hence, these emissions can lead to regional perturbations to the radiative forcing (Penner et al., 1999). The impact of aircraft on regional climate could be important, but is currently beyond the capability of the models used in this work. Despite these limitations, assessing short-lived effects on a globally averaged basis gives an indication of the total potential of mitigating climate change by including non-CO_2 forcing agents in climate policy (Solomon et al., 2007).

Following the framework outlined in Section 4.3, ratios were developed to scale the CO_2 emissions from fuel combustion to account for the climate forcing from non-CO_2 combustion effects. Ensuring consistency of metric and time window among emission species of any given analysis is essential; hence, the assessment was limited to integrated-radiative forcing over 20 year, 100 year and 500 year time windows to maintain consistency with the global warming potentials implemented in assessing life cycle methane and nitrous oxide emissions (Solomon et al., 2007). The life cycle emissions of a fuel pathway can be presented either with or without the inclusion of climate impacts from non-CO_2 combustion effects. When non-CO_2 effects are ignored, the emissions inventory is purely a GHG emissions inventory composed of only CO_2, CH_4 and N_2O. This is given by Equation 14 and is simply the summation of well-to-tank CO_2 equivalent with tank-to-wake CO_2.

$$\left(CO_2e\right)_{\text{well-to-wake}} = \left(CO_2 + CH_4 \cdot GWP_{CH_4} + N_2O \cdot GWP_{N_2O}\right)_{\text{well-to-tank}} + \left(CO_2\right)_{\text{combustion}} \qquad \text{Equation 14}$$

Although non-CO_2 combustion effects have climate impacts that have been represented in terms of CO_2, they are not themselves greenhouse gases (with the exception of water vapor). As such, integrating the non-CO_2 combustion effects into a GHG life cycle inventory results in a combination of a GHG inventory and an impact analysis. Recall from section 4.1, tank-to-wake (+)[41] was defined by Equation 2 as the combination of CO_2 and non-CO_2 effects from fuel combustion in aircraft. In a similar fashion, well-to-wake (+)[42] is now defined as the sum of well-to-tank GHG emissions and tank-to-wake (+) emissions. Equation 15 is the corollary of Equation 14, explicitly defining the functional form of a well-to-wake (+) emissions inventory.

$$\left(CO_2e\right)_{\text{well-to-wake (+)}} = \left(CO_2 + CH_4 \cdot GWP_{CH_4} + N_2O \cdot GWP_{N_2O}\right)_{\text{well-to-tank}} + \left(CO_2\right)_{\text{combustion}} \cdot \left(\text{non-}CO_2\text{ ratio}\right)$$

Equation 15

[41] Pronounced 'tank-to-wake plus'
[42] Pronounced 'well-to-wake plus'

9.3 Combustion of SPK Fuel Compared to Conventional Jet Fuel

Conventional jet fuel consists of roughly 60% paraffinic hydrocarbons (also known as alkanes), 20% naphthenes (also known as cycloparaffins or cycloalkanes), and 20% aromatic compounds. A recent survey of the sulfur content of jet fuel leaving US found the nationwide average as approximately 700ppm. By comparison, SPK fuel is composed of 100% paraffinic hydrocarbons, contains no aromatics and negligible sulfur (Hileman et al., 2010).

The purely paraffinic nature and lack of sulfur present in SPK fuels has been shown to result in increased specific energy, decreased energy density and changes to the emissions characteristics of CO_2, H_2O, soot, sulfates and NO_x (Bester and Yates, 2009; Whitefield, 2010; Miake-Lye, 2010; Hileman et al., 2010). Therefore, independent non-CO_2 ratios are required for conventional jet fuel and SPK fuel. The changes in combustion properties between conventional jet fuel and SPK fuel are summarized in Table 49.

Table 49: Emissions characteristics of SPK fuel relative to conventional jet fuel

Fuel Characteristics	SPK relative to Conventional Jet Fuel
Specific Energy (per kg_{fuel})	1.023
Energy Density (per L_{fuel})	0.963
CO_2 Emissions (per kg_{fuel})	0.98
H_2O Emissions (per kg_{fuel})	1.11
Sulfate Emissions (per kg_{fuel})	0.0
Soot Emissions (per kg_{fuel})	0.05-0.5
NO_x Emissions (per kg_{fuel})	0.9-1.0
Contrails (per kg_{fuel})	1.0
Contrail cirrus (per kg_{fuel})	1.0

A detailed characterization of conventional and synthetic jet fuel by Hileman et al. (2010) was used to determine changes in specific energy, energy density and CO_2 emissions. Water vapor emissions were modified based on the carbon to hydrogen ratio of Jet A and SPK fuel as presented by Hileman et al. (2010). Synthetic fuels contain negligible quantities of sulfur so all sulfate emissions were eliminated. The formation of contrails and contrail cirrus were assumed unchanged by the use of SPK fuel. Changes in soot and NO_x emissions were represented as probabilistic distributions due to a lower degree of agreement in the literature.

In maintaining the *lens* framework discussed in Section 4.3.2, the percentage reduction in soot and NO_x emissions attributed to the use of SPK fuel were given the distributions shown in Figure 36. Results using the low and high lenses reflect deterministic use of the low and high values while the mid-range lens reflects the results of Monte Carlo simulations using random variables drawn from distributions with the bounds and functional forms shown below.

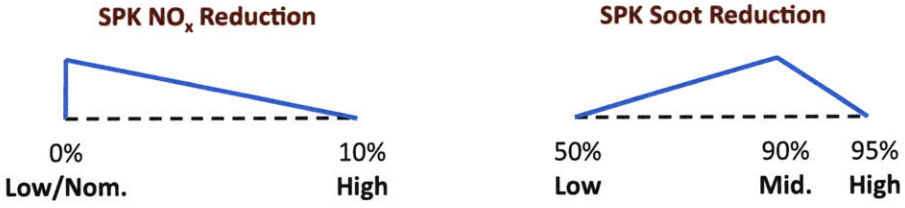

Figure 36: Input distributions for NO_x and soot reductions resulting from the use of SPK fuel

The upper and lower bounds of NO_x reduction were based on experimental results from Bester and Yates (2009), Dewitt et al. (2008), Timko et al. (2008) and Miake-Lye (2010). The functional form of the distribution was chosen to reflect a conservative estimate within the bounds of experimental data. NO_x emissions are strongly dependent on engine throttle setting, specific engine/combustor technology and ambient temperature; hence, it is little surprise that results of the aforementioned research efforts do not conclusively indicate a single value.

The upper and lower bounds of SPK induced soot reduction were based on experimental measurements from PW308 and CFM56 gas turbines. The data were reported by Donohoo (2010) and are dependent on throttle setting. Soot reductions from SPK use in the PW308 ranged from 95% at idle to 50% at 85% throttle; similarly, SPK fuel in the CFM56 led to a 98% reduction in soot at idle and a 70% reduction at 85% throttle. The mode of the distribution is consistent with measurements from Bester and Yates (2009) and Whitefield (2010), who measured an 87% reduction in soot at cruise conditions and an average reduction of 91% between throttle setting of 5% and 95%, respectively.

SPK fuel was assumed to have no impact on the radiative forcing from aircraft contrails and contrail cirrus because no data or scientific evidence has provided quantifiable evidence otherwise. Qualitatively, the magnitude of the atmospheric impact from contrails and contrail cirrus depends on details of plume evolution and the relative ability of aerosol particles to act as ice-forming nuclei (Wuebbles et al., 2007). The presence of ice-forming nuclei may trigger the formation of contrail cirrus much later than the original emission if the background atmosphere has changed to a state allowing for cloud formation (Sausen et al., 2005). Hence, the complete elimination of sulfate aerosols and the significant reduction of soot emissions caused by SPK fuel might serve to reduce contrail and contrail cirrus formation. Conversely, the increase in water vapor from SPK fuel may serve to stimulate additional contrails and contrail cirrus if their formation is more strongly dependent on background atmospheric aerosol concentrations rather than local concentrations in the exhaust jet. Wuebbles et al. (2007) emphasize that improving the understanding of contrails and contrail cirrus formation requires coordinated regional-scale measurements to correlate the growth, decay, and trajectories of contrail ice particles with the ambient aerosols and gaseous aerosol precursor concentrations.

The scaling factors for SPK fuel from Table 49 were implemented into the APMT climate impacts module and the results used to assess the climate effects of non-CO_2 combustion effects from SPK fuel and conventional jet fuel.

9.4 Non-CO_2 Ratios for Conventional and SPK Fuel

The non-CO_2 ratios derived for conventional jet fuel and SPK fuel are given in Figure 37 for time windows of 500 years, 100 years and 20 years. These time windows are consistent with the global warming potentials given by the IPCC for methane and nitrous oxide (Solomon et al., 2007). Each time window has ratios derived using the low impact lens, mid-range, and high impact lens to capture the uncertainties of the APMT climate model. The bars correspond to results using the mid-range lens while the low and high lenses are shown as the whiskers. Shorter time windows more strongly weigh short-lived effects. Assessing climate impacts using a short time window is analogous to adopting a high discount rate for a monetary impacts analysis; high discount rates are used to weight the present and near-term future more than the long-term future.

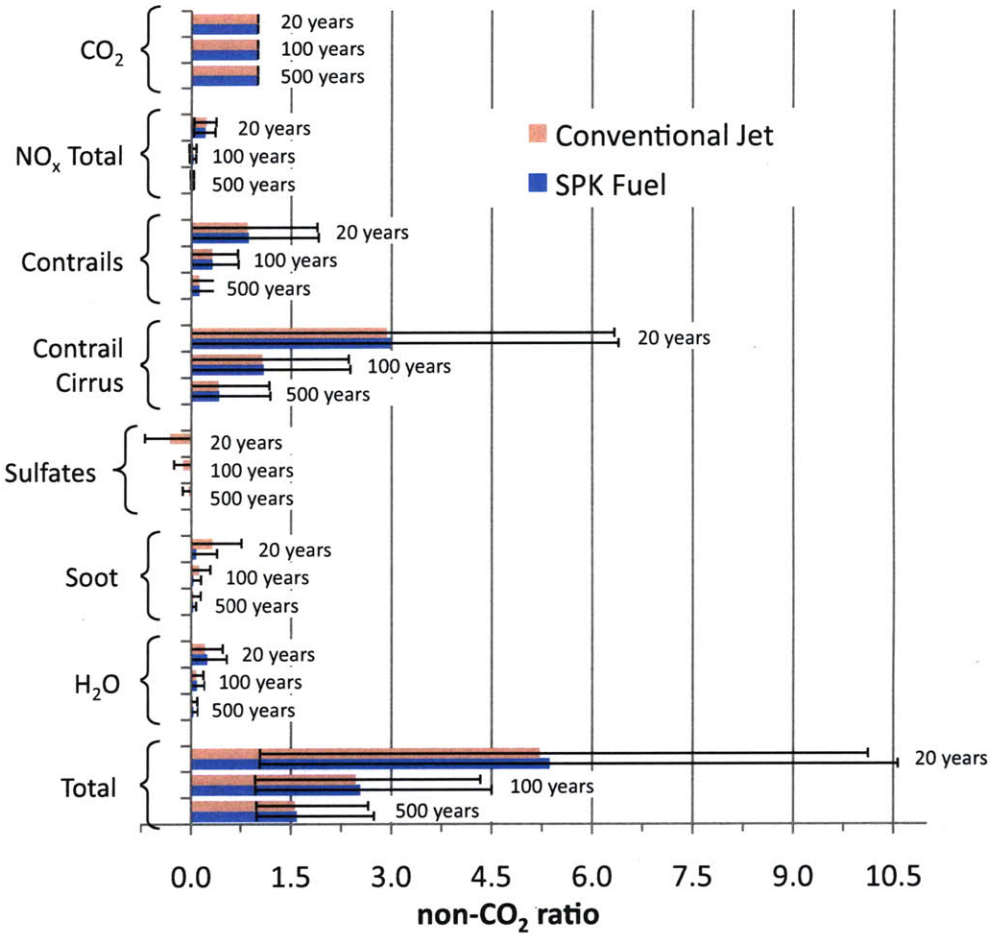

Figure 37: Non-CO_2 ratios disaggregated by species and time window for conventional and SPK fuel

These results indicate that both the time horizon and choice of lens play an important role in assessing the climate impacts of non-CO_2 combustion effects. As previously stated, a 100-year time window is most commonly used (Solomon et al., 2007); hence, results from the mid-range lens over a 100-year time window represent the nominal case.

The combustion of conventional jet fuel emits 73.2 g CO_2/MJ consumed by the engine. In the nominal case, the results from Figure 37 show that accounting for the climate impacts of all combustion products from aircraft is equivalent to emitting 2.47 times the amount of CO_2 actually produced from the combustion process, or 180.8 gCO_2e/MJ instead of 73.2 gCO_2/MJ.

Similarly, the combustion of SPK fuel emits 70.4 g CO_2/MJ consumed by the engine. When compared to conventional jet fuel, the elimination of sulfates and the increase in water vapor lead to warming while the reduction in NO_x and soot lead to cooling (in a few cases, the reduction in NO_x instead leads to a small warming effect). Additionally, small increases in the SPK non-CO_2 ratios occur as a result of normalizing by lower CO_2 emissions than conventional jet fuel. The net effect is a 0% to 4% increase in the total non-CO_2 ratio of SPK fuel compared to conventional jet fuel. The reader is reminded that the radiative forcing from contrails and contrail cirrus were assumed unchanged. As discussed in the section above, more detailed models and empirical

measurements are needed to determine what, if any, changes may actually occur. In the nominal case, Figure 37 shows that accounting for the climate impacts of the actual combustion products from aircraft consuming SPK fuel is equivalent to emitting 2.53 times the amount of CO_2 actually produced from the combustion process, or 178.2 gCO_2e/MJ instead of 70.4 gCO_2/MJ.

The lower CO_2 emissions per MJ of SPK fuel, compared to conventional jet fuel, more than offset the higher non-CO_2 ratio in the nominal case, resulting in a lower overall impact of combustion emissions. This fact is true for all lens and time windows except the high lens with a 20-year time window. The contribution of contrails and contrail cirrus to the total non-CO_2 ratio is sufficiently large that even a small change of either is more significant than a large change in other species; hence, the total non-CO_2 ratios are most sensitive to error in these two forcing agents. For conventional jet fuel, soot is the next most important effect after contrails and contrail cirrus; however, it is still only equivalent to maximum of approximately 40% and 10% of the effects from contrails and contrail cirrus, respectively. For SPK fuel, water vapor is the next most important effect after contrails and contrail cirrus; however, it is only equivalent to a maximum of approximately 8% and 30% of the effects from contrails and contrail cirrus, respectively. As such, additional research is needed to understand how SPK fuel consumption could affect contrail and contrail cirrus formation.

The differences in combustion CO_2 and total combustion emissions (as represented through the non-CO_2 ratios) between conventional jet fuel and SPK fuels is small by comparison to the variability in well-to-tank GHG emissions found in Chapters 5, 6 and 7. The differences in combustion CO_2 and total combustion emissions are only 2.8 gCO_2/MJ and 2.6 gCO_2e/MJ, respectively, but well-to-tank emissions were found to vary by over an order of magnitude. Therefore, while the inclusion of non-CO_2 effects in the fuel life cycle has been shown to be important, the influence of different emissions characteristics between SPK and conventional jet fuel is minimal on a life cycle basis.

The combination of these data with Equations 14 and 15 complete the framework required to include non-CO_2 effects in the fuel life cycle. The complete combustion products from aircraft can now be assessed in conjunction with the GHG inventories of Chapter 5, Chapter 6 and Chapter 7.

Chapter 10: Examination of Key Results

All results and discussion of this chapter is based on a combination of the work of Wong (2008) and this thesis. Since both results sets are complimentary and part of a common research initiative, the whole is more valuable than the sum of its individual parts.

10.1 Well to Wake Greenhouse Gas Inventories

Table 50 summarizes the results of the life cycle GHG emissions for the baseline scenario of the all fuel pathways considered as part of this research effort; this includes the work of Wong (2008) and the results from Chapters 5, 6 and 7 of this thesis. The data are broken out by life cycle step to allow for the identification of critical steps driving the GHG inventory of each fuel pathway. Figure 38 presents the same results in graphical form but does not show cumulative totals. Rather, it displays the contribution of emissions from each step in the fuel life cycle. The impact of the land use change scenarios, which are summarized in Table 51, is included in the form of two pathways for switchgrass fed F-T jet, three pathways for soy oil to HRJ, four pathways for palm oil HRJ, two pathways for rapeseed to HRJ and two pathways for salicornia oil HRJ. These results highlight the need to avoid land usage changes that result in positive GHG emissions. This method of presentation displays the 'biomass credits' that are given to biofuels from the CO_2 absorbed during biomass growth. With the exception of BTL and CBTL, the biofuel pathways all have similar 'biomass credits' and the magnitude of these credits is approximately the magnitude of the combustion emissions.[43] The 'biomass credit' for CBTL is smaller because the fuel is created from a combination of coal and biomass. The 'biomass credit' for BTL is larger because biomass is used to power the entire fuel production process.

The baseline life cycle GHG emissions values in Figure 38 were combined with the low and high emissions scenario values to create Figure 39. The purpose for life cycle GHG inventories is to compare an alternative jet fuel to jet fuel from conventional petroleum; hence, results are normalized by the life cycle GHG emissions of conventional jet fuel. The uncertainty bars represent the range of emissions as given by the low and high emissions cases. Many pathways have baseline life cycle GHG emissions that are lower than conventional jet fuel but have the potential to have GHG emissions that are higher than conventional jet fuel. For this reason, it is critical not to simply assume that biofuels are environmentally beneficial without knowing the specifics of how the fuel is produced.

A few of the key results are outlined below:

- *Life cycle GHG emissions are but one of many considerations when evaluating the feasibility and sustainability of an alternative fuel option.*

- *The data do not include all of the feedstock-to-fuel pathways that could be use to create jet fuel. Some interesting options not covered include camelina oil to jet fuel, fuels created from pyrolysis oils and advanced fermentation of sugars to hydrocarbons. These will be addressed as part of the ongoing work and will appear in future revisions to this report.*

[43] In some of the high and low emissions scenarios, the 'biomass credit' is not quite equal to the combustion emissions due to variations in the allocation ratios throughout the pathway. Since the biomass credit' is given in the first life cycle stage (feedstock recovery), it is subject to all allocation ratios.

- *Of the fuel options considered herein, conventional petroleum has the lowest emissions of any fossil-based jet fuel pathway.*
- *Few biofuels have zero life cycle GHG emissions.*
- *There is considerable variability in the life cycle GHG emissions; emissions from land use change contribute the most to this for the biofuel pathways considered.*

Table 50: Baseline life cycle GHG emissions for all fuel pathways studied. Land use change scenarios are described in Table 51

	Biomass Credit	Recovery	Feedstock Transport	Processing	Fuel Transport	Combustion	WTT N_2O	WTT CH_4	Land Use Change	Total
Crude to conventional jet fuel	0.0	4.2	1.5	5.5	0.8	73.2	0.1	2.3	0.0	87.5
Crude to ULS jet fuel	0.0	4.2	1.5	7.3	0.8	72.9	0.1	2.4	0.0	89.1
Oil sands to jet fuel	0.0	19.0	1.3	5.5	0.5	73.2	0.1	3.1	0.0	102.7
Oil shale to jet fuel	0.0	41.2	0.6	3.3	0.6	73.2	0.2	2.5	0.0	121.5
Natural gas to F-T fuel	0.0	4.6	0.0	20.2	1.2	70.4	0.0	4.6	0.0	101.0
Coal to F-T fuel (no carbon capture)	0.0	0.8	0.1	117.2	0.6	70.4	0.0	5.7	0.0	194.8
Coal to F-T fuel (with carbon capture)	0.0	0.8	0.1	19.4	0.6	70.4	0.0	5.9	0.0	97.2
Switchgrass to F-T fuel (LUC-B0)	-222.7	6.4	0.6	152.1	0.5	70.4	10.3	0.2	0.0	17.7
Switchgrass to F-T fuel (LUC-B1)	-222.7	6.4	0.6	152.1	0.5	70.4	10.3	0.2	-19.8	-2.0
Coal and Switchgrass to F-T fuel with CCS (LUC-B0)	-44.3	1.2	0.2	21.9	0.5	70.4	2.0	4.9	0.0	56.9
Coal and Switchgrass to F-T fuel w/o CCS (LUC-B1)	-44.3	1.2	0.2	21.9	0.5	70.4	2.0	4.9	-3.9	53.0
Soy oil to HRJ (LUC-S0)	-70.5	20.1	1.2	10.3	0.6	70.4	3.6	1.3	0.0	37.0
Soy oil to HRJ (LUC-S1)	-70.5	20.1	1.2	10.3	0.6	70.4	3.6	1.3	60.8	97.8
Soy oil to HRJ (LUC-S2)	-70.5	20.1	1.2	10.3	0.6	70.4	3.6	1.3	527.2	564.2
Palm oils to HRJ (LUC-P0)	-70.5	4.9	3.1	10.3	0.6	70.4	5.1	6.3	0.0	30.1
Palm oils to HRJ (LUC-P1)	-70.5	4.9	3.1	10.3	0.6	70.4	5.1	6.3	9.6	39.8
Palm oils to HRJ (LUC-P2)	-70.5	4.9	3.1	10.3	0.6	70.4	5.1	6.3	135.8	166.0
Palm oils to HRJ (LUC-P3)	-70.5	4.9	3.1	10.3	0.6	70.4	5.1	6.3	667.9	698.0
Rapeseed oil to HRJ (LUC-R0)	-70.5	17.2	3.1	10.3	0.6	70.4	22.4	1.3	0.0	54.9
Rapeseed oil to HRJ (LUC-R1)	-70.5	17.2	3.1	10.3	0.6	70.4	22.4	1.3	43.0	97.9
Jatropha oil to HRJ	-70.5	16.7	1.5	10.3	0.6	70.4	9.1	1.2	0.0	39.4
Algae oil to HRJ	-70.5	29.6	0.3	10.3	0.6	70.4	8.1	1.8	0.0	50.7
Salicornia to HRJ and F-T Fuel (LUC-H0)	-105.3	36.8	1.1	38.3	0.5	70.4	4.6	1.3	0.0	47.7
Salicornia to HRJ and F-T Fuel (LUC-H1)	-105.3	36.8	1.1	38.3	0.5	70.4	4.6	1.3	-41.9	5.8

Table 51: Land use change scenarios considered in this work

Land use change	Scenario 0	Scenario 1	Scenario 2	Scenario 3
Switchgrass (B0, B1)	None	Carbon depleted soils converted to switchgrass cultivation	n/a	n/a
Soy oil (S0-S2)	None	Grassland conversion to soybean field	Tropical rainforest conversion to soybean field	n/a
Palm oil (P0-P3)	None	Logged over forest conversion to palm plantation field	Tropical rainforest conversion to palm plantation field	Peat land rainforest conversion to palm plantation field
Rapeseed oil (R0, R1)	None	Set-aside land converted to rapeseed cultivation	n/a	n/a
Salicornia (H0, H1)	None	Desert land converted to salicornia cultivation field	n/a	n/a

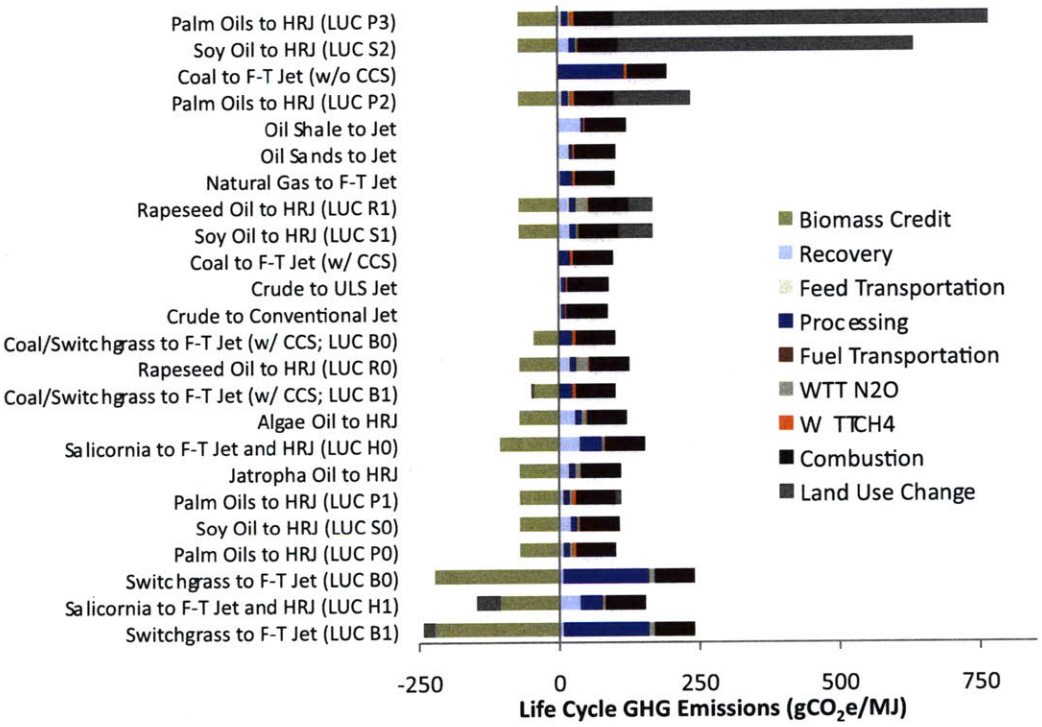

Figure 38: Life cycle GHG emissions for the baseline scenario of alternative jet fuel pathways under consideration

Notes: CCS denotes carbon capture and sequestration; land use change (LUC) scenarios are defined in Table 51.

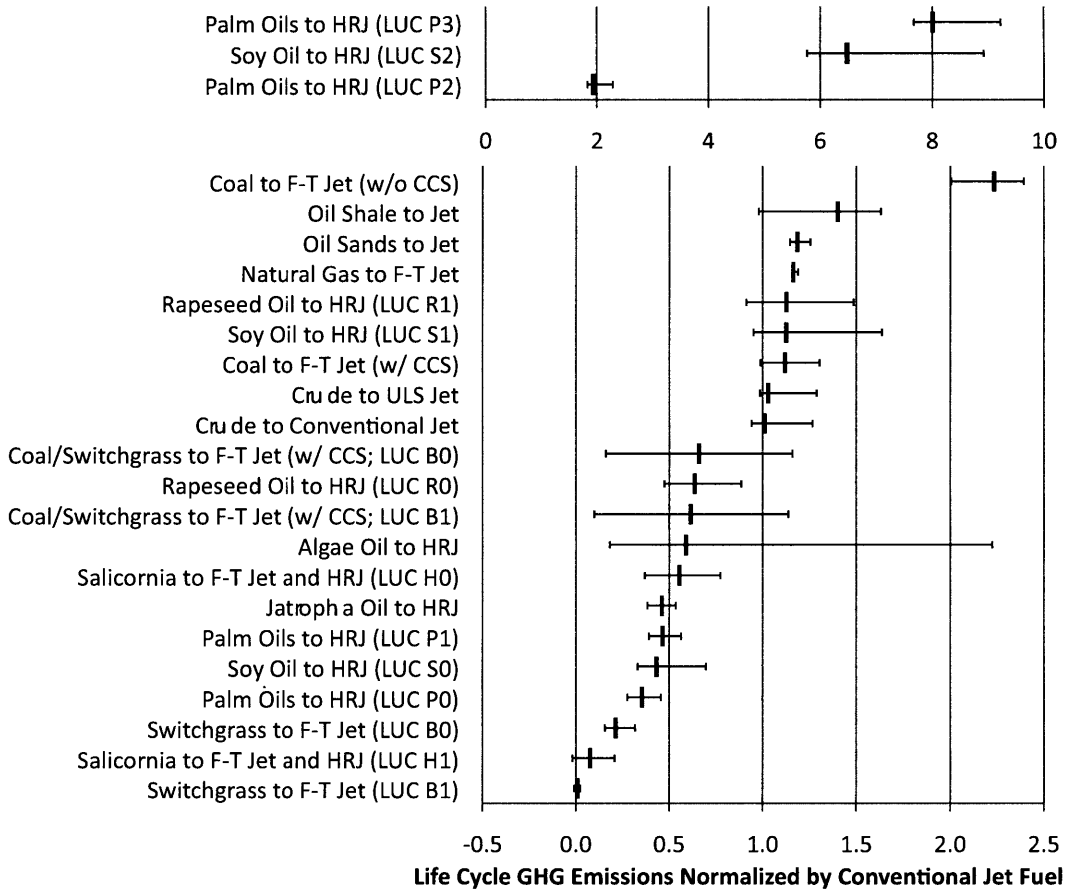

Figure 39: Life cycle GHG emissions for the alternative jet fuel pathways under consideration normalized by those of conventional jet fuel.

Notes: Different scales are used for the top and bottom portions of the figure; uncertainty bars represent the low emissions, baseline, and high emissions scenarios; CCS denotes Carbon Capture; storage and land use change (LUC) scenarios are defined in Table 51.

10.2 Well to Wake (+) Emissions Inventories

Using Equation 15, the well-to-wake GHG inventories were modified to include the climate effects of all combustion products from aircraft. The non-CO_2 ratios developed using the low impact, mid-range and high impact lenses of the APMT climate model were paired to the GHG inventories of the low emissions, baseline and high emissions scenarios. All results and discussion in this section is limited to a 100-year time window because of its prevailing use in the scientific community for global warming potentials. The sensitivity of results to choice of time window will be addressed separately in Section 10.3.

The well-to-tank (+) emissions inventory of the baseline scenario for all fuel pathways considered as part of this research effort are shown in Figure 40 broken out by life cycle step. Figure 40 differs from Figure 39 only in the addition of non-CO_2 effects expressed using the 100-year mid-range non-CO_2 ratio. Under these nominal assumptions, non-CO_2 effects are the largest emissions source for most fuel pathways; the exceptions are land use change scenarios S2, P2 and P3 (see Table 51) and the CO_2 emitted from F-T facilities without CCS.

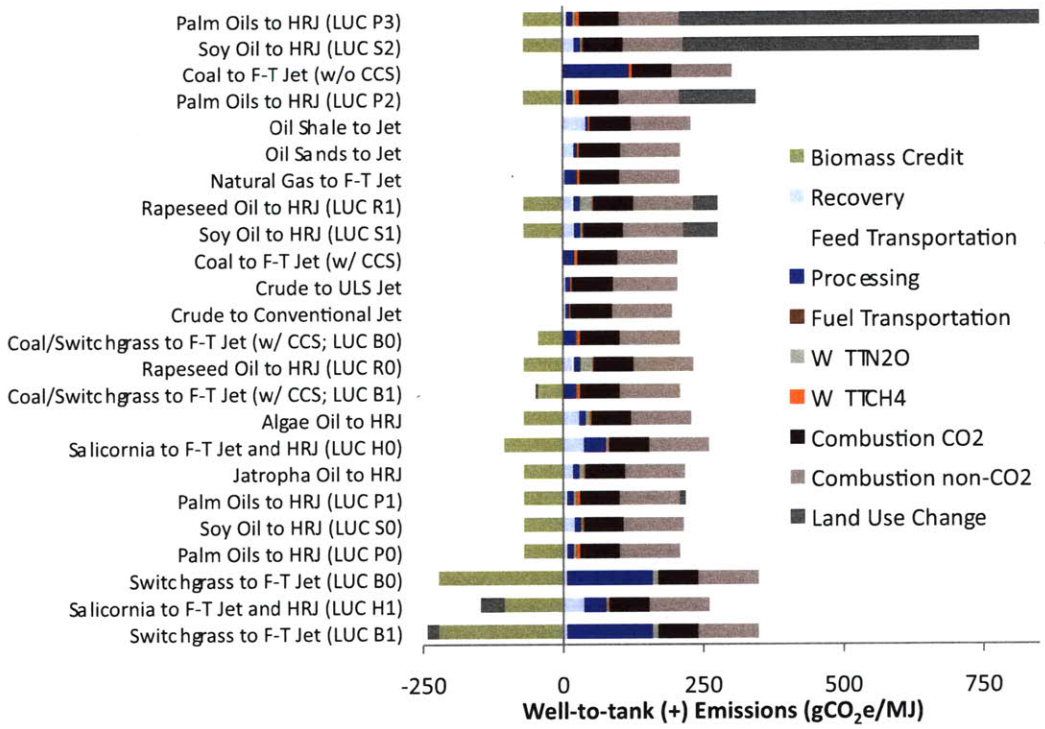

Figure 40: Well-to-Wake (+) emissions for the baseline scenario of alternative jet fuel pathways under consideration

Notes: CCS denotes carbon capture and sequestration; land use change (LUC) scenarios are defined in Table 51.

Figure 41 shows the well-to-wake (+) emissions inventories normalized by the baseline well-to-wake (+) emissions inventory of conventional jet fuel. The black error bars correspond to combining the 100-year mid-range non-CO_2 ratios with the well-to-wake low, baseline and high GHG emissions scenarios. The orange error bars correspond to pairing the 100-year low impact, mid-range and high impact non-CO_2 ratios with the well-to-wake low, baseline and high GHG emissions scenarios, respectively. Presenting the results in this manner separates the variability introduced by the GHG inventories from the climate modeling uncertainty of the non-CO_2 ratios. The uncertainty of the non-CO_2 ratios has a larger influence than the internal variability of the GHG inventories on the range of normalized well-to-wake (+) emissions for each fuel pathway.

While the intra-pathway variability is increased because of including non-CO_2 effects, inter-pathway variability in normalized well-to-wake (+) emissions is reduced. When only GHG emissions are considered, the range in life cycle GHG emissions was 0 to 9.1 times those of baseline conventional jet fuel. When GHG emissions and non-CO_2 combustion effect are considered, the range in well-to-wake (+) emissions is only 0 to 4.7 times those of baseline conventional jet fuel. This occurs because the well-to-tank GHG emissions represent a smaller fraction of the total when non-CO_2 effects are included in the fuel life cycle; well-to-tank GHG emissions drive the all inter- and intra-pathway variability in Figure 39. Hence, the inclusion of non-CO_2 effects in the fuel life cycle increases the absolute uncertainty of each fuel pathway but reduces the overall variability in the life cycle emissions of alternative fuels relative to conventional jet fuel.

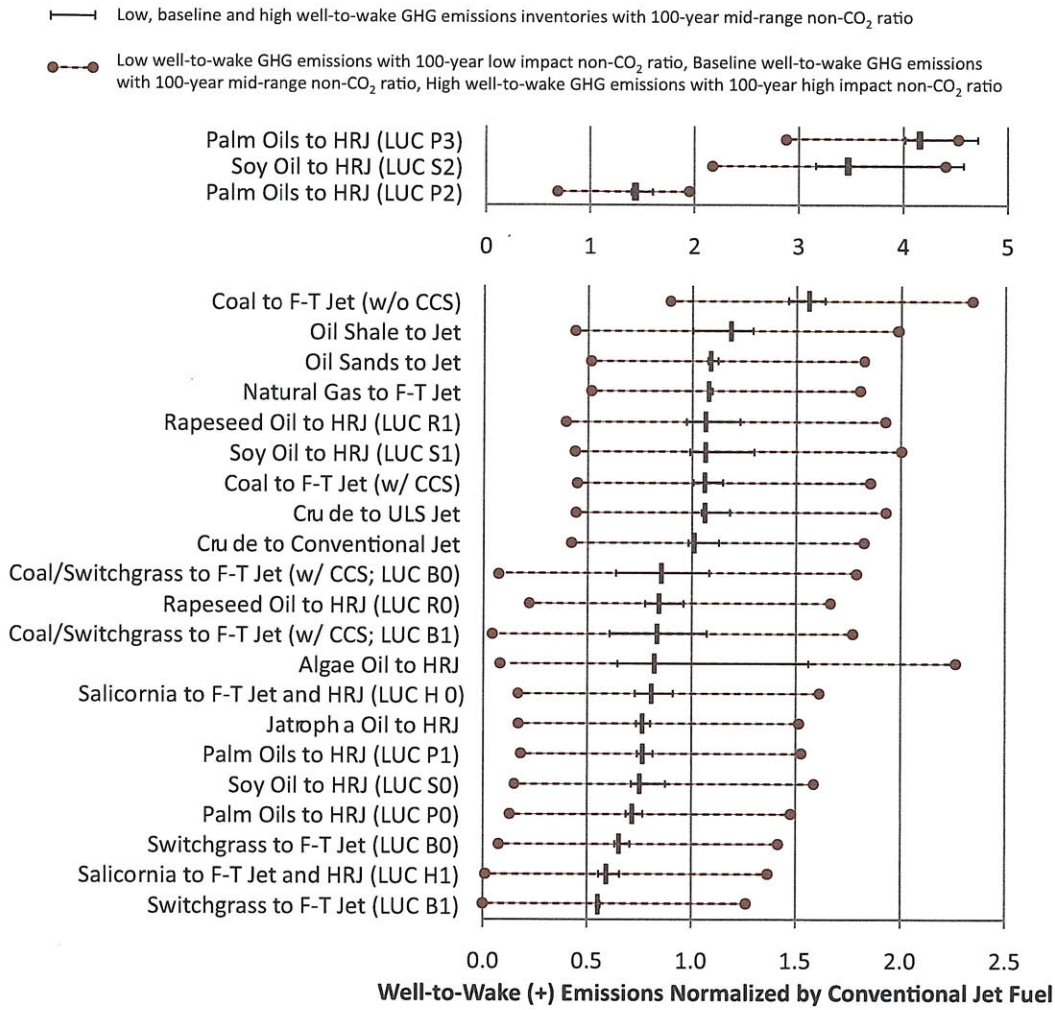

Figure 41: Well-to-tank (+) emissions for the alternative jet fuel pathways under consideration normalized by those of conventional jet fuel

Notes: Different scales are used for the top and bottom portions of the figure; uncertainty bars represent the low emissions, baseline, and high emissions scenarios; CCS denotes Carbon Capture; storage and land use change (LUC) scenarios are defined in Table 51.

10.3 Sensitivity of Results to Time Window

Thus far, a 100-year time window has been used to express all species and effects in terms of carbon dioxide equivalent. In a similar manner to the non-CO_2 ratios of Figure 37, the 500-year, 100-year and 20-year IPCC global warming potentials for methane and nitrous oxide are given in Table 52 (Solomon et al., 2007). Methane and nitrous oxide have atmospheric lifetimes of 12 and 114 years, respectively; therefore, a 20-year time window more heavily weights methane while a 100-year time window more heavily weights nitrous oxide.

Table 52: IPCC global warming potentials of methane and nitrous oxide

IPCC GWP	500 year	100 year	20 year
Methane (CH_4)	7.6	25	72
Nitrous Oxide (N_2O)	153	298	289

The sensitivity of the well-to-wake and well-to-wake (+) emissions inventories developed herein to the choice of time window is best examined through the use of case studies. Specifically, the well-to-wake GHG emissions inventories of baseline conventional jet fuel from US crude oil, baseline conventional jet fuel from Nigerian crude oil and baseline rapeseed oil to HRJ were chosen to span a CO_2 dominated fuel, a CH_4 intensive fuel and a N_2O intensive fuel. Additionally, the tank-to-wake (+) emissions of conventional jet fuel were evaluated using the mid-range lens 500-year, 100-year and 20-year non-CO_2 ratios from Figure 37.

10.3.1 Baseline Conventional Jet Fuel from US Crude Oil

The life cycle GHG inventory of conventional jet fuel from US crude oil is almost entirely composed of CO_2 emissions. Only a small fraction is CH_4 or N_2O; therefore, this inventory is insensitive to the choice of time window chosen to represent CH_4 and N_2O in terms of CO_2. This is demonstrated in Figure 42 where the choice of time window causes only a 1.3gCO_2e/MJ change in the well-to-wake GHG emissions the fuel.

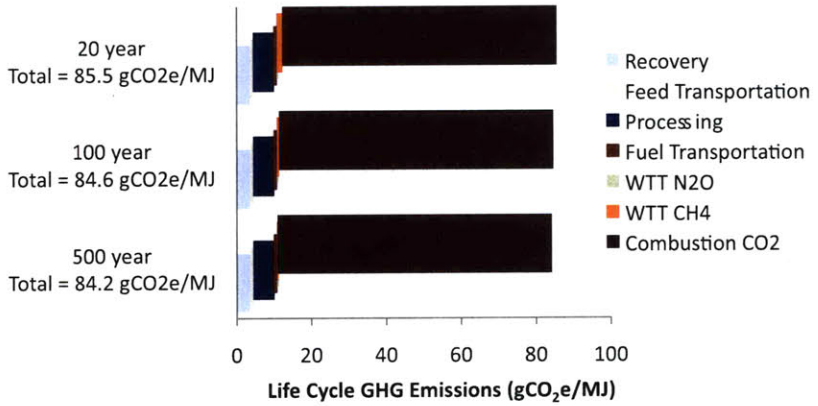

Figure 42: Life cycle GHG inventory of conventional jet fuel from US crude oil using 20-year, 100-year and 500-year global warming potentials for CH_4 and N_2O

10.3.2 Baseline Conventional Jet Fuel from Nigerian Crude Oil

The life cycle GHG inventory of conventional jet fuel from Nigerian crude oil is subject to substantial methane emissions from the venting processes used in Nigeria for crude oil extraction. The global warming potential of CH_4 varies by approximately an order of magnitude when evaluated using a 20-year time window or a 500-year time window. This variation is carried through to the life cycle GHG inventories of fuels where CH_4 is an important contributor to the total. As shown in Figure 43, choosing different time windows to assess the life cycle GHG emissions of baseline conventional jet fuel from Nigerian crude oil results in a range of 33.6 gCO_2e/MJ.

10.3.3 Baseline Rapeseed Oil to HRJ Fuel

The life cycle GHG inventory of HRJ form rapeseed oil is strongly influenced by N_2O emissions from direct and indirect conversion of synthetic nitrogen and nitrogen rich crop residues applied to the field. The global warming potential for N_2O is less sensitive to time window than that of

CH_4; however, it still varies by approximately a factor of 2 and this variation is carried through to the life cycle GHG inventories of fuels where N_2O is an important contributor to the total. Figure 44 demonstrates this effect for baseline HRJ from rapeseed oil (no land use change), where the use of 500-year and 20-year time windows results in a range of 13.5 gCO_2e/MJ.

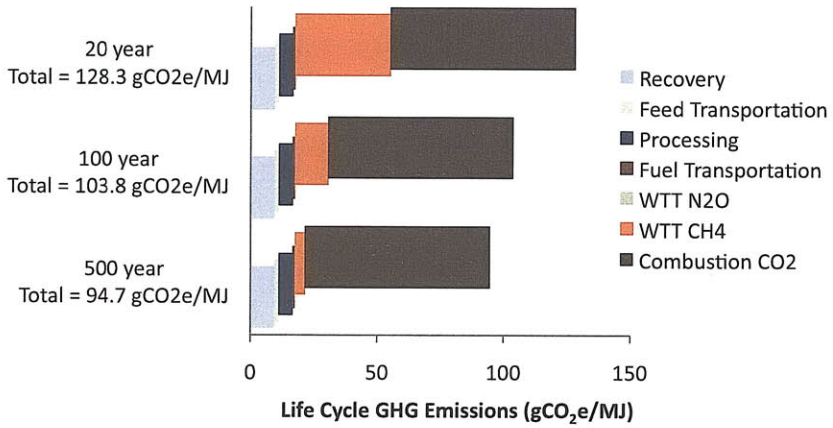

Figure 43: Life cycle GHG inventory of conventional jet fuel from Nigerian crude oil using 20-year, 100-year and 500-year global warming potentials for CH_4 and N_2O

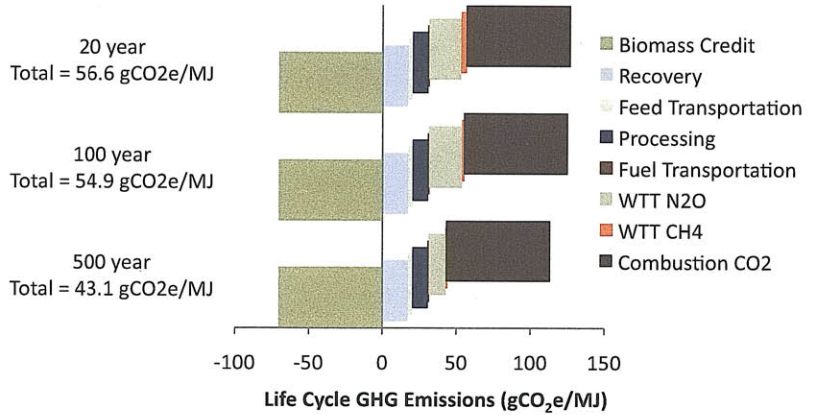

Figure 44: Life cycle GHG inventory of HRJ fuel from rapeseed oil using 20-year, 100-year and 500-year global warming potentials for CH_4 and N_2O

10.3.4 Tank-to-Wake (+) Emissions of Conventional Jet Fuel

Tank-to-wake (+) emissions are subject to a choice of time windows through the non-CO_2 ratios presented in Figure 37. As shown in Section 9.4, both the time horizon and choice of lens are important when assessing the climate impacts of non-CO_2 combustion effects. The focus of this section is assessing the influence of the time window; therefore, the mid-range lens was used as a representative assumptions set. Figure 45 shows that the tank-to-wake (+) emissions from conventional jet fuel vary by 267.7 gCO_2e/MJ, from 114.1 gCO_2e/MJ to 381.8 gCO_2e/MJ, with the use of a 500-year or 20-year time window, respectively. SPK fuels are subject to the same influence because of the similarity in the non-CO_2 ratios of SPK fuel and conventional jet fuel.

As a result, all fuel pathways are affected by the substantial influence of time window choice on well-to-wake (+) emissions. The scope is not limited to fuel pathways that are strong in a particular type of emissions and the magnitude is several times larger than the CH_4 or N_2O cases considered in Sections 10.3.2 and 10.3.3. Despite this undesirable variability, the time window used to assess non-CO_2 combustion effects must be the same as that used in the global warming potentials of well-to-tank CH_4 and N_2O. In the majority of cases, a 100-year time window is chosen for CH_4 and N_2O; hence, the need for consistency serves as a constraint in choosing the appropriate time window over which to consider non-CO_2 combustion effects.

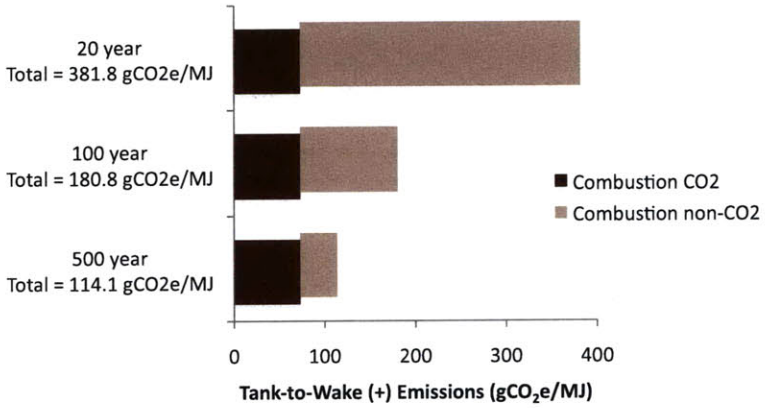

Figure 45: Tank-to-wake (+) emissions of conventional jet fuel using 20-year, 100-year and 500-year mid-range non-CO_2 ratios

10.4 Synthesis of Findings

The focus of this work was to evaluate the environmental feasibility of a variety of alternative jet fuels and to determine the scales at which these fuels would need to be implemented in order to represent a meaningful contribution to the petroleum-based jet fuel industry. The former was covered from the perspective of life cycle GHG emissions, non-CO_2 combustion effects, freshwater use and potential for introducing invasive species into an unprepared ecosystem in Sections 10.1, 10.2, 8.2 and 8.3, respectively. The latter was addressed in Section 8.1 by combining the analysis of fuel yield with the production scales of the petroleum-based jet fuel industry.

The life cycle GHG emissions from Figure 39 and production potentials from Figure 31 can be combined to select fuel pathways that hold the most potential for reducing aviation's GHG emissions. While the complete well-to-wake (+) emissions inventories of Figure 41 are required to evaluate the true climate change mitigation potential of alternative fuels, only the well-to-wake emissions of Figure 39 are necessary to compare one fuel option to another. This combination is needed to reduce aviation's GHG emissions because fuel pathways having both low life cycle GHG emissions as well as large fuel production potential are required.

Fossil-to-jet fuel pathways have large production potential, but they have comparable or higher emissions than conventional jet fuel; therefore, their use will not reduce GHG emissions. BTL fuels have low GHG emissions, but they also have limited fuel production potential due to the large capital costs for F-T production facilities. With the use of excess rapeseed, palm or soy (available after food needs are met) for HRJ production, rapeseed to HRJ, soy to HRJ and palm to HRJ have low life cycle GHG emissions; however, there is little excess available and new cropland is required for additional production. Current global production of soy, palm and

rapeseed oil translate to only 34%, 43% and 18% of US jet fuel demand, respectively (FAPRI, 2009). As such, expanded production of soy oil and palm oil for large-scale HRJ production could result in significant GHG emissions from land use change. Because of its toxic characteristics and low yield, jatropha is likely limited to small regional applications making it inappropriate to replace considerable quantities of conventional jet fuel. Hence, BTL fuels as well as HRJ fuels from soy, palm, and jatropha have limited potential for reducing GHG emissions. The production potential of CBTL is largely dependent on the biomass weight fraction of the feedstock. Switchgrass was found to yield three times more volume of jet per hectare than corn stover when fed with a weight fraction of 25%; however, corn is a co-product of corn stover and could be used for other purposes. Salicornia holds promise if it is used to make both HRJ and BTL (or CBTL) fuels as it could reduce life cycle GHG emissions by 25% compared to conventional jet fuel and has a production potential equivalent to one third of palm. The most obvious opportunity for large-scale production is using algae to make HRJ, which explains the recent wave of investments in the algae industry.

By comparing Figure 39 to Figure 41, including non-CO_2 combustion effects has been shown to change the emissions of an SPK fuel relative to those of conventional jet fuel. The magnitude of this change is dependent on both the magnitude of the SPK and conventional jet fuel non-CO_2 ratios as well as the well-to-tank GHG emissions of the fuel. In general, fuels with life cycle GHG emissions less than conventional jet fuel experience an increase in their normalized emissions after including non-CO_2 combustion effects. For example, a fuel option with zero life cycle GHG emissions would offer a 100% reduction in well-to-wake emissions but only a 45% reduction in well-to-wake (+) emissions using a 100-year mid-range non-CO_2 ratio. Conversely, fuels with life cycle GHG emissions greater than those of conventional jet fuel experience a decrease in their normalized emissions after including non-CO_2 combustion effects.

As discussed in Section 2.2, a motivation for considering alternative fuels for use in aviation is to reduce the environmental impact of the aviation industry; hence, interest is primarily focused on fuels with GHG emissions lower than those of conventional jet fuel. Since the normalized well-to-wake (+) emissions of fuels in this category are higher than their normalized well-to-wake GHG emissions, a percentage reduction in life cycle GHG emissions of the jet fuel mix is less than the actual percentage reduction in aviation related climate impacts. Therefore, aviation GHG reduction scenarios (e.g. emissions wedge charts) that rely exclusively on relative well-to-wake life cycle GHG emissions may overestimate the impact of alternative fuel use on the global climate system. Both the renewable fuels standard of 2010 and Section 526 of the Energy Independence and Security Act of 2007 rely on relative well-to-wake GHG emissions (EISA, 2007; EPA, 2010). The degree of overestimation is dependent on the assumptions used for the climate impact analysis of non-CO_2 combustion effects. While the results of this thesis were developed using the current best available data, climate forcing from contrails and contrail cirrus remains uncertain, especially for SPK fuel; hence, these results should be used with caution until further research is available.

Chapter 11: Conclusions and Future Work

11.1 Conclusions

As part of continuing research on alternative jet fuels, a screening level life cycle assessment of a wide range of potential drop-in alternative jet fuels was conducted. Three scenarios were developed for each pathway corresponding to optimistic, nominal and pessimistic assumptions regarding specific process inputs and production characteristics. In most fuel pathways, the choice of allocation methodology and potential for GHG emissions from land use change were found to have the largest impact on the results.

Consistent allocation methodologies were implemented across multiple pathways to facilitate equitable comparisons of different alterative fuels. In all analyses, the use of displacement or system expansion was minimized to reduce the variability of the results to subjective assumptions. The displacement method was only implemented where assumptions could be made that minimize the impact of allocation on the result (e.g. electricity generation as a CO_2 source for algae). Energy allocation was used for any process that resulted in a product slate of liquid hydrocarbons (e.g., jet, diesel and naphtha from F-T synthesis). Market value allocation was used for processes resulting in a combination of oil and meal (e.g. separation of soybeans into soy oil and soy meal). In all such cases, the oil price was assumed equal to that of soy oil and the price of meal assumed relative to soy meal based on relative protein content. The use of mass or volume allocation was avoided.

The treatment of land use change emissions (both positive and negative) in this work was developed to provide an understanding for the reader of how land use change emissions compare with the emissions from the other five life cycle stages. It was not intended to explicitly quantify the specific land use change emissions that would result from expanded production of any given feedstock. The scope of this work was limited to only quantifying the impacts of direct land use change; emissions from indirect land use change were not considered. Multiple scenarios were used to explore the range of magnitudes of GHG emissions due to land use change; these included a scenario where no land use change emissions were incurred. This approach allowed the impacts of different land use change scenarios to be isolated from the other emissions from fuel production and use.

Given their reduced life cycle GHG emissions relative to conventional jet fuel, some alternative fuels could play a central role in mitigating aviation's contribution to climate change, including helping aviation to achieve carbon-neutral growth when combined with improved technology and more efficient operations. If appropriate renewable feedstocks were used, both Fischer-Tropsch (F-T) fuels and Hydroprocessed Renewable Jet (HRJ) fuel could provide aviation with modest (~10%) to large (~50%) reductions in GHG emissions. If projections of soil carbon sequestration prove valid, a salicornia-based biofuel could have a 100% reduction in life cycle GHG emissions.

Life cycle GHG inventories of bio-based fuels consider the emissions from fuel combustion equal and opposite to the emissions absorbed from the atmosphere during growth of the feedstock; however, this neglects the climate forcing from non-CO_2 combustion effects resulting from the combustion of jet fuel in the upper atmosphere. Using a modified version of the APMT climate impacts module, ratios were developed to scale the CO_2 from fuel combustion to account for the

additional climate forcing from the non-CO_2 combustion effects of SPK fuel and conventional jet fuel. The uncertainty in the non-CO_2 ratios was found to have a larger influence on the overall emissions range for each fuel pathway than the internal variability of the GHG inventories. This thesis defined the term 'well-to-wake (+)' as the combination of life cycle GHG emissions and non-CO_2 effects from fuel combustion in aircraft. While the intra-pathway variability was increased because of including non-CO_2 effects, inter-pathway variability in normalized well-to-wake (+) emissions was reduced. Hence, the inclusion of non-CO_2 effects in the fuel life cycle increases the absolute uncertainty of each fuel pathway but reduces the overall variability in the life cycle emissions of alternative fuels relative to conventional jet fuel.

National policies responsible for the environmental requirements for alternative fuels (e.g. EISA Section 526) are based on the ratio of well-to-wake GHG emissions of the alternative fuel to those of the displaced petroleum product. In general, fuels with well-to-wake GHG emissions less than conventional jet fuel experience an increase in their normalized emissions when non-CO_2 combustion effects are included. A motivation for considering alternative fuels for use in aviation is to reduce the environmental impact of the aviation industry; hence, interest is primarily focused on fuels with well-to-wake GHG emissions lower than those of conventional jet fuel. Therefore, aviation GHG reduction scenarios (e.g. emissions wedge charts) that rely exclusively on relative well-to-wake life cycle GHG emissions may overestimate the impact of alternative fuel use on the global climate system. Only a percentage reduction in fuel burn is equivalent to the same percentage reduction in aviation related climate forcing. Future policies for aviation should reflect this important difference between changing consumption and changing the product consumed.

Although this thesis has identified several shortcomings that could prevent biofuels from being a complete environmental solution for the aviation industry, they could still be an important part of the aviation industry's strategy for reducing life cycle GHG emissions. Current actions with regard to biofuel expansions are important in realizing the potential of this industry. Not all feedstocks need to have the potential to displace large volumes of petroleum fuel. Any feedstock produced today can lead to valuable experience through benefitting local economies and providing essential lessons in production and processing techniques. This experience would be invaluable should a higher yield crop, such as algae, become commercially viable.

The most significant challenge is not in developing viable alternative fuels that could reduce aviation's environmental impacts – the technology exists; rather, the challenge lies in developing and commercializing the large scale production of next generation of biomass feedstocks that could be grown in a sustainable manner.

11.2 Recommendations of Future Work

Some key areas of additional research are outlined below as potential extensions of the work presented in this thesis.

Indirect Land Use Change Emissions

As part of ongoing research, a more complete assessment of land use change emissions that includes indirect effects should be developed. Proper evaluation of the indirect effects of alternative fuels within aviation requires modeling of the demand for renewable energy resources within the transportation sector, including aviation, as well as the demand for renewable energy resources from the energy sector as a whole. Most indirect effects are expected to occur on an international scale; hence, domestic analyses, such as those in this work, need to be done in the context of the global market.

Next Generation Fuel Pathways

Aviation is not the only potential user of renewable biomass resources, and it will have to compete for these limited resources. Furthermore, large land area requirements indicate that it is unlikely that a single region could create sufficient biomass to supply the entire planet with biofuels. Hence, it is probable that large-scale implementation of biofuels would arise as a superposition of regionally appropriate feedstocks. It is critical to continue to examine feedstocks that could be used to create transportation fuels, such as jet fuel, without the need for arable land, with a minimum of fresh water, and with large yields per hectare. Immediate attention should be given to advanced fermentation of sugars to create a paraffinic fuel for aviation gas turbines and pyrolysis of organic material to create synthetic aromatics that could be blended with SPK fuels to create a fully synthetic jet fuel. Both these fuel options are potentially viable alternatives.

Blending HRD into jet fuel to maximize utility from renewable oil feedstocks

For renewable oils with a carbon chain length distribution similar to soil oil (e.g. palm oil, rapeseed oil, salicornia oil and jatropha oil), the hydroprocessing step of HRD of converting renewable oil into HRD has a mass yield of 84%; however, hydroprocessing renewable oil into HRJ has a mass yield below 60%. The decrease in yield is accompanied by an increase in naphtha production. Although naphtha is used as a blending stock in gasoline, it has a lower economic value than HRD, which is a high performance diesel fuel. While the naphtha could be used as an internal process fuel or catalytically reformed at a petroleum refinery, the aviation community could consider using HRD as a dilute blend stock in gas turbine engines (~10%). The combined domestic jet and diesel consumption is approximately 6 million bbl/day; hence, blending HRD into all jet and diesel fuel at 10% by volume amounts to a consumption of 600,000 bbl/day, or an order of magnitude more than the anticipated worldwide hydroprocessing capacity of 60,000 bbl/day (Hileman et al., 2009). Since producing HRD is a more effective use of a currently limited resource, the same total hydroprocessed fuel could be produced from 28% less feedstock while still contributing to the aviation industry. This option would require further research to ensure viability with the current fleet of aircraft.

Life cycle water consumption

Most alternative fuels will require at least the quantity of water that refineries currently consume and have the potential to consume several orders of magnitude more (DOE, 2006). Without considering any specific examples, water consumption from feedstock recovery and processing would likely dominate the life cycle water consumption while water consumption from feedstock and fuel transportation will be secondary through consuming fuels requiring water for their production. The current state of research on water consumption of fuel production was limited to citing the results of other studies. This approach identified that biofuel production would aggravate regional strains on freshwater supply and local infrastructure but was not extended to consider which fuel pathways would be best suited to which region. Water availability was qualitatively recognized as a limiting factor for biofuel production but water consumption was not assessed on a life cycle basis for any fuels. Future work in considering the role of water use in alternative fuels may seek to develop a life cycle water consumption model in a framework similar to that of GREET. A database of freshwater availability and corresponding local water laws should be developed to compliment the fuel/feedstock specific life cycle water consumption inventories.

Contrail and contrail cirrus formation from aircraft burning SPK fuel

The formation of exhaust contrails occurs through the mixing of hot and moist exhaust air with cold and drier ambient air. This combination can cause a temporary water saturated, or even supersaturated, state that is conducive to water condensation on aerosol particles. The scientific understanding of this process is characterized by the Schmidt-Appleman criterion. When contrails

persist and spread, contrail cirrus can eventually be formed in regions that are supersaturated with respect to ice. Although contrails are known to lead to contrail cirrus formation, our current capacity to predict the creation of contrail cirrus is limited. Because of the uncertainties in the relative magnitudes of IR transmission through thin clouds, the understanding of climate forcing from this aviation related effect is poor. This thesis assumed no change in the formation of contrails and contrail cirrus between aircraft burning conventional jet fuel and aircraft burning SPK fuel. To make a better estimate of any possible change in contrails, existing large eddy simulations could be used to quantify the correlation of soot and sulfate aerosol emissions in the exhaust to the formation and properties of contrails. Changes in contrail cirrus are dependent on both changes in contrails and a better understanding of impacts from existing contrail cirrus on the climate system. Improved characterization of contrail cirrus requires coordinated regional-scale measurements to correlate the growth, decay, and trajectories of contrail ice particles with the ambient aerosols and gaseous aerosol precursor concentrations (Wuebbles et al., 2007).

Appendix A – General Feedstock and Fuel Properties

The properties of the main feedstocks and fuels used in this analysis are given in Table 97. In most cases, these properties represent only a single value within the typical range of each characteristic. While these data are appropriate for the level of detail of this work, sample specific data should be used (where available) in conducting analyses of individual production configurations.

Table 53: Feedstock and Fuel Properties

Feedstock or Fuel	LHV (MJ/kg)	Density (kg/L)	Carbon content (wt %)	Sulfur content (wt ppm)	Source(s)
Crude oil or syncrude	41.3[1]	0.878[2]	84.6[1]	16,900[2]	EIA, 2008a
Conventional Jet A	43.2	0.802	86.2	600	Hileman et al., 2010
ULS Jet A	43.3	0.791	85.9	15	Hileman et al., 2010
F-T Jet Fuel / HRJ	44.1	0.76	84.7	0	Hileman et al., 2010
F-T Diesel / HRD	44.0	0.78	84.9	0	Norton et al.,1998; GREET, 2008
F-T Naphtha / HR Naphtha	44.4	0.70	84.2	0	GREET, 2008
Coal (U.S. average)[4]	22.7	-	59.0	11,100	GREET 2007; EIA, 2006
Bituminous coal[4]	26.4	-	64.8	29,400	SSEB, 2006
Sub-bituminous coal[4]	18.4	-	49.2	3,500	SSEB, 2006
Petroleum coke[5]	33.2	-	92.3	68,000	EIA, 2006; GREET, 2008
Biomass (forest residue)[6]	15.4	-	51.7	0	GREET, 2008
Biomass (corn stover)[6]	16.3	-	44.5	0	GREET, 2008
Biomass (switchgrass)[6]	17.6	-	47.0	900	GREET, 2008
Natural gas	47.1	0.00078	72.4	6	GREET, 2007
Hydrogen	120	0.00009	0	0	GREET, 2007

Notes:

1) Energy content of crude oil assumed to be 5.8 million Btu per barrel (HHV); carbon content calculated from formula: percent carbon = 76.99 + (10.19×Specific Gravity) + (-0.76×Sulfur Content). (EIA, 1999)
2) Density and sulfur content derived using historical data (1995-2006) provided in EIA, 2008a
3) As source of process energy (e.g. electricity generation). LHV and sulfur content from GREET, 2007; carbon content derived from coal HHV and U.S. average coal carbon emission factor of 26.0 million metric tons per quadrillion Btu for the electric power sector in 2004. (EIA, 2006)
4) For Coal-To-Liquids (CTL) process.
5) Used as a source of process energy in the refining of jet fuel. LHV and carbon content from EIA, 2006, sulfur content from GREET, 2008.
6) For Biomass-To-Liquids (BTL) process.

[Page Intentionally Left Blank]

References

Achten, W.M.J.; Verchot, L.; Franken, Y.J.; Mathijs, E.; Singh, V.P.; Aerts, R.; Muys, B. Jatropha Bio-diesel Production and Use. *Biomass and Bioenergy* **2008**, 32 (12), 1063-1084.

Adler, P.R.; Del Grosso, S.J.; Parton, W.J. Life-cycle Assessment of Net Greenhouse-gas Flux for Bioenergy Cropping Systems. *Ecological Applications* **2007**, 17 (3), 675-691.

AFLCAWG , Aviation Fuel Life Cycle Analysis Working Group, *Framework and Guidance for Estimating Greenhouse Gas Footprints of Aviation Fuels*, AFRL-RZ-Wp-TR-2009-2206, Air Force Research Laboratory: Wright Patterson Air Foce Base: Ohio, 2009; http://www.netl.doe.gov/energy-analyses/pubs/EstGHGFtprntsAvFuels2009.pdf (accessed March 11, 2010).

Ahmed, I.; Decker, J.; Morris, D. How Much Energy Does it Take to Make a Gallon of Soy diesel. Institute for Local Self Reliance: Minneapolis, Minnesota, 1994; http://www.carbohydrateeconomy.org/library/admin/uploadedfiles/How_Much_Energy_Does_It_Take_To_Make_A_Gallon_.pdf (accessed May 20, 2010).

APMT, Aviation Portfolio Management Tool, Climate Impacts Methodology, 2010; http://web.mit.edu/aeroastro/partner/apmt/climateimpact.html (accessed April 14, 2010).

ASTM D1655-09, Standard Specification for Aviation Turbine Fuels, DOI: 10.1520/D1655-09, ASTM International, West Conshohocken, PA, 2009; http://www.astm.org/Standards/D1655.htm (accessed April 14, 2010).

ASTM D7566-09, Standard Specification for Aviation Turbine Fuel Containing Synthesized Hydrocarbons, DOI: 10.1520/D7566-09, ASTM International: West Conshohocken, Pennsylvania, 2009; http://www.astm.org/Standards/D7566.htm (accessed March 11, 2010).

ATA, Air Transport Association, Annual Crude Oil and Jet Fuel Prices, 2010a; http://www.airlines.org/Economics/DataAnalysis/Pages/AnnualCrudeOilandJetFuelPrices.aspx (accessed May 16, 2010).

ATA, Air Transport Association, U.S. Air Carrier Traffic Statistics, 2010b; http://www.bts.gov/xml/air_traffic/src/index.xml#CustomizeTable (accessed May 16, 2010).

Anderi Silva, G.; Alexandre Kuley, L. Application of Life Cycle Assessment to the LCA Case Studies Single Superphosphate Production, *International Journal of Life Cycle Assessment* **2003**, 8 (4), 209-214.

Anwar, F.; Bhanger, M.I.; Khalil, M.; Nasir, A.; Ismal, S. Analytical Characterization of *Salicornia bigelovii* Seed Oil Cultivated in Pakistan. *Journal of Agricultural and Food Chemistry* **2002**, 50 (15), 4210-4214.

Armitage, D.M.; Prickett, A.J.; Norman, K.; Wildey, K.B. *Survey of current harvesting, drying and storage practices with oilseed rape*, Home-Grown Cereals Authority: London, UK, 2005; http://www.hgca.com/document.aspx?fn=load&media_id=2180&publicationId=2556 (accessed March 11, 2010).

Bartis, J.T.; Camm, F.; Ortiz, D.S. *Producing Liquid Fuels from Coal: Prospects and Policy Issues*, MG-754-AF/NETL, RAND Corporation: Santa Monica, California, 2008; http://www.rand.org/pubs/monographs/2008/RAND_MG754.pdf (accessed October 12, 2009).

Becker, E.W. Micro-algae as a source of protein, *Biotechnology Advances* **2007**, 25 (2), 207-210.

Ben-Amotz, A. *Bio-Fuel and CO_2 Capture by Marine Microalgae*, Oral Presentation, Seambiotic, 2008 Algae Biomass Summit, Seattle, Washington, October 23, 2008; Obtained from conference organizers.

Bergman, P.C.A.; Boersma, A.R.; Kiel, J.H.A.; Prins, M.J.; Ptasinski, K.J.; Janssen, F.J.J.G.; *Torrefaction for Entrained-Flow Gasification of Biomass*, ECN-C-05-067, Energy Research Center of the Netherlands and Eindhoven University of Technology: Netherlands, 2005; http://www.techtp.com/recent%20papers/Rome2004_Bergman_et_al.pdf (accessed October 12, 2009).

Bernesson, S.; Nilsson, D.; Hansson, P. A limited LCA comparing large- and small scale production of rape methyl ester (RME) under Swedish conditions, *Biomass and Bioenergy* **2004**, *26* (6) 545-559.

Bester, N. and Yates, A. Assessment of the Operational Performance of Fisher-Tropsch Synthetic Paraffinic Kerosene in a T63 Gas Turbine Compared to Conventional Jet A-1 Fuel, GT200960333, In Power for Land, Sea and Air, Proceedings of ASME Turbo Expo 2009, Orlando, Florida, June 8-12, 2009.

Broch, A.; Hoekman, S. K.; Gertler, A.; Robbins, C.; Natarajan, M. Biodistillate Transportation Fuels 3 – Life Cycle Impacts, *SAE International* **2009**, 2009-01-2768.

Broder, J. M. Obama to Go to Copenhagen With Emissions Target. *The New York Times*, November 25, 2009; http://www.nytimes.com/2009/11/26/us/politics/26climate.html (accessed May 16, 2010).

Campbell, F.T. Killer pigs, vines, and fungi: Alien species threaten native ecosystems. *Endangered Species Technical Bulletin* **1994** 19 (5), 3-5.

Chynoweth, D.P.; Owens, J.M.; Legrand, R. Renewable Methane from Anaerobic Digestion of Biomass. *Renewable Energy* **2001**, 22, 1-8.

CONCAWE, *Energy and Greenhouse Gas Balance of Biofuels for Europe – An Update*, CONCAWE Ad Hoc Group on Alternative Fuels. Brussels, Belgium, 2002; http://www.see.ed.ac.uk/~jwp/research/sustainable/various/CONCAWE-26601_tcm24-124161.pdf (accessed March 11, 2010).

Coşge, B.; Gürbüz, B; Kiralan, M. Oil Content and Fatty Acid Composition of Some Safflower (Carthamus tinctorius L.) Varieties Sown in Spring and Winter, *International Journal of Natural and Engineering Sciences* **2007**, 1 (3), 11-15.

Daggett, D.L. *Advances in Adapting the Fleet to Alternative Fuel Use*, Boeing, Oral Presentation to Transportation Research Board: Washington, DC, 2008; http://www.trbav030.org/pdf2008/TRB08_Daggett.pdf (accessed October 12, 2009).

De Klein, C.; Novoa, R.S.A.; Ogle, S.; Smith, K.A.; Rochette, P.; Wirth, T.C.; McConkey, B.G.; Mosier, A.; Rypdal, K.; Walsh, M.; Williams, S.A. *N_2O Emissions from Managed Soils, and CO_2 Emissions from Lime and Urea Application*. Volume 4: Agriculture, Forestry and Other Land Use, 2006 IPCC Guidelines for National Greenhouse Gas Inventories, Intergovernmental Panel on Climate Change, Institute for Global Environmental Strategies: Hayama, Japan, 2006; http://www.ipcc-nggip.iges.or.jp/public/2006gl/pdf/4_Volume4/V4_11_Ch11_N2O&CO2.pdf (accessed February 8, 2010).

DeMan, J.M. Lipids. In *Principles of Food Chemistry (3rd Edition)*; Springer – Verlag, 1999; pp 33-94; http://www.knovel.com/knovel2/Toc.jsp?BookID=1093&VerticalID=0 (accessed May 16, 2010).

Deutch, J.; Moniz, E. *The Future of Coal: Options for a Carbon Constrained World*, Massachusetts Institute of Technology: Cambridge, Massachusetts, 2007; http://web.mit.edu/coal/ (accessed October 12, 2009).

Dewitt , M.J.; Corporan, E.; Graham, J.; Minus, D. Effects of Aromatic Type and Concentration in Fischer-Tropsch Fuels on Emissions Production and Material Compatibility, *Energy and Fuels* **2008**, *22*, 2411-2418.

Dilmore, R. and Skone, T. Personal communication with R. Stratton, November 25, 2009.

DOE, Department of Energy, *How Anaerobic Digestion (Methane Recovery) Works*, 2008; http://www.energysavers.gov/your_workplace/farms_ranches/index.cfm/mytopic=30003 (accessed October 12, 2009).

DOE, Department of Energy, *Energy Demands on Water Resources*, Report to Congress on the Interdependency of Energy and Water, Sandia National Labs, 2006; http://www.sandia.gov/energy-water/docs/121-RptToCongress-EWwEIAcomments-FINAL.pdf (accessed October 12, 2009).

Donohoo, P. Scaling Air Quality Effects from Alternative Jet Fuel in Aircraft and Ground Support Equipment, M.Sc. Thesis, Massachusetts Institute of Technology, Cambridge, MA, 2010.

Dorbian, C. Estimating the environmental benefits of aviation fuel and emissions reductions, Masters Thesis, Massachusetts Institute of Technology, Cambridge, MA, 2010.

Edwards, T. Personal Communication with R. Stratton, October 13, 2009.

Edwards, R.; Larivé, J.; Mahieu, V.; Rouveirolles, P. *Well-to-Wheels Analysis of Future Automotive Fuels and Powertrains in the European Context, Tank-to-Wake Report Version 2c,* EUCAR, CONCAWE, & JRC: Ispra, Italy, 2007; http://ies.jrc.ec.europa.eu/WTW (accessed March 22, 2010).

EIA, Energy Information Administration, *Emissions of Greenhouse Gases in the United States 1998, Appendix B: Carbon Coefficients Used in This Report,* EIA/DOE-0573(98), U.S. Government Printing Office: Washington, DC, 1999; ftp://ftp.eia.doe.gov/pub/oiaf/1605/cdrom/pdf/ggrpt/057398.pdf (accessed October 12, 2009).

EIA, Energy Information Administration, *Nonconventional Liquid Fuels*, Annual Energy Outlook, 2006; http://www.eia.doe.gov/oiaf/aeo/otheranalysis/aeo_2006analysispapers/nlf.html (accessed October 12, 2009).

EIA, Energy Information Administration, *Emissions of Greenhouse Gases in the United States 2006*, DOE/EIA-0573(2006), Washington, DC, 2007; ftp://ftp.eia.doe.gov/pub/oiaf/1605/cdrom/pdf/ggrpt/057306.pdf (accessed October 12, 2009).

EIA, Energy Information Administration, *Crude Oil Input Qualities*, 2008a; http://tonto.eia.doe.gov/dnav/pet/pet_pnp_crq_dcu_nus_a.htm (accessed October 12, 2009).

EIA, Energy Information Administration, *Annual Coal Report 2007*, DOE/EIA-0584(2007), 2008b; http://www.eia.doe.gov/cneaf/coal/page/acr/acr_sum.html (accessed November 19, 2008).

EIA, Energy Information Administration, *Annual Energy Review 2007: Coal*, DOE/EIA-0384(2007), 2008c; http://www.eia.doe.gov/aer/coal.html (accessed November 19, 2008).

EIA, Energy Information Administration, *Annual Energy Outlook 2008, with Projections to 2030*, EIA/DOE-0383(2008), U.S. Government Printing Office: Washington, DC, 2008d; http://tonto.eia.doe.gov/ftproot/forecasting/0383(2008).pdf (accessed October 12, 2009).

EIA, Energy Information Administration, *Average Cost of Coal Delivered for Electricity Generation by State*, Electric Power Monthly, 2009a; http://www.eia.doe.gov/cneaf/electricity/epm/table4_10_a.html (accessed October 12, 2009).

EIA, Energy Information Administration, *US Weekly Product Supplied*, Petroleum Navigator, 2009b; http://tonto.eia.doe.gov/dnav/pet/pet_cons_wpsup_k_w.htm (accessed October 12, 2009).

EIA, Energy Information Administration, *Refinery Yield*, 2010a; http://tonto.eia.doe.gov/dnav/pet/pet_pnp_pct_dc_nus_pct_m.htm (accessed May 16, 2010).

EIA, Energy Information Administration, *Crude oil production*, 2010b; http://www.eia.doe.gov/dnav/pet/pet_crd_crpdn_adc_mbbl_m.htm (accessed May 20, 2010).

EIA, Energy Information Administration, *Product Supplied*, 2010c; http://tonto.eia.doe.gov/dnav/pet/pet_cons_psup_dc_nus_mbblpd_a.htm (accessed May 16, 2010).

EISA, Energy Independence and Security Act, Section 526, Procurement and Acquisition of Alternative Fuels, 2007; http://frwebgate.access.gpo.gov/cgi-bin/getdoc.cgi?dbname=110_cong_public_laws&docid=f:publ140.110 (accessed April 14, 2010).

EPA, Environmental Protection Agency, Climate Change Glossary of Terms, 2009; http://www.epa.gov/climatechange/glossary.html#Aerosol (accessed April 14, 2010).

EPA, Environmental Protection Agency. *Renewable Fuel Standard Program (RFS2) Regulatory Impact Analysis*, EPA-420-R-10-006, Assessment and Standards Division, Office of Transportation and Air Quality, US Environmental Protection Agency: Washington, DC, 2010; http://www.epa.gov/otaq/fuels/renewablefuels/regulations.htm (accessed March 11, 2010).

Eurostat, *Agriculture Database*, European Commission, 2010; http://epp.eurostat.ec.europa.eu/portal/page/portal/agriculture/data/database (accessed March 7, 2010).

FAO, Food and Agriculture Organization, *Agricultural Production Domain*, Commodities by Country, 2010; http://faostat.fao.org/site/339/default.aspx (accessed March 9, 2010).

FAPRI, Food and Agricultural Policy Research Institute, *FAPRI 2009 U.S. and World Agricultural Outlook*, Database Query, 2009; http://www.fapri.iastate.edu/tools/outlook.aspx (accessed June 6, 2009).

Forbes.com. *Malaysian government not concerned with rising palm oil prices – minister*, December 12, 2007; http://www.forbes.com/feeds/afx/2007/12/16/afx4445844.html (accessed March 12, 2010).

Fuglestvedt, J.S.; Berntsen, T.K.; Godal, O.; Sausen, R.; Shine, K.P.; Skodvin, T. Metrics of climate change: Assessing radiative forcing and emission indices. *Climatic Change* **2003**, *58(3),* 267 – 331.

Gandhi, V.M.; Cherian, K.M.; Mulky, M.J. Toxicological Studies on Ratanjyot Oil. *Food and Chemical Toxicology* **1995**, 33 (1), 39-42.

Glenn, E.P.; O'Leary, J.W.; Watson, M.C.; Thompson, T.L. Salicornia bigelovii Torr: An Oilseed Halophyte for Seawater Irrigation. *Science* **1991**, 251 (4997), 1065-1067.

Glenn, E.P.; Pitelka, L.F.; Olsen, M.W. The Use of Halophytes to Sequester Carbon. *Water, Air & Soil Pollution* **1992**, 64 (1-2), 251-263.

Glenn, E.P.; Squires, V.; Olsen, M.; Frye, R. Potential for Carbon Sequestration in the Drylands. *Water, Air & Soil Pollution* **1993**, 70 (1-4), 341-355.

Glenn, E.P.; Brown, J.J.; O'Leary, J.W. Irrigating Crops with Seawater, *Scientific American Magazine* **August 1998**, 76-81.

Gray, D.; White, C.; Tomlinson, G.; Ackiewicz, M.; Schmetz, E.; Winslow, J. *Increasing Security and Reducing Carbon Emissions of the U.S. Transportation Sector: A Transformational Role for Coal with Biomass*, DOE/NETL-2007/1298, National Energy Technology Laboratory: Pittsburgh, 2007; http://www.netl.doe.gov/energy-analyses/pubs/NETL-AF%20CBTL%20Study%20Final%202007%20Aug%2024.pdf (accessed October 12, 2009).

Gray, L. Farmers agree to set aside land for wildlife. *The Telegraph*, November 5, 2009; http://www.telegraph.co.uk/earth/earthnews/6501679/Farmers-agree-to-set-aside-land-for-wildlife.html (accessed March 7, 2010).

Green Car Congress. *DESC Awards Solazyme Contract for Naval Renewable F-76 from Algae, Sustainable Oils Contract for Renewable JP-5 from Camelina*, September 10, 2009; http://www.greencarcongress.com/2009/09/desc-f76-hrj5-20090910.html (accessed March 11, 2010).

Green Car Congress. UOP, Masdar Institute, Boeing and Etihad Airways Establish Sustainable Aviation Biofuels Project Using Integrated Saltwater Agricultural Systems; Support from Global Seawater Inc., January 17, 2010; http://www.greencarcongress.com/2010/01/sbrp-20100117.html (accessed March 18, 2010).

GREET, The Greenhouse Gases, Regulated Emissions, and Energy Use in Transportation (GREET) Model, version 1.8a, developed by Systems Assessment Section, Center for Transportation Research, Argonne National Laboratory, August 2007.

GREET, The Greenhouse Gases, Regulated Emissions, and Energy Use in Transportation (GREET) Model, version 1.8b, developed by Systems Assessment Section, Center for Transportation Research, Argonne National Laboratory, May 2008.

Gunderson, C.; Davis, E.; Jager, H.; West, T., Perlack, R.; Brandt, C.; Wullschleger, S.; Baskaran, L.; Wilkerson, E.; Downing, M. *Exploring Potential U.S. Switchgrass Production for Lignocellulosic Ethanol*, ORNL/TM-2007/183, Oak Ridge National Laboratory: Oak Ridge, Tennessee, 2008; http://digitalcommons.unl.edu/cgi/viewcontent.cgi?article=1016&context=usdoepub (accessed February 8, 2010).

Hansen, J.; Sato, M.; Ruedy, R. and et al. Efficacy of climate forcings. *Journal of Geophysical Research Atmospheres* **2005**, *110* (D18104).

Hasselmann, K.; Hasselmann, S.; Giering, R.; Ocana, V. and Storch, H. V. Sensitivity study of optimal CO2 emission paths using a simplified structural integrated assessment model (SIAM). *Climatic Change* **1997**, *37 (2)*, 345 – 386.

Heaton, E.; Voigt, T.; Long, S.P. A quantitative review comparing the yields of two candidate C_4 perennial biomass crops in relation to nitrogen, temperature and water. *Biomass and Bioenergy* **2004**, 27 (1), 21-30.

Hedegaard, K.; Thyo, K.A.; Wenzel, H. Life Cycle Assessment of an Advanced Bioethanol Technology in the Perspective of Constrained Biomass Availability. *Environmental Science and Technology* **2008**, 42 (21), 7992-7999.

Hendricks, R.C. Potential Carbon Negative Commercial Aviation Through Land Management, Proceedings of the 12th International Symposium on Transport Phenomena and Dynamics of Rotating Machinery, Honolulu, Hawaii, February 17-22, 2008; http://ntrs.nasa.gov/archive/nasa/casi.ntrs.nasa.gov/20080000860_2007039194.pdf (accessed May 16, 2010).

Hendricks, R.C.; Bushnell, D.M. *Halophytes Energy Feedstocks: Back to Our Roots*. NASA Glenn Research Center: Cleveland, Ohio, 2008; http://ntrs.nasa.gov/archive/nasa/casi.ntrs.nasa.gov/20080001445_2007039195.pdf (accessed October 12, 2009).

Herzog, H.; Golomb, D.; Zemba, S. Feasibility, Modelling and Economics of Sequestering Power Plant CO_2 Emissions in the Deep Ocean. *Environmental Progress* **1991**, 10 (1), 64-74.

Hileman, J.I.; Ortiz, D.S.; Bartis, J.T.; Wong, H.M.; Donohoo, P.E.; Weiss, M.A.; Watiz, I.A. *Near Term Feasibility of Alternative Jet Fuels*, Massachusetts Institute of Technology and RAND Corporation, Santa Monica, CA, 2009; http://web.mit.edu/aeroastro/partner/reports/proj17/altfuelfeasrpt.pdf (accessed February 17, 2010).

Hileman, J.I. Alternative Jet Fuel Feasibility, *Transport Policy*, submitted for publication, 2010.

Hileman, J. I.; Stratton, R. W.; Donohoo. P. E. Energy Content and Alternative Fuel Viability, Submitted to *Journal of Propulsion and Power* **2010**, in press.

Hoor, P.; Borken-Kleefeld, J.; Caro, D.; Dessens, O.; Endresen, O.; Gauss, M.; Grewe, V.; Hauglustaine, D.; Isaksen, I. S. A.; J¨ockel, P.; Lelieveld, J.; Myhre, G.; Meijer, E.; Olivie, D.; Prather, M.; Schnadt Poberaj, C.; Shine, K. P.; Staehelin, J.; Tang, Q.; van Aardenne, J.; van Velthoven, P. and Sausen, R. The impact of traffic emissions on atmospheric ozone and oh: results from quantify. *Atmospheric Chemistry and Physics* **2009**, *9*, 3113–3136.

Huo, H., Wang, M.; Bloyd, C.; Putsche, V. *Life Cycle Assessment of Energy and Greenhouse Gas Effects of Soybean-Derived Biodiesel and Renewable Fuels*, ANL/ESD/08-2, Argonne National Laboratory, 2008; http://www.biodiesel.org/resources/reportsdatabase/reports/gen/20080301_gen-395.pdf (accessed October 12, 2009).

ICAO, International Civil Aviation Organization, GIACC/4 – IP/12, U.S. Fuel Trends Analysis And Comparison To GIACC/4-IP/1, Group on International Aviation and Climate Change (GIACC) Fourth Meeting, 2009; http://web.mit.edu/aeroastro/partner/reports/proj28/fueltrend-analy.pdf (accessed May 16, 2010).

ISO, International Organization of Standardization, *Environmental management – Life cycle assessment – Requirements and guidelines*, ISO 14044:2006(E), ISO: Switzerland, 2006, http://www.iso.org/iso/catalogue_detail.htm?csnumber=38498 (accessed October 12, 2009).

Kadam, K. *Microalgae Production from Power Plant Flue Gas: Environmental Implications on a Life Cycle Basis*, NREL/TP-510-29417, National Renewable Energy Laboratory: Golden Colorado, 2001; http://www.nrel.gov/docs/fy01osti/29417.pdf (accessed October 12, 2009).

Kalnes, T. Personal communication with R. Stratton, January 9-February 18, 2009.

Karaosmanoglu, F.; Tetik, E.; Gurboy, B.; Sanli, I. Characterization of the Straw Stalk of the Rapeseed Plant as a Biomass Energy Source, *Energy Sources* **1999**, 21 (9), 801-810.

King, C.W.; Webber, M.E. Water Intensity of Transportation. *Environmental Science and Technology* **2008**, 42 (21), 7866-7872.

Kreutz, T.G.; Larson, E.D.; Liu, G.; Williams, R.H. *Fischer-Tropsch Fuels from Coal and Biomass*, Princeton Environment Institute, Princeton University: Princeton, New Jersey, 2008; http://www.princeton.edu/pei/energy/publications/texts/Kreutz-et-al-PCC-2008-10-7-08.pdf (accessed October 12, 2009).

Kumabe, K.; Hanaoka, T.; Fujimoto, S.; Minowa, T.; Sakanishi, K. Co-gasification of Woody Biomass and Coal with Air and Steam. *Fuel* **2007**, 86 (5-6), 684-689.

Lamprecht, D. Fisher-Tropsch Fuel for Use by the US Military as Battlefield-Use Fuel of the Future. *Energy Fuels* **2007**, 21 (3), 1448-1453.

Luoma, J.R. Hailed as a Miracle Biofuel, Jatropha Falls Short of the Hype. *Yale Environment 360*, May 4, 2009; http://e360.yale.edu/content/feature.msp?id=2147 (accessed March 22, 2010)

Mahashabde, A. Assessing Environmental Benefits and Economic Costs of Aviation Environmental Policy Measures, Ph.D. Thesis, Massachusetts Institute of Technology, Cambridge, MA, 2009.

Mahmudi, H.; Flynn, P.C. Rail vs truck transport of biomass, *Applied Biochemistry and Biotechnology* **2006**, 129 (1-3), 88-103.

Mani, B. Personal communication with R. Stratton, March 16, 2010.

Marais, K.; Lukachko, S. P.; Jun, M.; Mahashabde, A.; Waitz, I.A. Assessing the impact of aviation on climate. *Meteorologische Zeitschrift* **2008**, *17*, 157–172.

Marathon Electric, *Black Max Vector Duty Motors*, 2009; Retrieved October 12, 2009 at http://www.automationdirect.com/static/specs/motorsblackmax.pdf (accessed October 12, 2009).

Marker, T.; Petri, J.; Kalnes, T.; McCall, M.; Mackowiak, D.; Jerosky, B.; Reagan, B.; Nemeth, L.; Krawczyk, M.; Czernik, S.; Elliott D.; Shonnard D. *Opportunities for Biorenewables in Oil Refineries*, DE-FG36-05GO15085, UOP: Des Plaines, Illinois, 2005; http://www.osti.gov/bridge/servlets/purl/861458-Wv5uum/861458.pdf (accessed October 12, 2009).

McLaughlin, S.B.; Delatorreugarte, D.G.; Garten Jr, C.T.; Lynd, L.R.; Sanderson, M.A.; Tolbert, V.R.; Wolf, D.D. High-Value Renewable Energy from Prairie Grasses, *Environmental Science and Technology* **2002**, 36 (10), 2122-2129.

Melillo, J.M.; Reilly, J.M.; Kicklighter, D.W.; Gurgel, A.C.; Cronin, T.W.; Paltsev, S.; Felzer, B.S.; Wang, X.; Sokolov, A.P.; Schlosser, C.A. Indirect Emissions from Biofuels: How Important?, *Science* **2009**, 326 (5958), 1397-1399.

Miake-Lye, R.C. AAFEX Gaseous Emissions: Criteria, Greenhouse Gases and Hazardous Air Pollutants, Oral presentation at the AAFEX Workshop of AIAA Meeting, Orlando, FL, January 22-25, 2010.

Minnis, P.; Nguyen, L.; Garber, D. P.; Duda, D. P.; Palikonda, R.; Doelling, D. R. Simulation of Contrail Coverage Over the USA Missed During the Air Traffic Shutdown, In *European Conference on Aviation, Atmosphere, and Climate Friedrichschafen*, Lake Constance, Germany, June 30-July3, 2003; http://www-pm.larc.nasa.gov/sass/pub/conference/Minnis.sim.AAC03.pdf (accessed April 14, 2010).

Mission Biofuels Limited. *Mission Biofuels officially opens first biodiesel plant in Kuantan, Malaysia*, December 18, 2007; http://www.missionnewenergy.com/uploads/127.pdf (accessed March 12, 2010).

Molina Grima, E.; Belarbi, E.H.; Acien Fernandez, F.G.; Robles Medina, A.; Yusuf Chisti. Recovery of Microalgal Biomass and Metabolites: Process Options and Economics, *Biotechnology Advances* 2003, 20 (7-8), 491-515.

Mortimer, N.D. and Elsayed, M.A. *North East Biofuel Supply Chain Carbon Intensity Assessment*, North Energy Associates Ltd: Sheffield, UK, 2006; http://www.northenergy.co.uk/c/pdf/Life_Cycle_Assessment-Reports-2_1.pdf (accessed March 11, 2010).

National Academies, National Academy of Sciences; National Academy of Engineering; National Research Council. *Liquid Transportation Fuels from Coal and Biomass*, Washington, DC, National Academies Press, 2009; http://www.nap.edu/catalog/12620.html (accessed February 8, 2010)

Norton, P.; Vertin, K.; Bailey, B.; Clark, N.N.; Lyons, D.W.; Goguen, S.; Eberhardt, J. Emissions from Trucks using Fischer-Tropsch Diesel Fuel, *SAE International Journal* **1998**, Paper number 982526.

Mouawad, J. Exxon to Invest Millions to Make Fuel from Algae. *The New York Times*, July 13, 2009; http://www.nytimes.com/2009/07/14/business/energy-environment/14fuel.html?_r=1 (Accessed March 11,2010).

O'Leary, J.W.; Glenn E.P.; Watson, M.C. Agricultural Production of Halophytes Irrigated with Seawater. *Plant and Soil* **1985**, 89 (1-3), 311-321.

OpenCongress, H.R.2454 - American Clean Energy And Security Act of 2009, 2009; http://www.opencongress.org/bill/111-h2454/show (accessed May 16, 2010).

Ozata, I.; Ciliz, N.; Mammadov, A.; Buyukbay, B.; Ekinci, E. *Comparative Life Cycle Assessment Approach for Sustainable Transport Fuel Production from Waste Cooking Oil and Rapeseed*, Istanbul Technical University, Bogazici University and Isik University: Istanbul, Turkey, 2009; http://gin.confex.com/gin/2009/webprogram/Manuscript/Paper2602/Ilker%20paper%2011.05.2009.pdf (accessed March 11, 2010).

Penner, J. E.; Lister, D. H.; Griggs, D. J.; Dokken, D. J.; McFarland, M. *Aviation and the Global Atmosphere: A special report in collaboration with the Scientific Assessment Panel to the Montreal Protocol on Substances that Deplete the Ozone Layer*, Intergovernmental Panel on Climate Change, Cambridge University Press, Cambridge, UK, 1999.

Pimentel, D.; Lach, L.; Zuniga, R.; Morrison, D. Environmetal and Economic Costs of Nonondigenous Species in the United States. *Bioscience* **2000**, 50 (1), 53-65.

Pimentel D.; Greiner, A. Environmental and socio-economic costs of pesticide use. In *Techniques for Reducing Pesticide Use: Economic and Environmental Benefits*; John Wiley & Sons: Chichester, UK 1997; pp 51-78.

Prieur, A.; Bouvert, F.; Gabrielle, B.; Lehuger, S. Well to Wheels Anaysis of Biofuels vs. Conventional Fossil fuels: A Proposal for Greenhouse Gases and Energy Savings Accounting the French Context, *SAE International Journal* **2008**, Paper number 2008-01-0673.

Putt. R, *Algae as a Biodiesel Feedstock: A Feasibility Assessment,* Center for Microfibrous Materials Manufacturing, Department of Chemical Engineering, Auburn University: Alabama, 2007; http://bioenergy.msu.edu/feedstocks/algae_feasibility_alabama.pdf (accessed October 12, 2009).

Reinhardt, G.; Gartner, S.; Rettenmaier, N.; Munch, J.; von Falkenstein, E. Screening Life Cycle Assessment of Jatropha Biodiesel, Institute for Energy and Environmental Research: Heidelberg, 2007; http://www.ifeu.org/landwirtschaft/pdf/jatropha_report_111207.pdf (accessed October 12, 2009).

Reinhardt, G.; Becker, K.; Chaudhary, D.R.; Chikara, J.; Falkenstein, E.; Francis, G.; Gartner, S.; Gandhi, M.R.; Ghosh, A.; Ghosh, P.K.; Makkar, H.; Munch, J.; Patolia, J.S.; Reddy, M.P.; Rettenmaier, N.; Upadhyay, S.C. *Basic Data for Jatropha Production and Use*, Institute for Energy and Environmental Research, Central Salt and Marine Chemicals Research Institute, University of Hohenheim: Heidelberg, Bhavnagar and Hohenheim, 2008; Obtained by request from G. Reinhardt.

Richards, I.R. *Energy Balances in the Growth of Oilseed Rape for Biodiesel and of Wheat for Bioethanol*, British Association for Bio Fuels and Oils: Suffolk, UK, 2000; http://bloomingfutures.com/uploads/Levington%20Agricultural%20Report%202000.pdf (accessed March 11, 2010).

Rumizen, M. (CAAFI steering committee member). Personal communication with R. Stratton, March 12, 2010.

Sausen, R. and Schumann, U. Estimates of the climate response to aircraft CO_2 and NO_x emissions scenarios. *Climatic Change* **2000**, *44* (1-2), 27–58.

Sausen, R.; Isaksen, I.; Grewe, V.; Hauglustaine, D.; Lee, D. S.; Myhre, G.; K¨ohler, M. O.; Pitari, G.; Schumann, U.; Stordal, F.; Zerefos, C. Aviation radiative forcing in 2000: An update on IPCC (1999). *Meteorologische Zeitschrift* **2005**, *14*, 555– 561.

Schmer, M.R.; Vogel, K.P.; Mitchell, R.B.; Perrin, R.K. Net Energy of Cellulosic Ethanol from Switchgrass, *Proceedings of the National Academy of Sciences* **2008**, 105 (2), 464-469.

Schmidt, J.H. Life cycle assessment (LCA) of rapeseed oil and palm oil, Part 3: Life cycle inventory of rapeseed oil and palm oil, Ph.D. Thesis, Aalborg University, Aalborg, Denmark, 2007; http://vbn.aau.dk/fbspretrieve/10388016/inventory_report (accessed March 11, 2010).

Sheehan, J.; Aden, A.; Paustian, K.; Killian, K.; Brenner, J.; Walsh, M.; Nelson, R. Energy and Environmental Aspects of Using Corn Stover for Fuel Ethanol, *Journal of Industrial Ecology* **2004**, *7(3-4)*, 117-146.

Sheehan, J.; Camobreco, V.; Duffield, J.; Graboski, M.; Shapouri, H. *Life Cycle Inventory of Biodiesel and Petroleum Diesel for Use in an Urban Bus*, NREL/SR-580-24089, National Renewable Energy Laboratory: Golden Colorado, 1998a; http://www.nrel.gov/docs/legosti/fy98/24089.pdf (accessed October 12, 2009).

Sheehan, J.; Dunahay, T.; Benemann, J.; Roessler, P. *A Look Back at the U.S. Department of Energy's Aquatic Species Program—Biodiesel from Algae*, NREL/TP-580-24190, National Renewable Energy Laboratory: Golden, Colorado, 1998b; http://www.nrel.gov/docs/legosti/fy98/24190.pdf (accessed October 12, 2009).

Shelef, G.; Sukenik, A.; Green, M. *Microalgae Harvesting and Processing: A Literature Review*, SERI/STR-231-2396, Solar Energy Research Institute: Golden Colorado, 1984; http://www.nrel.gov/docs/legosti/old/2396.pdf (accessed October 12, 2009).

Shine, K. P.; Fuglestvedt, J. S.; Hailemariam, K.; Stuber, N. Alternatives to the global warming potential for comparing climate impacts of emissions of greenhouse gases. *Climatic Change* **2005**, *68* (3), 281 – 302.

Shweta, S.; Shweta, S.; and Gupta, M.N. Biodiesel Preparation by Lipase-Catalyzed Transesterification of Jatropha Oil, *Energy Fuels* **2004**, 18 (1) 154-159.

Skone, T and Gerdes, K, *Development of Baseline Data and Analysis of Life Cycle Greenhouse Gas Emissions of Petroleum-Based Fuels*, DOE/NETL-2009/1346, National Energy and Technology Laboratory: Pittsburgh, Pennsylvania, 2008; http://www.netl.doe.gov/energy-analyses/pubs/NETL%20LCA%20Petroleum-Based%20Fuels%20Nov%202008.pdf (accessed October 12, 2009).

Skone, T and Gerdes, K, *Consideration of Crude Oil Source in Evaluating Transportation Fuel GHG Emissions*, DOE/NETL-2009/1360, National Energy and Technology Laboratory: Pittsburgh, Pennsylvania, 2009; http://www.netl.doe.gov/energy-analyses/pubs/Life%20Cycle%20GHG%20Analysis%20of%20Diesel%20Fuel%20by%20Crude%20Oil%20Source%202.pdf (accessed October 12, 2009).

Solomon, S.; Qin, D.; Manning, M.; Chen, Z.; Marquis, M.; Averyt, K. B.; Tignor, M.; Miller, H. L. *Contribution of Working Group I to the Fourth Assessment Report*, Intergovernmental Panel on Climate Change, Cambridge University Press, Cambridge, UK, 2007; http://www.ipcc.ch/ipccreports/ar4-wg1.htm (accessed October 12, 2009).

Sommer, R.; Denich, M.; Vlek, P.L.G. Carbon storage and root penetration in deep soils under small farmer land-use systems in the Eastern Amazon region, Brazil. *Plant and Soil* **2000**, 219 (1-2), 231-241.

Spicer, J.; Richardson, C.; Ehrlich, M.; Bernstein, J.; Fukuda, M.; Terada, M. Effects of Frictional Loss on Bicycle Chain Drive Efficiency. *Journal of Mechanical Design* **2001**, 123 (4), 598-605.

SSEB, Southern States Energy Board, *American Energy Security: Building a Bridge to Energy Independence and to a Sustainable Energy Future*, Appendix D: *Coal-to-Liquids Case Studies*, Southern States Energy Board: Norcross, Georgia, 2006; http://americanenergysecurity.org/wordpress/wp-content/uploads/2009/02/aes-appendices.pdf (accessed October 12, 2009).

Stevenson, S. D.; Doherty, R. M.; Sanderson, M. G.; Collins, W. J.; Johnson, C. E.; Derwent, R. G. Radiative forcing from aircraft NO_x emissions: Mechanisms and seasonal dependence. *Journal of Geophysical Research* **2004**, 109 (D17307).

Stratton, R. W.; Wong, H. M.; Hileman, J. I. *Life Cycle Greenhouse Gas Emissions from Alternative Jet Fuels*, Partnership for Air Transportation Noise and Emissions Reduction, Massachusetts Institute of Technology: Cambridge, MA, 2010; http://web.mit.edu/aeroastro/partner/reports/proj28/partner-proj28-2010-001.pdf.

Tarka, T., *Affordable, Low-Carbon Diesel Fuel from Domestic Coal and Biomass*, DOE/NETL-2009/1349, National Energy Technology Laboratory: Golden Colorado, 2009; http://www.netl.doe.gov/energy-analyses/pubs/CBTL%20Final%20Report.pdf (accessed October 12, 2009).

Timko, M.T. et al. The Impact of Alternative Fuels on Aircraft Emissions, In *AAAR 27th Annual Conference*, Orlando, FL, October 20-24, 2008.

UNFCCC, United Nations Framework Convention on Climate Change, *Project Salicornia, Halophyte Cultivation in Sonora*, 1998;

http://unfccc.int/kyoto_mechanisms/aij/activities_implemented_jointly/items/1784.php (accessed October 12, 2009).

Vadas, P.A.; Barnett, K.H.; Undersander, D.J. Economics and Energy of Ethanol Production from Alfalfa, Corn, and Switchgrass in the Upper Midwest, USA, *Bioenergy Research* **2008**, 1 (1), 44-55.

van der Drift, A.; Boerrigter, H.; Coda, B.; Cieplik, M.K.; Hemmes, K. *Entrained Flow Gasification of Biomass – Ash behaviour, feeding issues and system analyses*, Energy Recerch Center of the Netherlands: Petten, Netherlands, 2004; http://www.ecn.nl/docs/library/report/2004/c04039.pdf (accessed October 12, 2009).

Virki, T. Neste to Build US$814 Million Singapore Biofuel Plant, *Planet Arc*, December 3, 2007; http://www.planetark.org/dailynewsstory.cfm/newsid/45658/story.htm (accessed March 12, 2010).

Weissman, J. C.; Goebel, R. P. *Design and Analysis of Micro algal Open Pond Systems for the Purpose of Producing Fuels*, SERI/STR-231-2840, Solar Energy Research Institute: Golden Colorado, 1987; http://www.nrel.gov/docs/legosti/old/2840.pdf (accessed October 12, 2009).

Whisenant, S. G. *Changing fire frequencies on Idaho's Snake River Plains: Ecological and Management Implications*. Proceedings: Symposium on Cheatgrass Invasion, Shrub Die-Off, and Other Aspects of Shrub Biology and Management. US Department of Agriculture, Forest Service, Intermountain Research Station 4–10: Ogden, UT, 1990.

Whitefield, P.; Hagen, D.; Lobo, P. Particle Emissions II: Fuel Effects Relative to Other Sources of Emission Variability, Oral presentation at AAFEX Workshop, Orlando, FL, January 18, 2010.

Wild, O.; Prather, M. J.; Akimoto, H. Indirect long-term global radiative cooling from NO_x emissions. *Geophysical Research Letters* **2001**, *28* (9), 1719–1722.

Wilhelm, W.W.; Johnson, J.; Karlen, D.L.; Lightle, D.T. Corn Stover to Sustain Soil Organic Carbon Further Constrains Biomass Supply, *Agronomy Journal* **2007**, 99, 1665-1667.

Wong, H.M. Life-cycle Assessment of Greenhouse Gas Emissions from Alternative Jet Fuels, Master of Science Thesis, Massachusetts Institute of Technology, Cambridge, Massachusetts, 2008.

Wuebbles, D.; Gupta, M.; Ko, M. Evaluating the Impacts of Aviation on Climate Change, *EOS* **2007**, *88 (14)*, 157-168.

Weubbles, D. J.; Yang, H.; Herman, R. *Climate Metrics and Aviation: Analysis of Current Understanding and Uncertainties*, Subject Specific white paper on Metrics for Climate Impacts, University of Illinois and Western Illinois University: Urbana and Macomb, IL, 2008.